극성/강유전 산화물 기초이론, 제일원리 계산 및 응용

부산대 물리학과 이재광 교수

부산대학교
PUSAN NATIONAL UNIVERSITY

I. Polar oxide stabilization

- Why are polar oxides unstable
  - fundamental mechanism: $\vec{P} \cdot \vec{n} = \sigma_b$

- Novel stabilization mechanism
  - polar oxide stabilization via vicinal surface: $\vec{P} \cdot \vec{n} = 0$

II. Magnetoelectric effect

- Depolarizing field $E_d = -\frac{2\lambda}{\varepsilon_0 d} P$

- Magnetoelectric coupling $\alpha = \mu_0 \frac{\delta \Delta M}{\delta E_d}$

III. Ferroelectric tunneling junction (FTJ)

$$T_{j+1,j} = \begin{pmatrix} \frac{k_j + k_{j+1}}{2k_j} e^{-ikjdx} & \frac{k_j - k_{j+1}}{2k_j} e^{-ikjdx} \\ \frac{k_j - k_{j+1}}{2k_j} e^{ik_jdx} & \frac{k_j + k_{j+1}}{2k_j} e^{ik_jdx} \end{pmatrix}$$

$$J(V_{DC}) \sim \int T(E) \left(\int f(E) - f(E + eV_{DC}) \right) dE$$

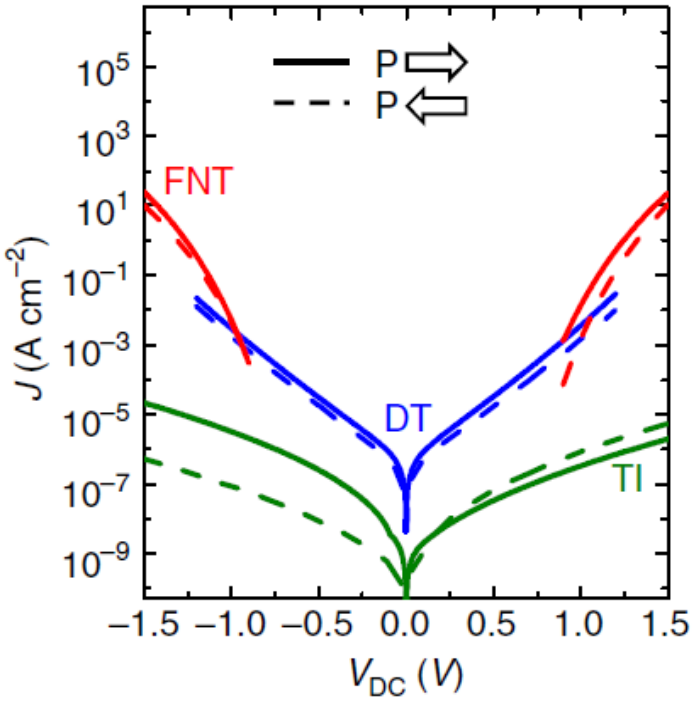

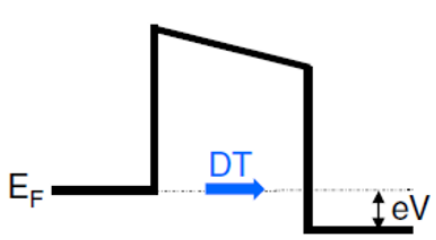

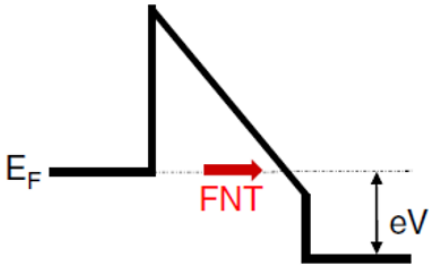

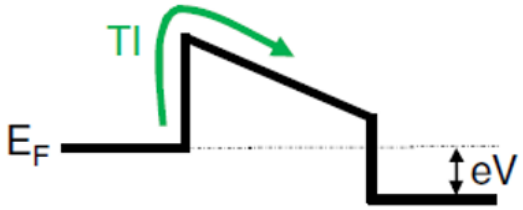

Polar oxides

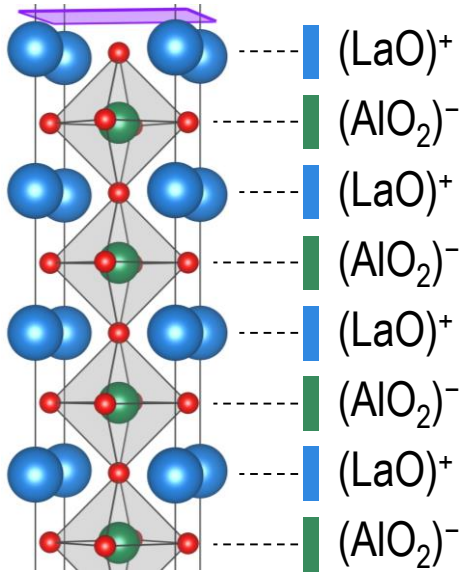



$LaAlO_3$, ZnO, $SrTiO_3$ (111)…

Ferroelectric oxides

$BaTiO_3$, $PbTiO_3$…

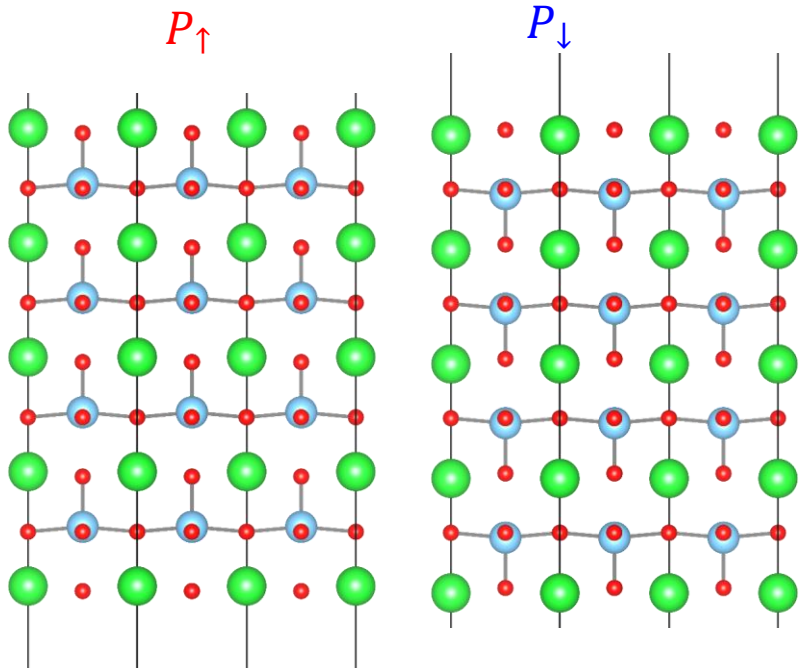



Surface reconstruction in polar ZnO

- Zn
- O

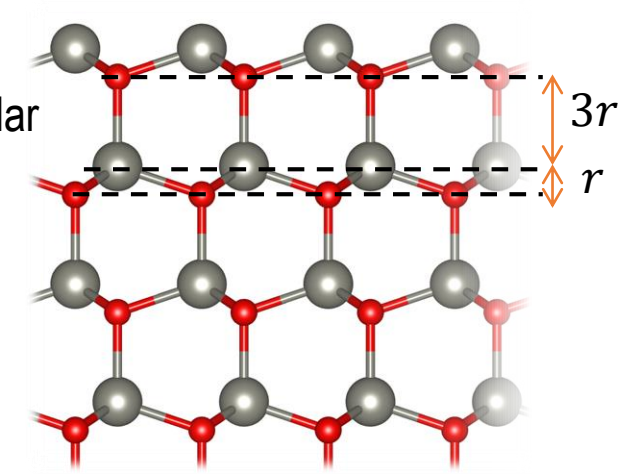

Surface metallization

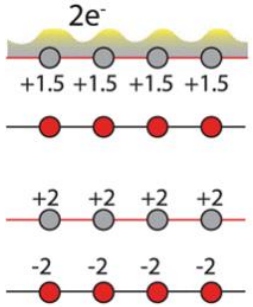

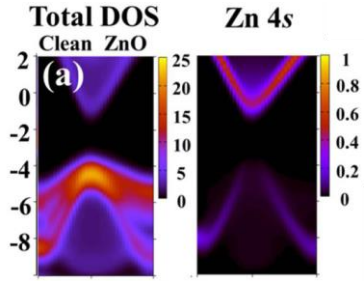

Silva, *et al*, *Phys. Rev. B*. **98** (2018)

C.C. Tseng, *J. Appl. Phys.* **38** (1967)

A. Wander and N. M. Harrison *J. Chem. Phys.* **115** (2001)

Kresse, *et al*, *Phys. Rev. B*. **68** (2003)

K. Ozawa and K. Mase, *Phys. Rev. B*. **83** (2011)

Absorption of foreign species

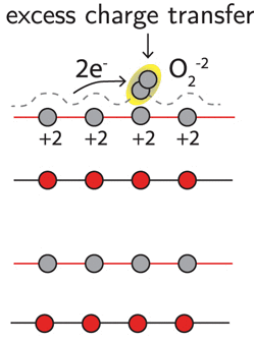

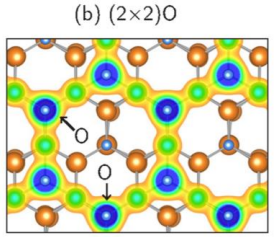

Gorai, *et al*, *J. Chem. Phys.* **144** (2016)

A. Wander and N. M. Harrison, *J. Chem. Phys.*, **115** (2001)

Ito *et al, J. Chem. Phys.* **135** *(2011)*

Wahl*, et al, Phys. Rev. B*, **87** (2013)

Jacobs *et al, J. Phys. Chem. Lett.* **7** (2016)

Formation of Zn vacancy (V_{Zn})

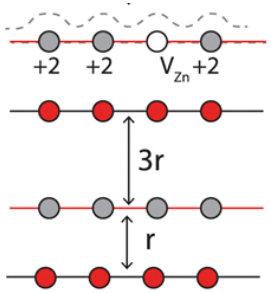

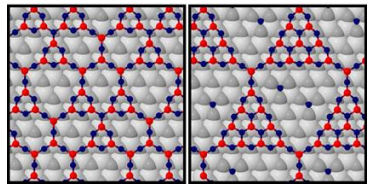

Fonz *et al*, *Chem. Mater.*, **29** (2017)

Dulub, *et al*, *Phys. Rev. Lett.* **90** (2003)

Gorai, *et al*, *J. Chem. Phys.* **45** (2016)

Lauritsen, *et al*, *ACS Nano* **5** (2011)

Diebold U, *et al*, *Annu. Rev. Phys. Chem.* **61** (2010)

H. Meskine and P. A. Mulheran, *Phys. Rev. B*, **84** (2011)

Tang *et al, Phys. Chem. Chem. Phys.*,**16** (2014)

Dynamic surface reconstruction in polar ZnO

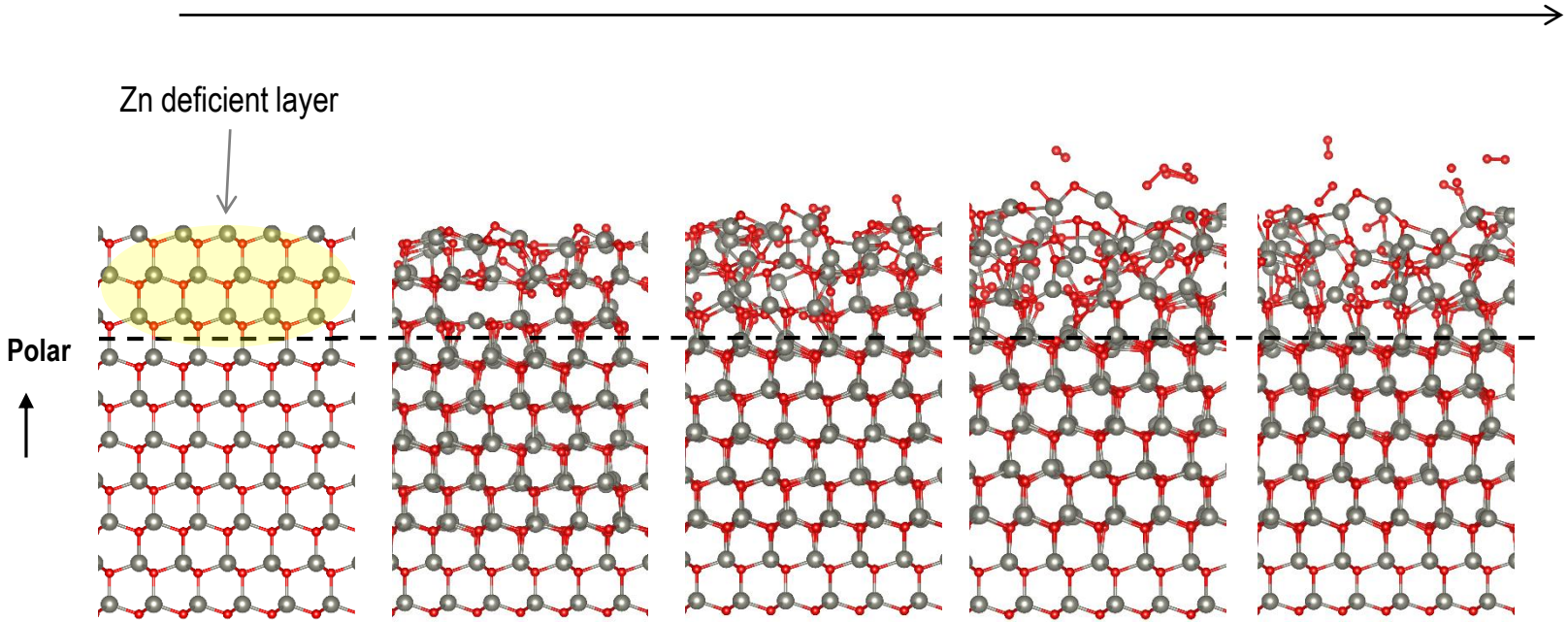

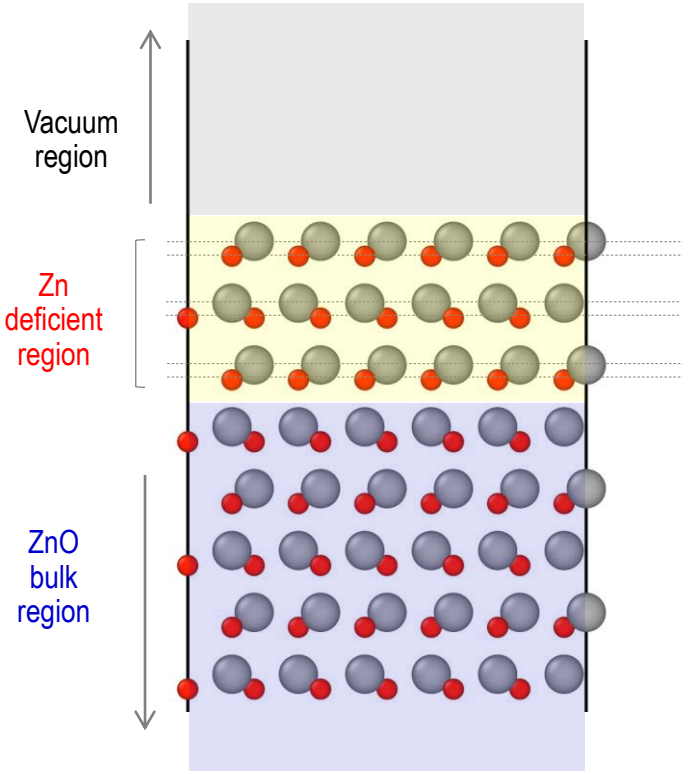

V_{Zn} induce the strongly distorted lattice and fast evaporation of oxygen molecules (O_2) from the surface

Z. Wang, J. Byun *et al., Nature communications 13, 1-12 (2022)*

Surface reconstruction in polar LAO

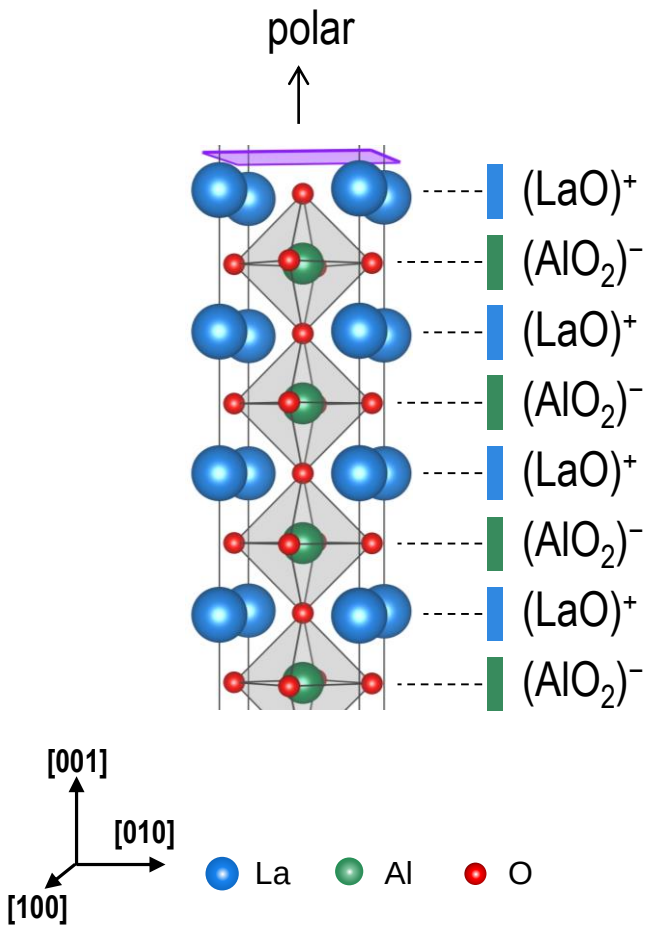

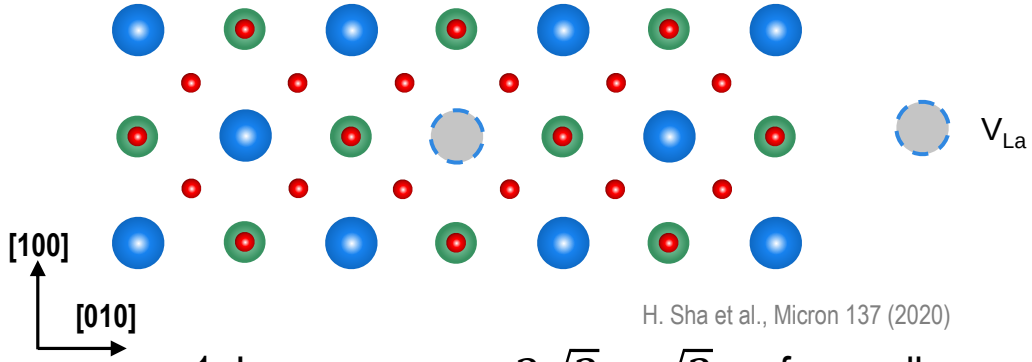

H. Sha et al., Micron 137 (2020)

1. La vacancy per $3\sqrt{2} \times \sqrt{2}$ surface cell

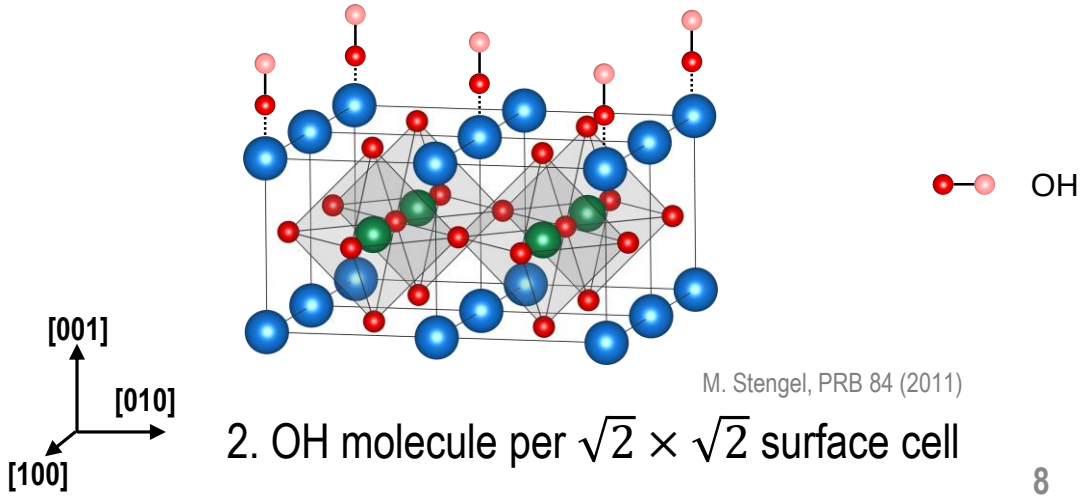

M. Stengel, PRB 84 (2011)

2. OH molecule per $\sqrt{2} \times \sqrt{2}$ surface cell

2DEG formation at STO/LAO(001) heterostructure

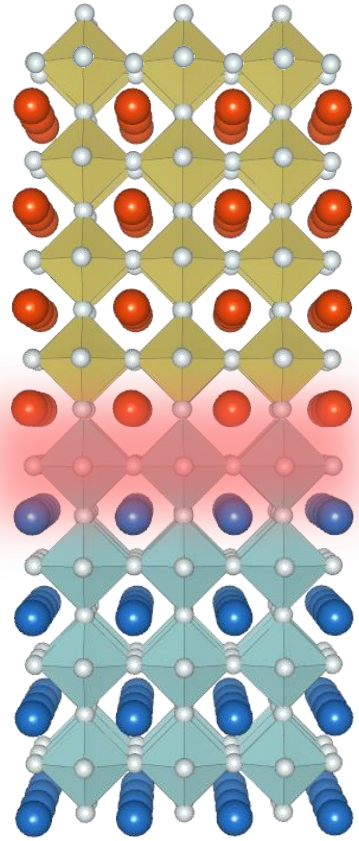

Intrinsic doping

Electronic reconstruction

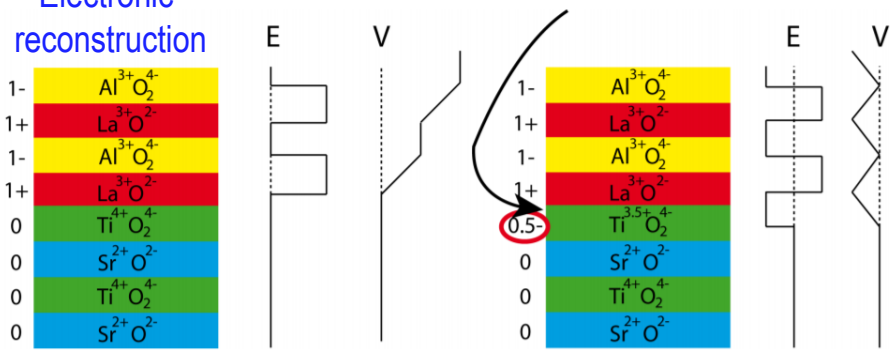

A. Ohtomo & H. Y. Hwang, Nature 427, 423–426 (2004)
S. Thiel, et al., Science 313, 1942–1945 (2006)
J. Lee & A. A. Demkov, Phys. Rev. B 78, 193104 (2008)

Extrinsic doping

Cation intermixing (interdiffusion of La)

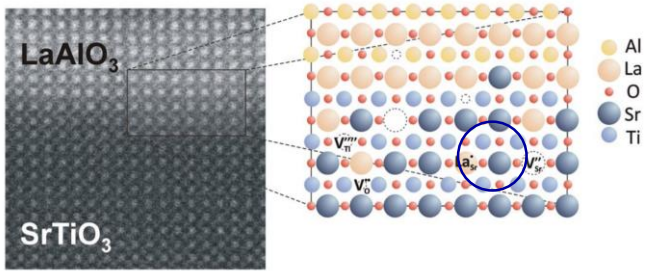

N. Nakagawa, *et al.,* Nat. Mater. 5, 204–209 (2006)
P. R. Willmott, *et al.,* Phys. Rev. Lett. 99, 155502 (2007)
A. S. Kalabukhov, *et al.*, Phys. Rev. Lett. 103, 146101 (2009)
R. Yamamoto, *et al.*, Phys. Rev. Lett. 107, 036104 (2011)
L. Qiao, *et al.*, Surf. Sci. 605, 1381–1387 (2011)
V. Vonk, *et al.*, Phys. Rev. B 85, 045401 (2012)
F. Gunkel, *et al.*, Appl. Phys. Lett. 100, 052103 (2012)

Oxygen vacancy on the LAO surface

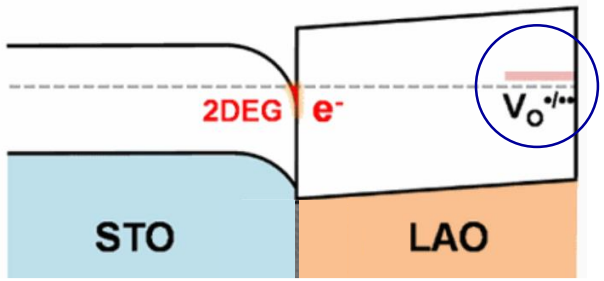

C. Cen, *et al.,* Nat. Mater. 7, 298–302 (2008)
Z. C. Zhong, *et al.*, Phys. Rev. B 82, 165127 (2010)
N. C. Bristowe, *et al.,* Phys. Rev. B 83, 205405 (2011)
Y. Li, *et al.,* Phys. Rev. B 84, 245307 (2011)
M. Takizawa*et al.,* Phys. Rev. B 84, 245124 (2011)
G. Berner, *et al.,* Phys. Rev. Lett. 110, 247601 (2013)
L. Yu & A. Zunger, Nat. Comms. 5, 6118 (2014)
T. Min *et al.*, Science Advances 7 (17) eabe9053 (2021)

Cooperative coupling of FE distortion and AFD rotation

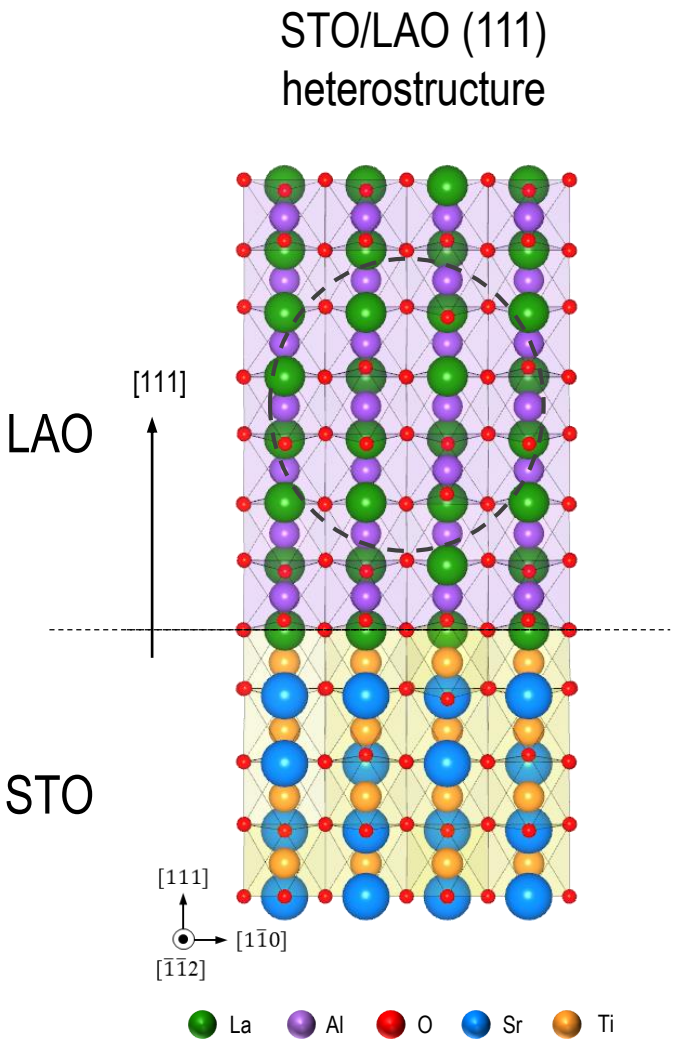

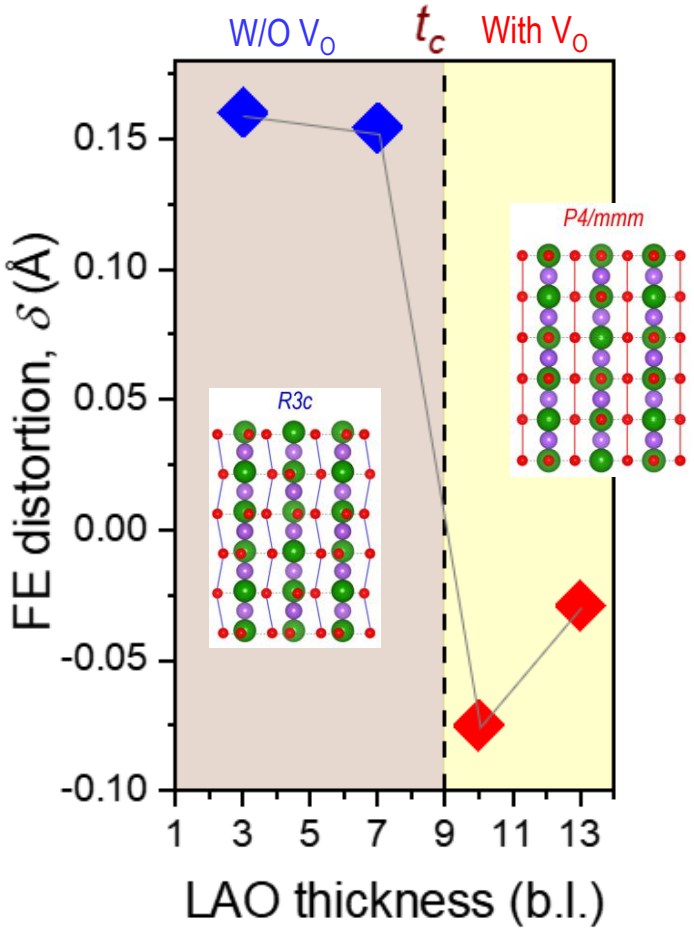

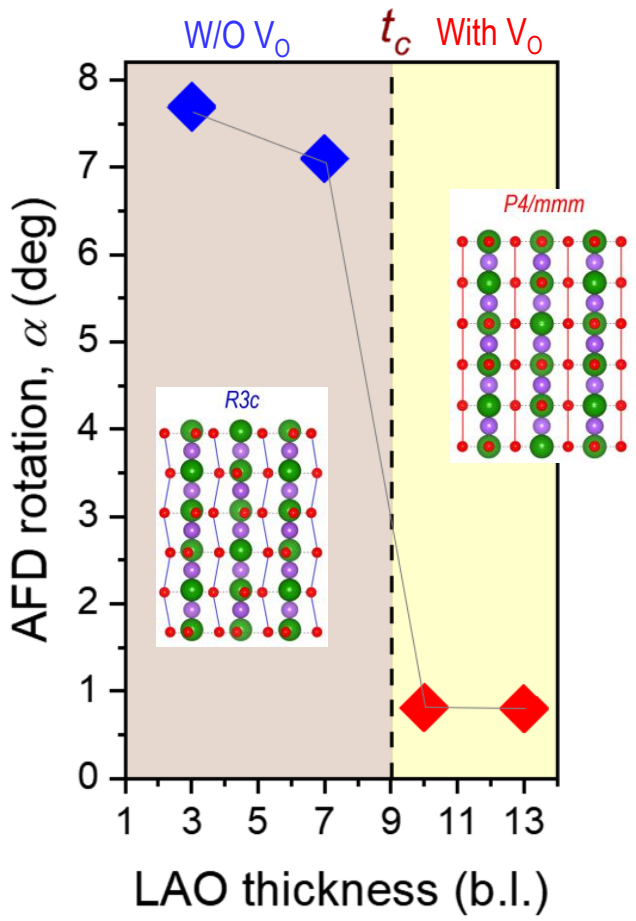

T. Min *et al., Science Advances 7, eabe9053 (2021)*

Contents

- Why are polar oxides unstable
  - fundamental mechanism: $\vec{P} \cdot \vec{n} = \sigma_b$

- Novel stabilization mechanism
  - polar oxide stabilization via vicinal surface: $\vec{P} \cdot \vec{n} = 0$

Polarization and surface bound charge in polar oxide

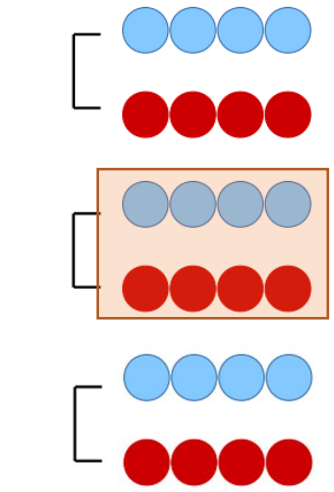

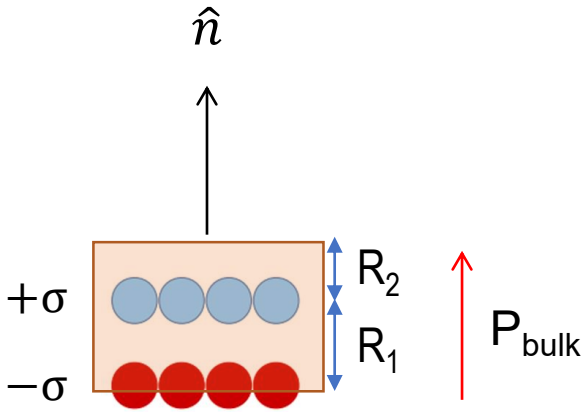

Cation (+σ)

Anion (−σ)

Bulk Polarization

$$\overrightarrow{P_{bulk}} = \frac{\sum_i q_i z_i}{\Omega}\hat{n} = \frac{\sigma R_1}{R_1+R_2}\hat{n}$$

Surface bound charge

$$\sigma_b = \overrightarrow{P_{bulk}} \cdot \hat{n} = \frac{\sigma R_1}{R_1+R_2}$$

Goniakowski, Jacek, and Claudine Noguera. *Comptes Rendus Physique* 17.3-4 (2016): 471-480.

Polar oxide is unstable : polar-catastrophe

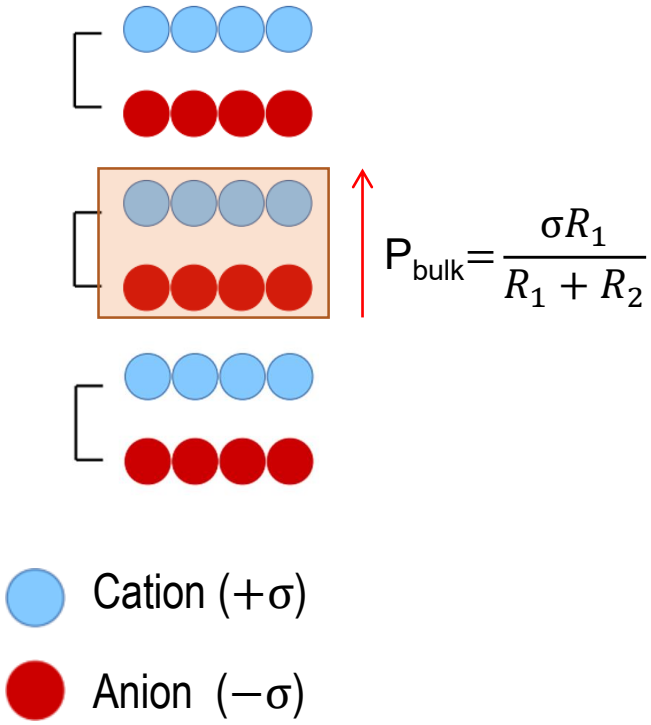

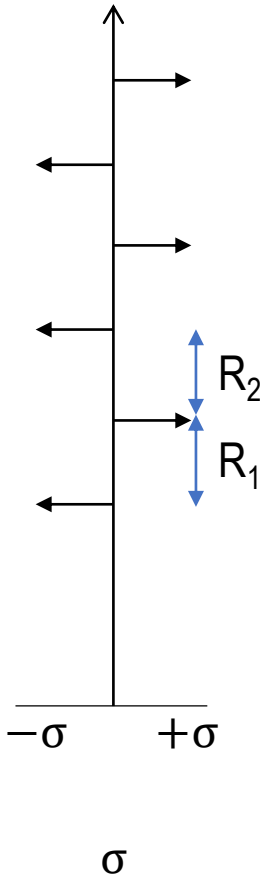

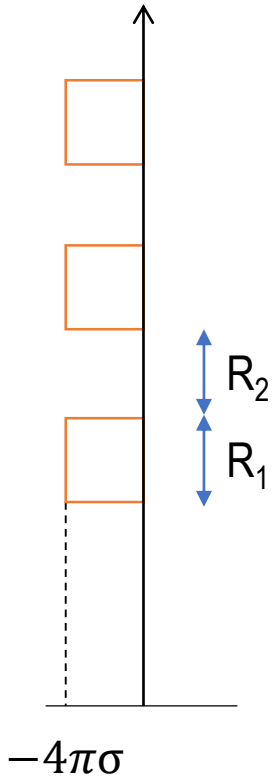

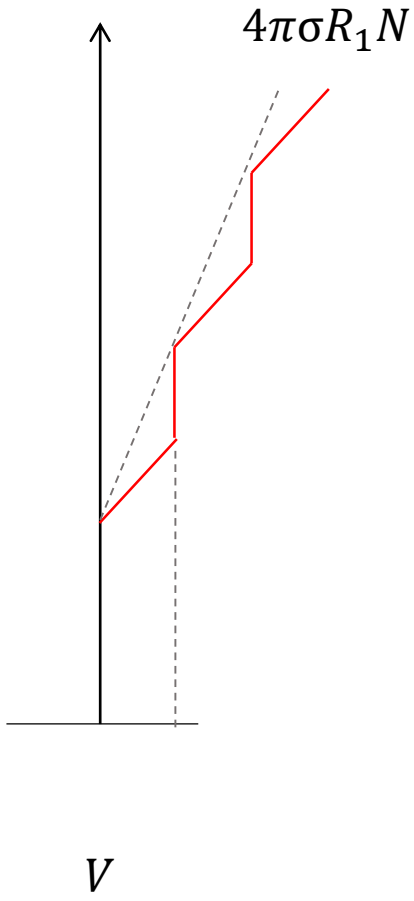

Goniakowski, Jacek, and Claudine Noguera. *Comptes Rendus Physique* 17.3-4 (2016): 471-480.

Stabilization of polar oxide

$$\boldsymbol{\sigma_{comp}} + \sigma_{bound} = 0$$

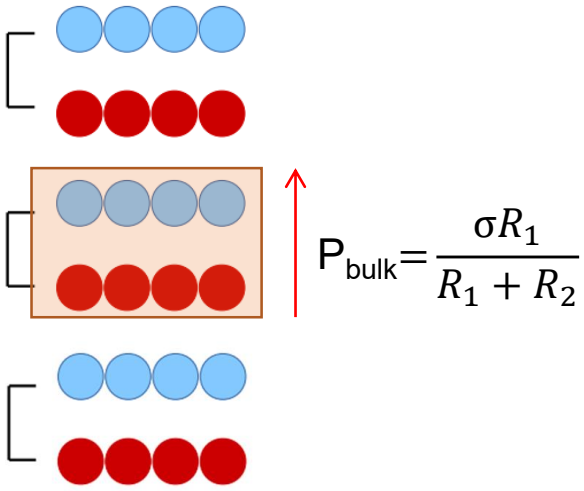

$$P_{bulk} = \frac{\sigma R_1}{R_1 + R_2}$$

Cation $(+\sigma)$

Anion $(-\sigma)$

$$\boldsymbol{\sigma_{comp}} + \sigma_{bound} = 0$$

$$\rightarrow \quad \boldsymbol{\sigma_{comp}} = -\frac{\boldsymbol{\sigma R_1}}{\boldsymbol{R_1 + R_2}}$$

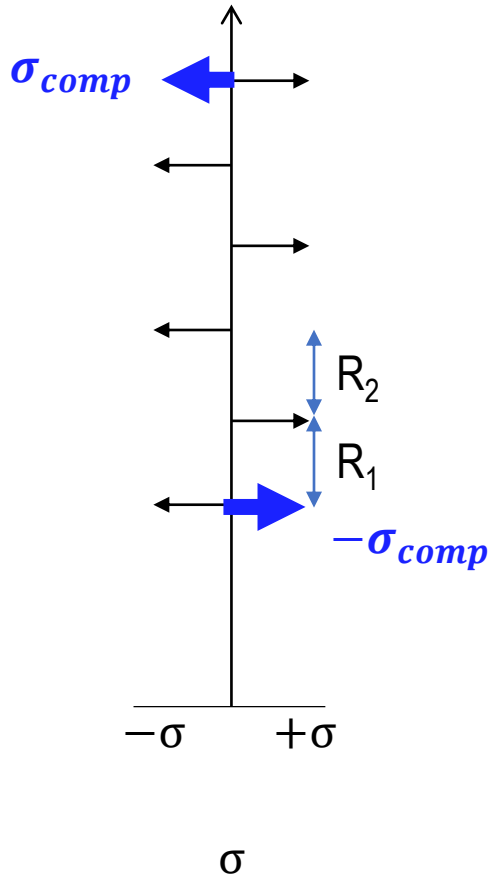

Goniakowski, Jacek, and Claudine Noguera. *Comptes Rendus Physique* 17.3-4 (2016): 471-480.

$$\sigma_{comp} = - \frac{\sigma R_1}{R_1 + R_2}$$

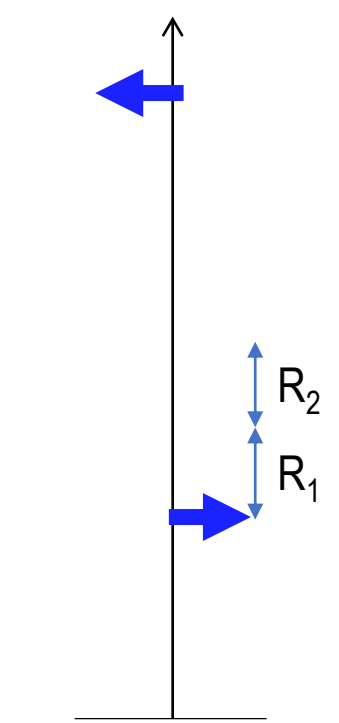

σ

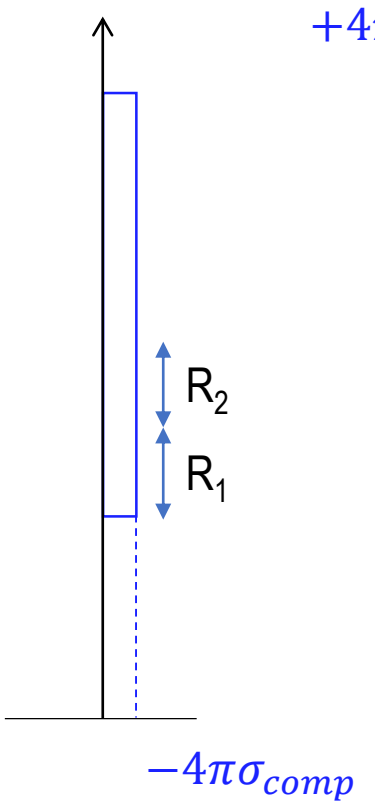

E

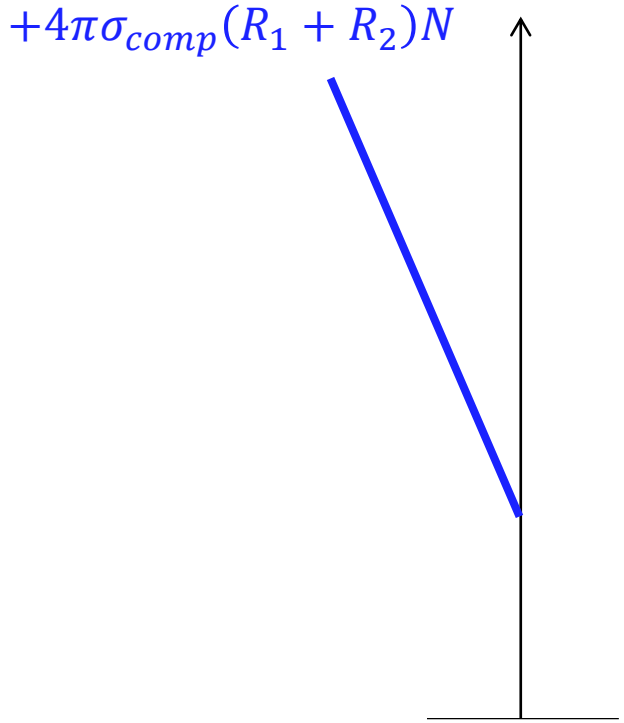

V

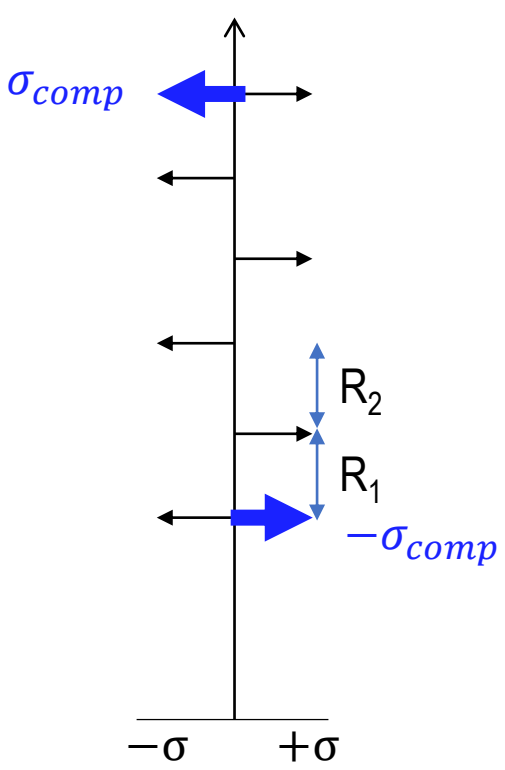
σ_{comp}
R2
R1
$-\sigma_{comp}$
$-\sigma$
$+\sigma$

σ

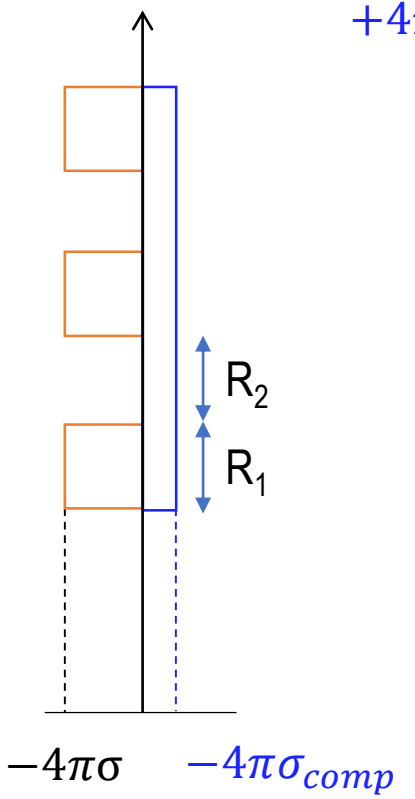
R2
R1
$-4\pi\sigma$
$-4\pi\sigma_{comp}$

E

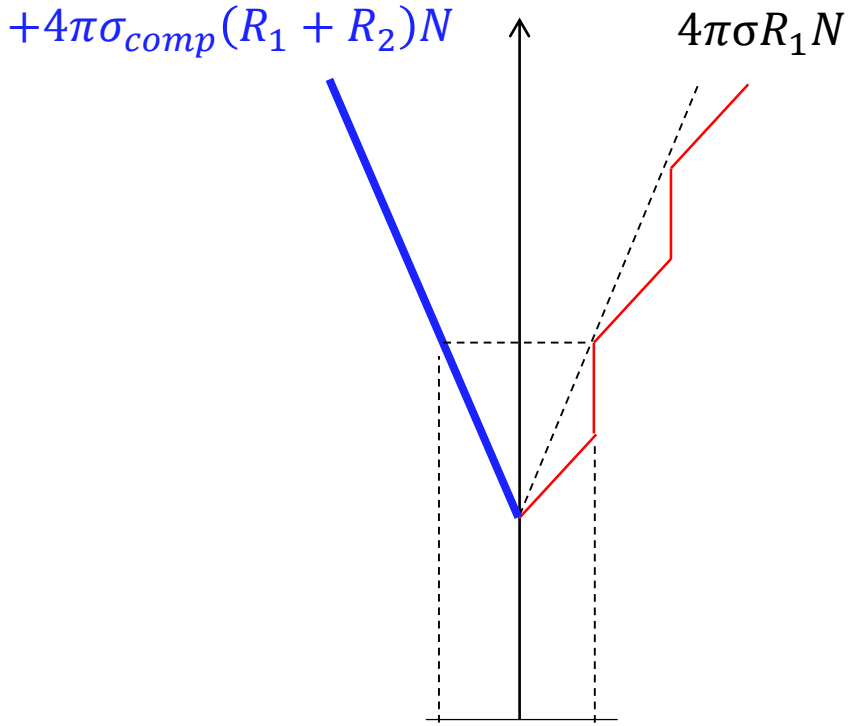
$+4\pi\sigma_{comp}(R_1+R_2)N$
$4\pi\sigma R_1 N$

V

Stabilization of polar oxide by charge compensation

$\sigma_{comp} = -\frac{\sigma R_1}{R_1+R_2}$

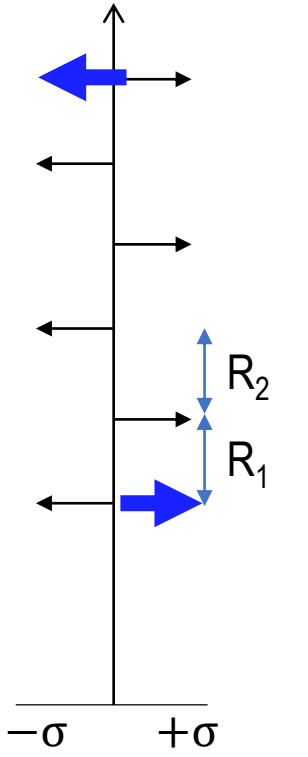

σ

$-4\pi\sigma_{comp} = \frac{4\pi\sigma R_1}{R_1+R_2}$

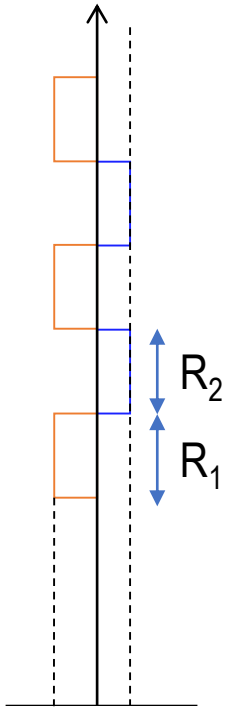

$-4\pi\sigma - 4\pi\sigma_{comp} =$

$-4\pi\sigma + \frac{4\pi\sigma R_1}{R_1+R_2} = -\frac{4\pi\sigma R_2}{R_1+R_2}$

E

$4\pi\sigma_{comp}(R_1+R_2)N + 4\pi\sigma R_1 N = 0$

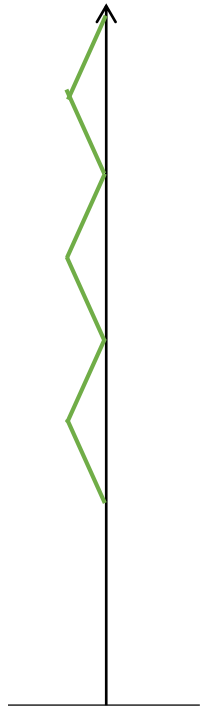

V

ZnO bulk polarization

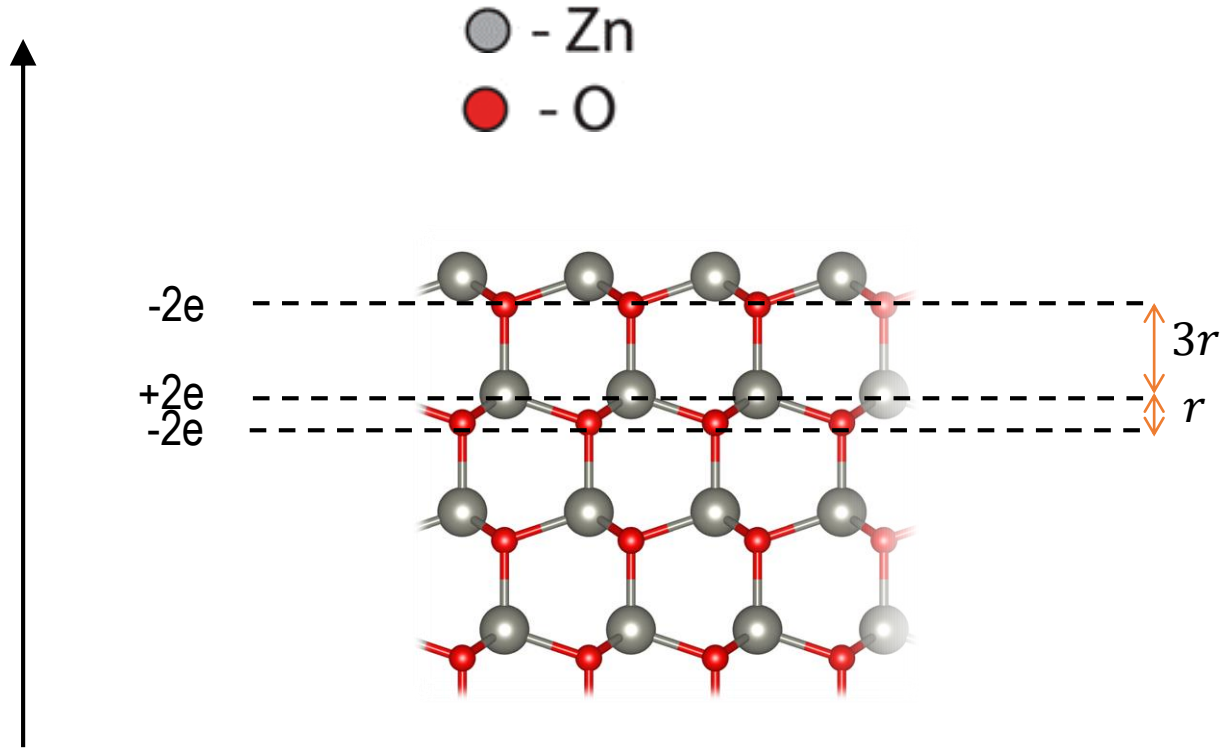

$$P_{bulk} = \frac{\sigma R_1}{R_1 + R_2} = \frac{\left(\frac{2e}{S}\right) r}{r + 3r} = 0.5e/S$$

$$\sigma_{comp} = -P_{bulk} \cdot n = -0.5e/S$$

Polar compensation in ZnO

- Zn
- O

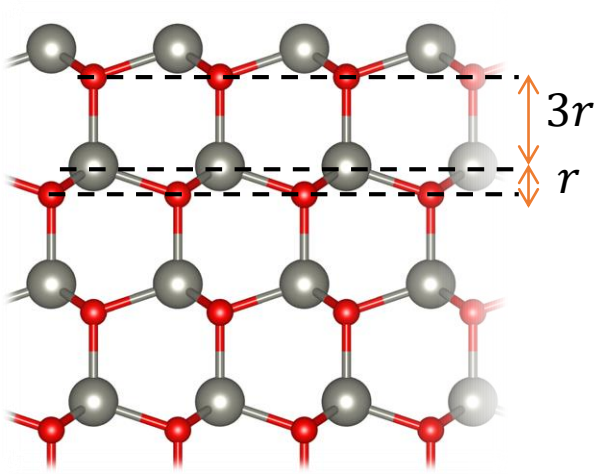

$\sigma_{comp} = -0.5e/S$

Surface metallization

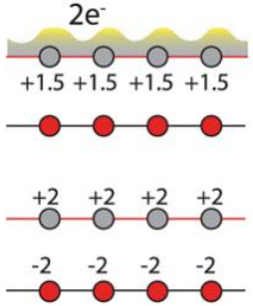

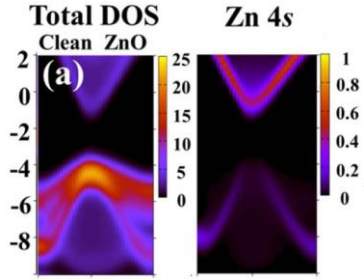

Silva, *et al*, *Phys. Rev. B.* **98** (2018)

C.C. Tseng, *J. Appl. Phys.* **38** (1967)

A. Wander and N. M. Harrison *J. Chem. Phys.* **115** (2001)

Kresse, *et al*, *Phys. Rev. B.* **68** (2003)

K. Ozawa and K. Mase, *Phys. Rev. B.* **83** (2011)

Absorption of foreign species

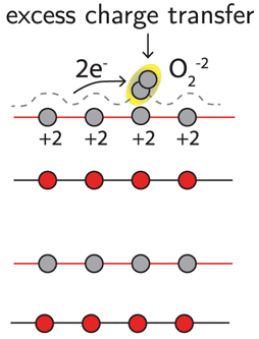

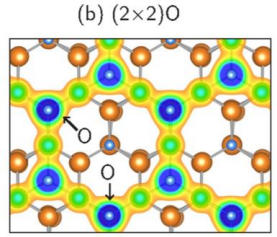

Gorai, *et al*, *J. Chem. Phys.* **144** (2016)

A. Wander and N. M. Harrison, *J. Chem. Phys.*, **115** (2001)

Ito *et al, J. Chem. Phys.* **135** *(2011)*

Wahl*, et al, Phys. Rev. B*, **87** (2013)

Jacobs *et al, J. Phys. Chem. Lett.* **7** (2016)

Formation of Zn vacancy (V_{Zn})

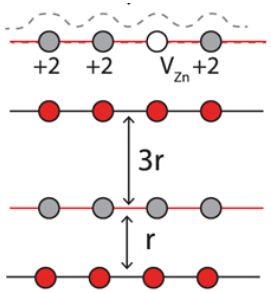

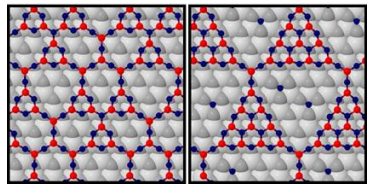

Fonz *et al*, *Chem. Mater.*, **29** (2017)

Dulub, *et al*, *Phys. Rev. Lett.* **90** (2003)

Gorai, *et al*, *J. Chem. Phys.* **45** (2016)

Lauritsen, *et al*, *ACS Nano* **5** (2011)

Diebold U, *et al*, *Annu. Rev. Phys. Chem.* **61** (2010)

H. Meskine and P. A. Mulheran, *Phys. Rev. B*, **84** (2011)

Tang *et al, Phys. Chem. Chem. Phys.*,**16** (2014)

Polarity compensation in polar LAO

LAO (001) surface

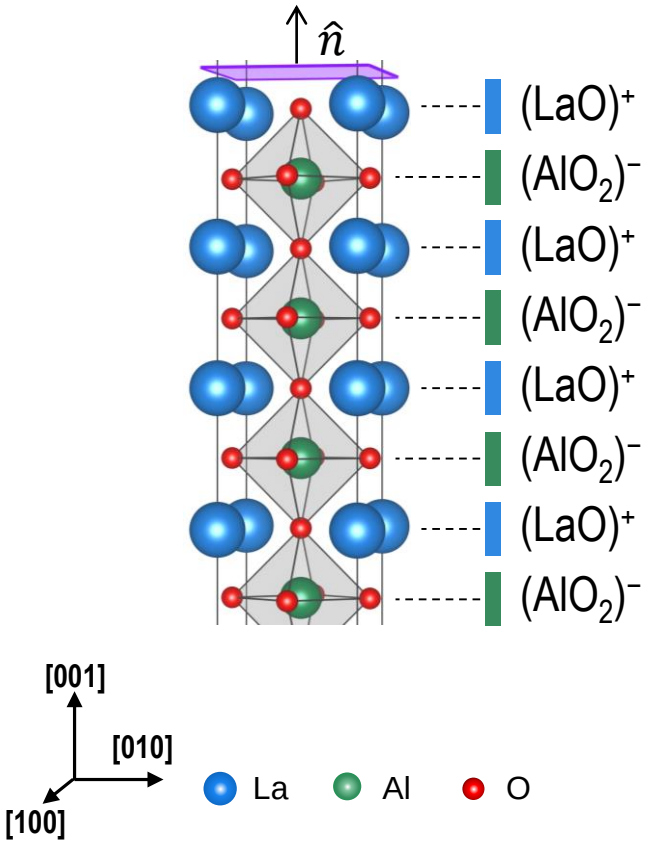

Side view of LAO unit cell

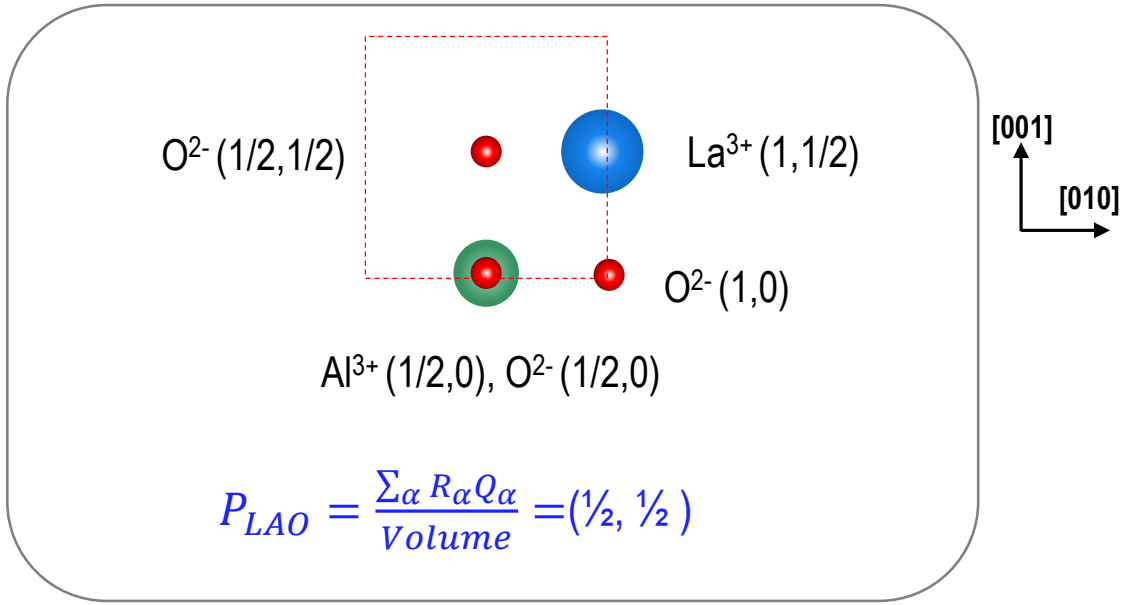

$$P_{LAO} = \frac{\sum_\alpha R_\alpha Q_\alpha}{Volume} = (½, ½)$$

$$\sigma_{bound} = P_{LAO} \cdot \hat{n} = 0.5e/S$$

$$\sigma_{comp} = -0.5e/S$$

Polar compensation in LAO

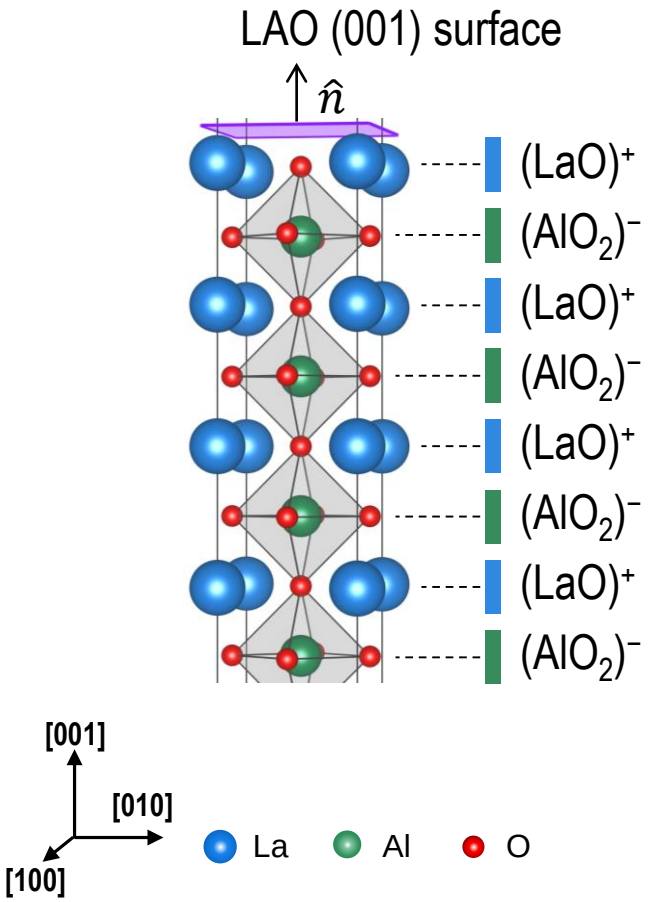

$\sigma_{comp} = -0.5e/S$

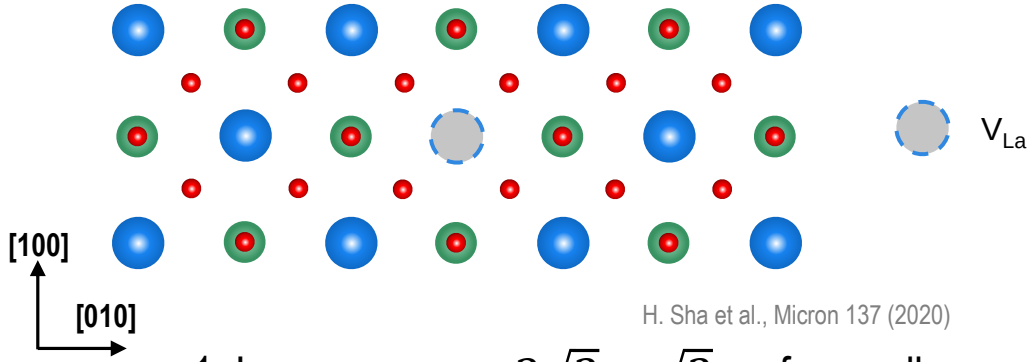

H. Sha et al., Micron 137 (2020)

1. La vacancy per $3\sqrt{2} \times \sqrt{2}$ surface cell

$\sigma_{comp} = -0.5e/S$

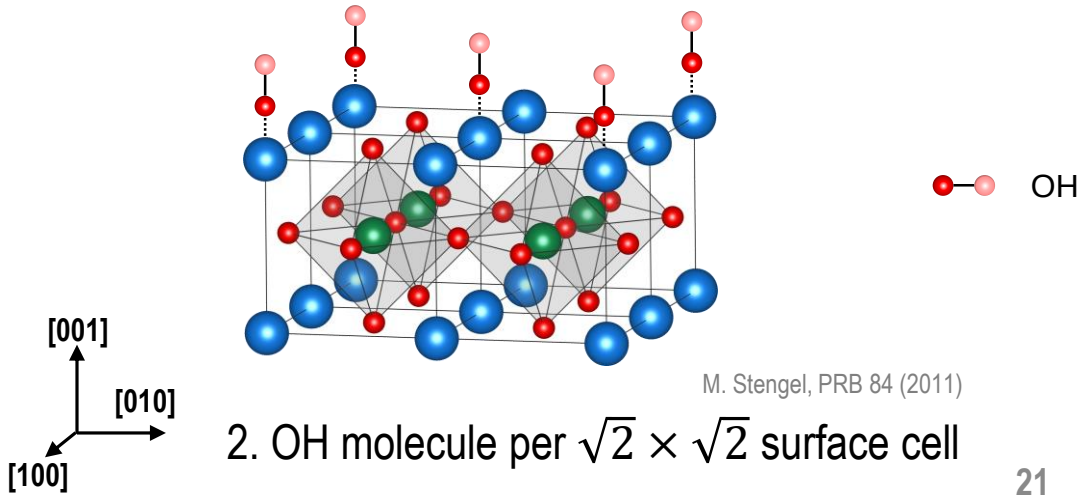

M. Stengel, PRB 84 (2011)

2. OH molecule per $\sqrt{2} \times \sqrt{2}$ surface cell

Contents

- Why are polar oxides unstable
  - fundamental mechanism: $\vec{P} \cdot \vec{n} = \sigma_b$

- Novel stabilization mechanism
  - polar oxide stabilization via vicinal surface: $\vec{P} \cdot \vec{n} = 0$

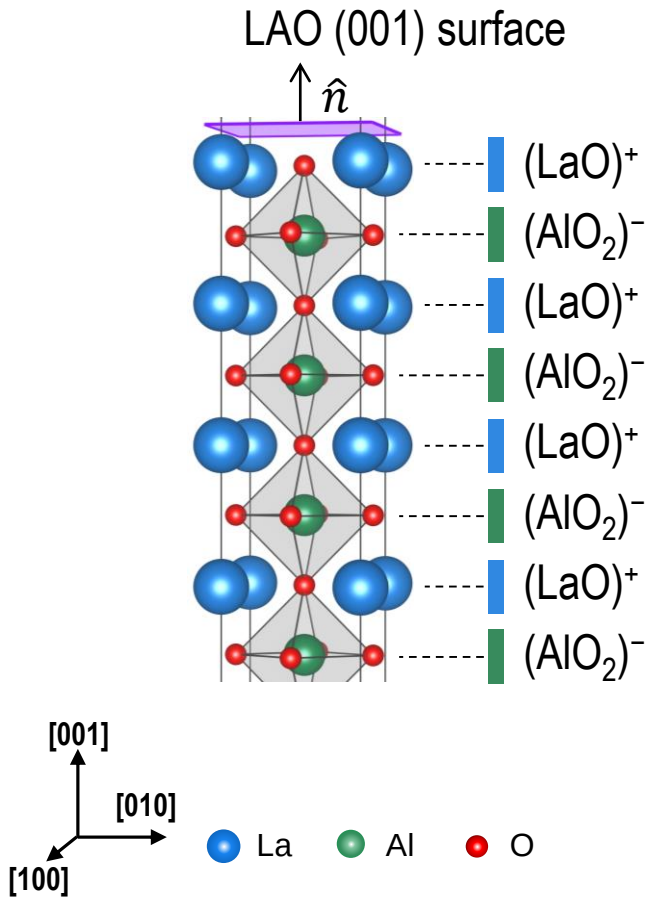

⟶ Polar surface stabilization without σ_{comp} ?

$$P_{LAO} \cdot \hat{n} \rightarrow 0$$

P $\frac{1}{2}(1, 1)$

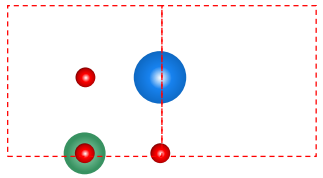

Side view of LAO unit cell

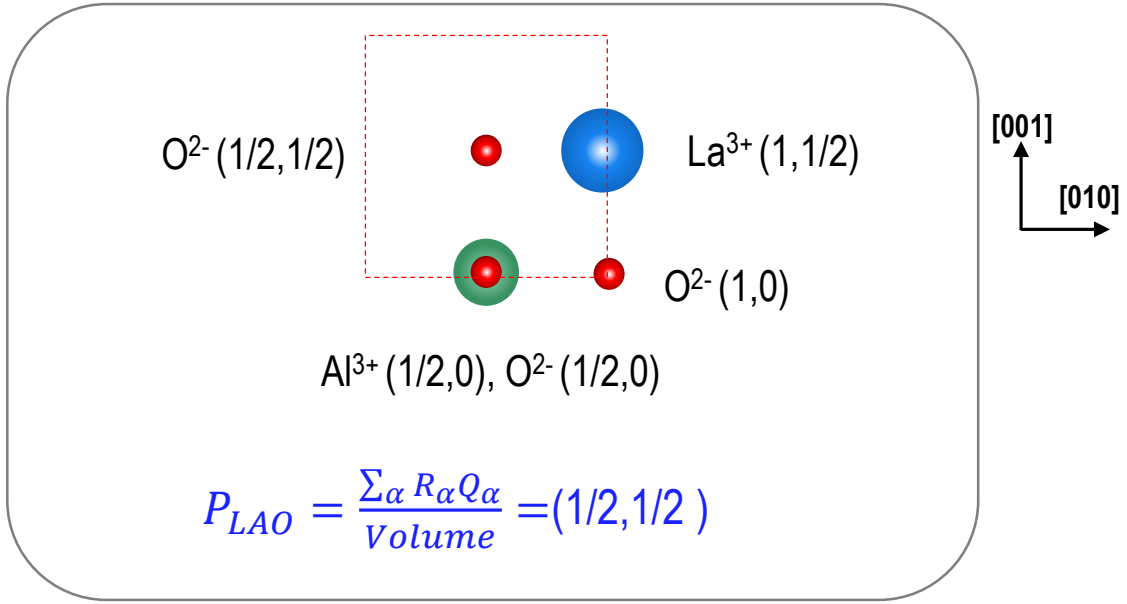

$$P_{LAO} = \frac{\sum_\alpha R_\alpha Q_\alpha}{Volume} = (1/2, 1/2)$$

P $\frac{1}{2}(3, 1)$

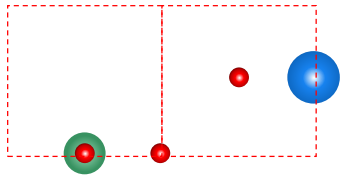

Side view of LAO unit cell

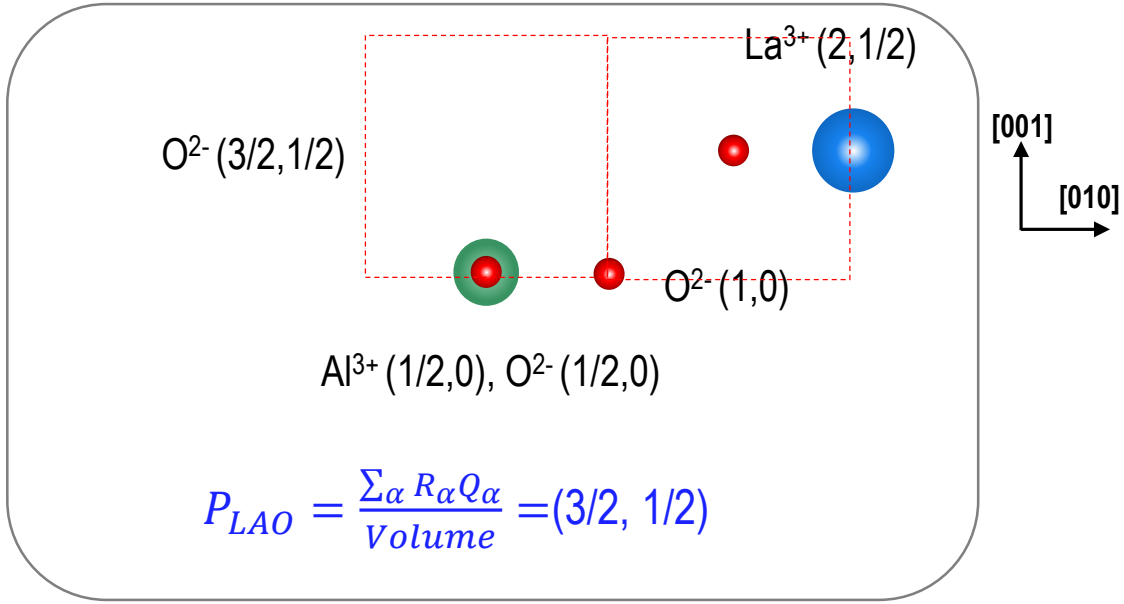

$$P_{LAO} = \frac{\sum_\alpha R_\alpha Q_\alpha}{Volume} = (3/2,\ 1/2)$$

P $\frac{1}{2}(3, 1)$

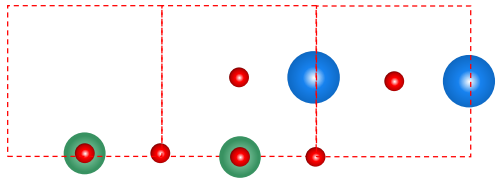

P $\frac{1}{2}(3, 1)$

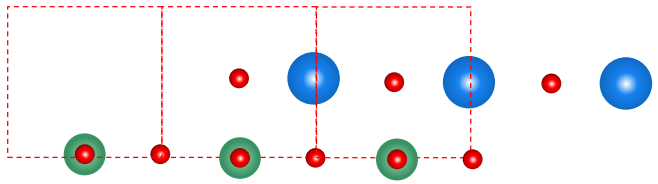

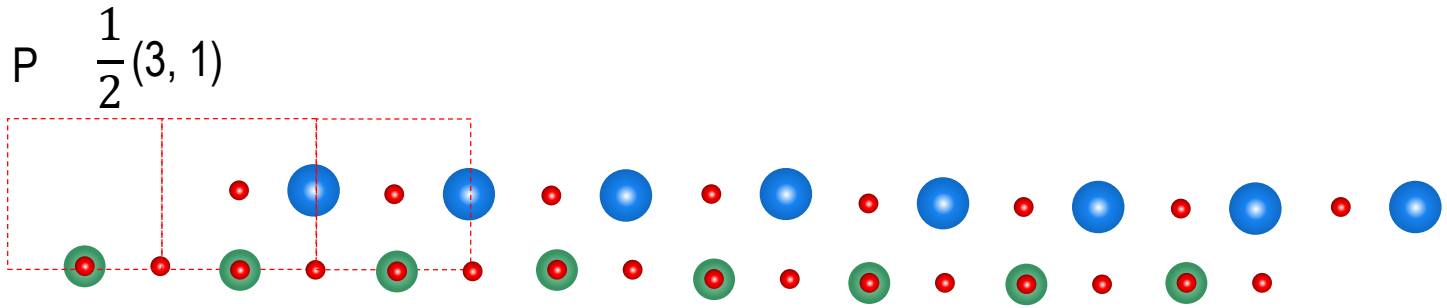
P
1/2(3, 1)

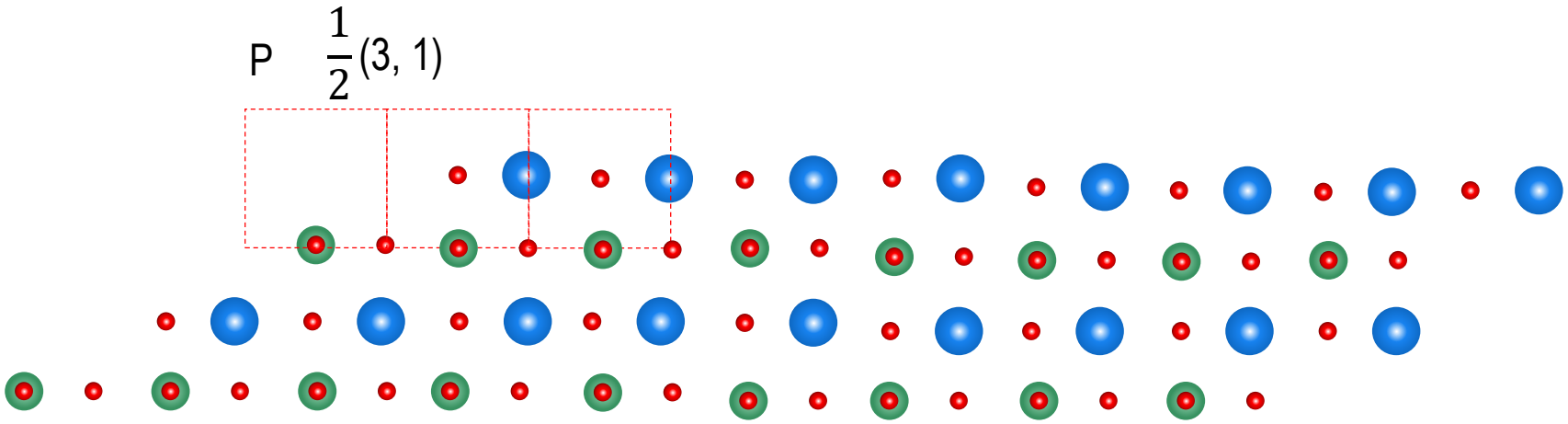
P $\frac{1}{2}(3, 1)$

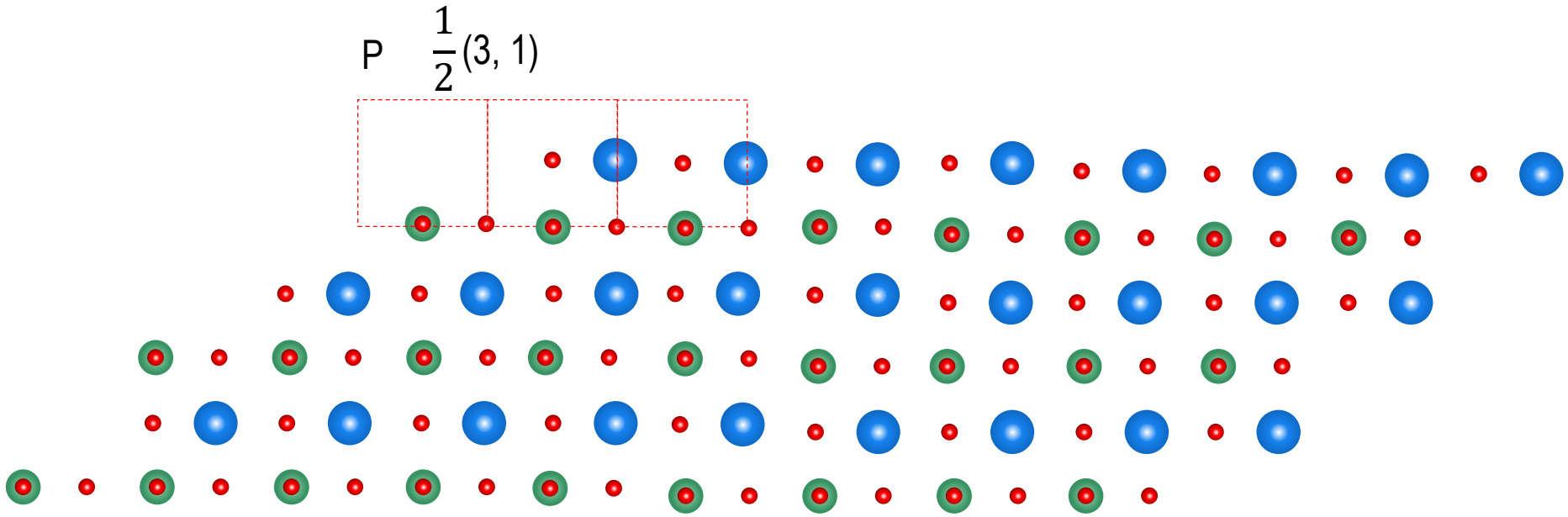
P $\frac{1}{2}(3, 1)$

vicinal surface

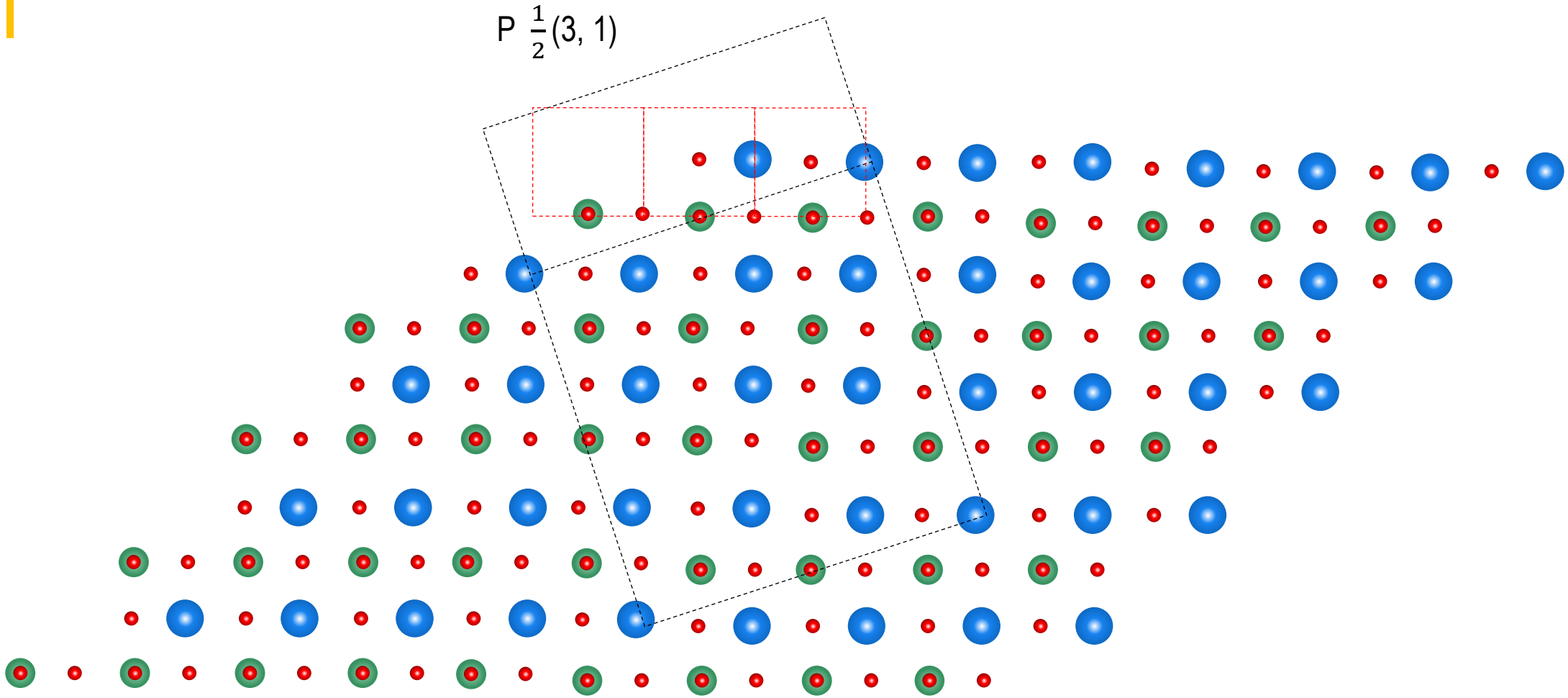

$P\ \frac{1}{2}(3,\ 1)$

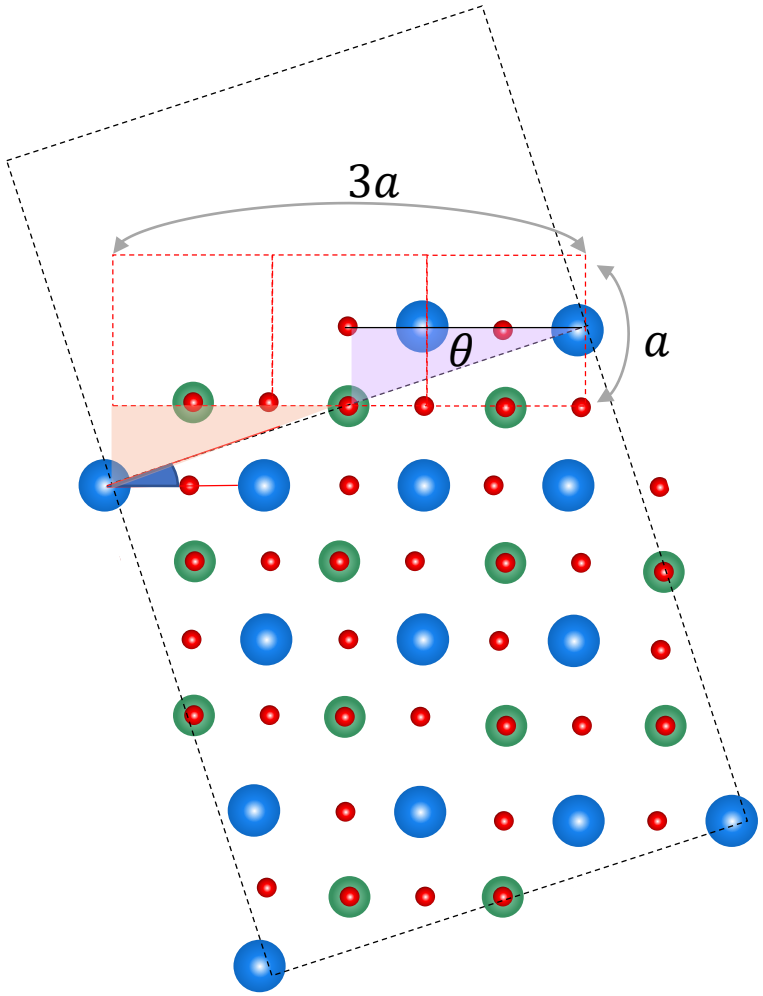

Computational Physics & Materials Design Lab.

$P\ \frac{1}{2}(3,\ 1)$

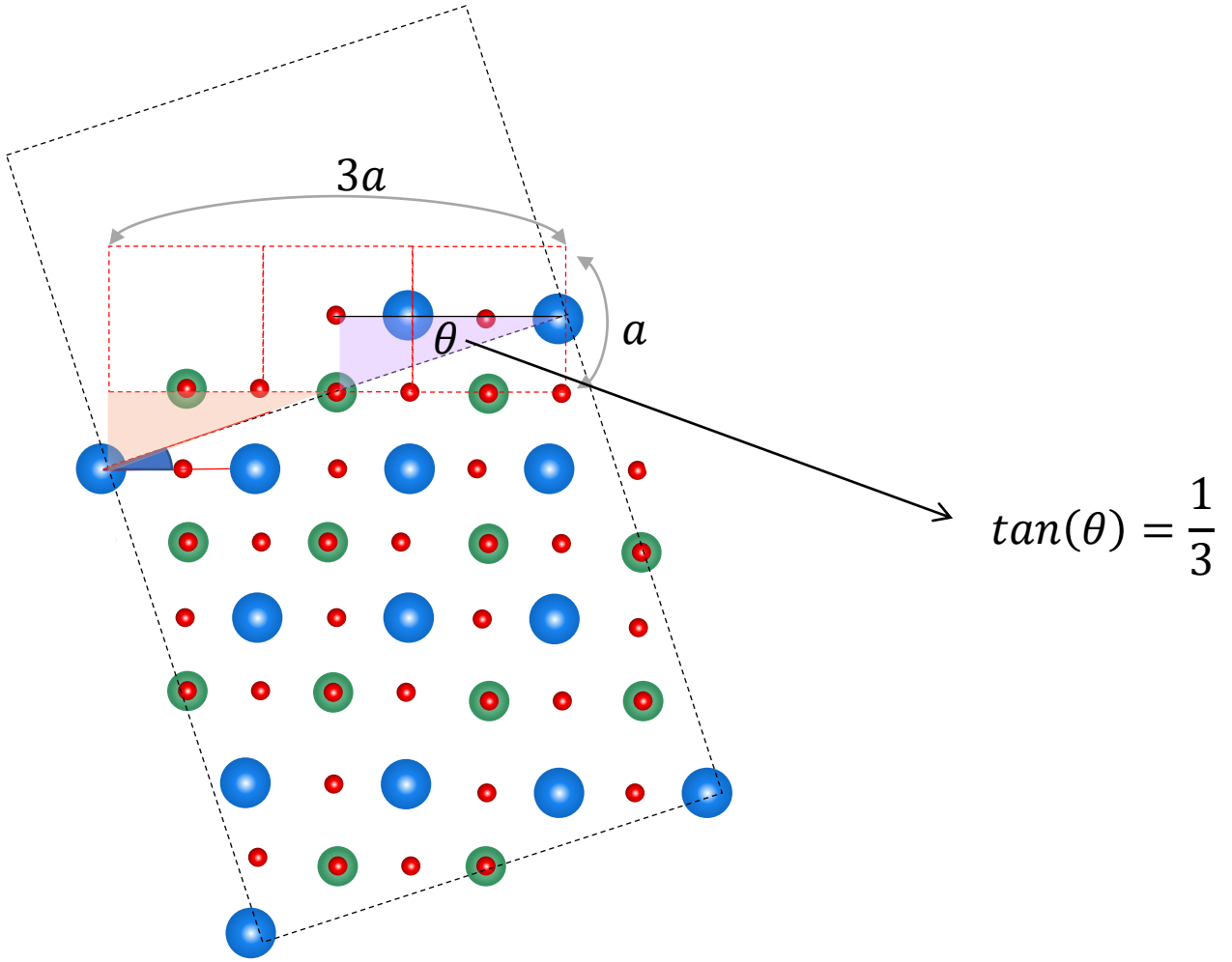

Computational Physics & Materials Design Lab.

$P\ \frac{1}{2}(3,\ 1)$

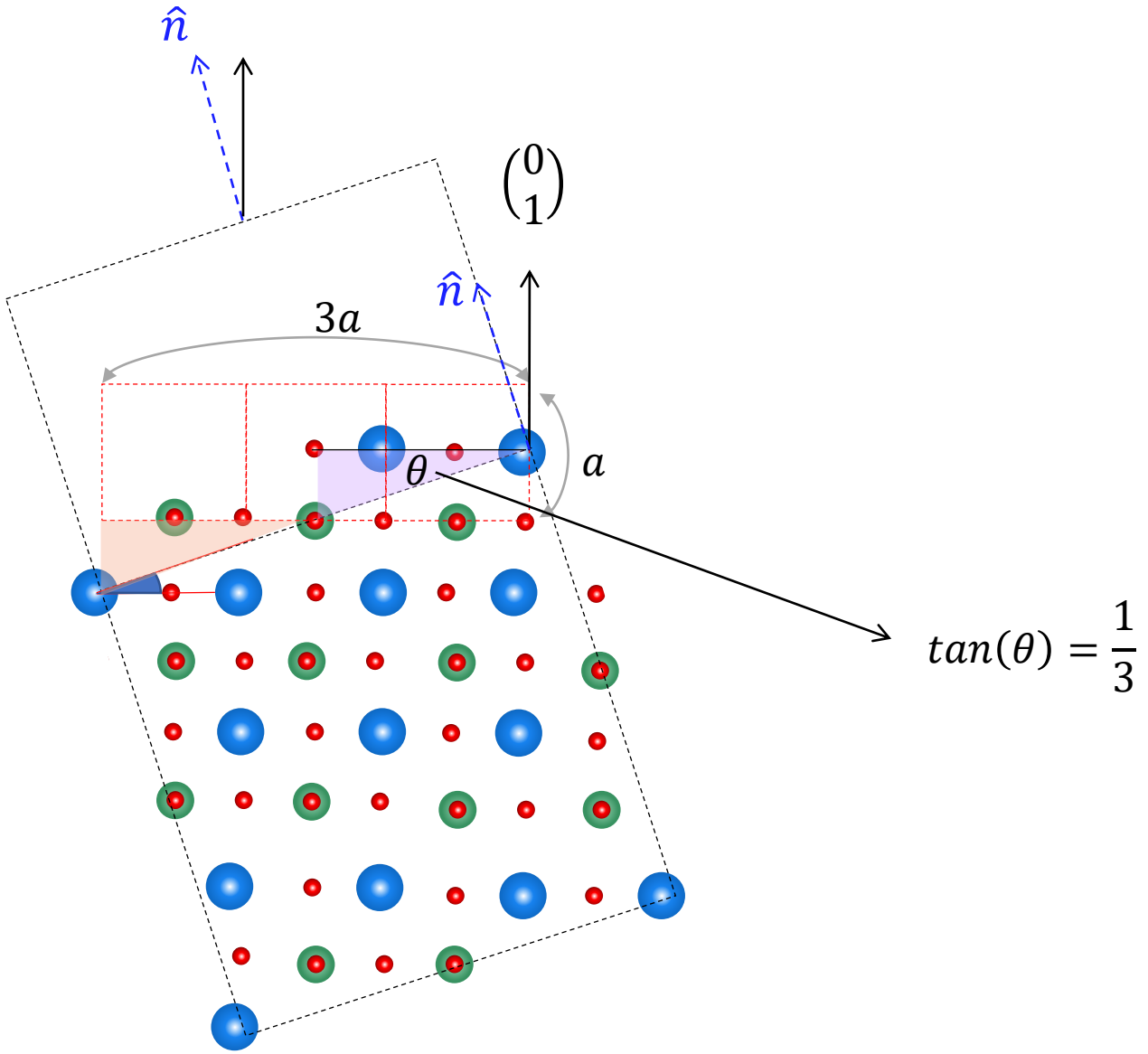

Computational Physics & Materials Design Lab.

$P\ \frac{1}{2}(3,\ 1)$

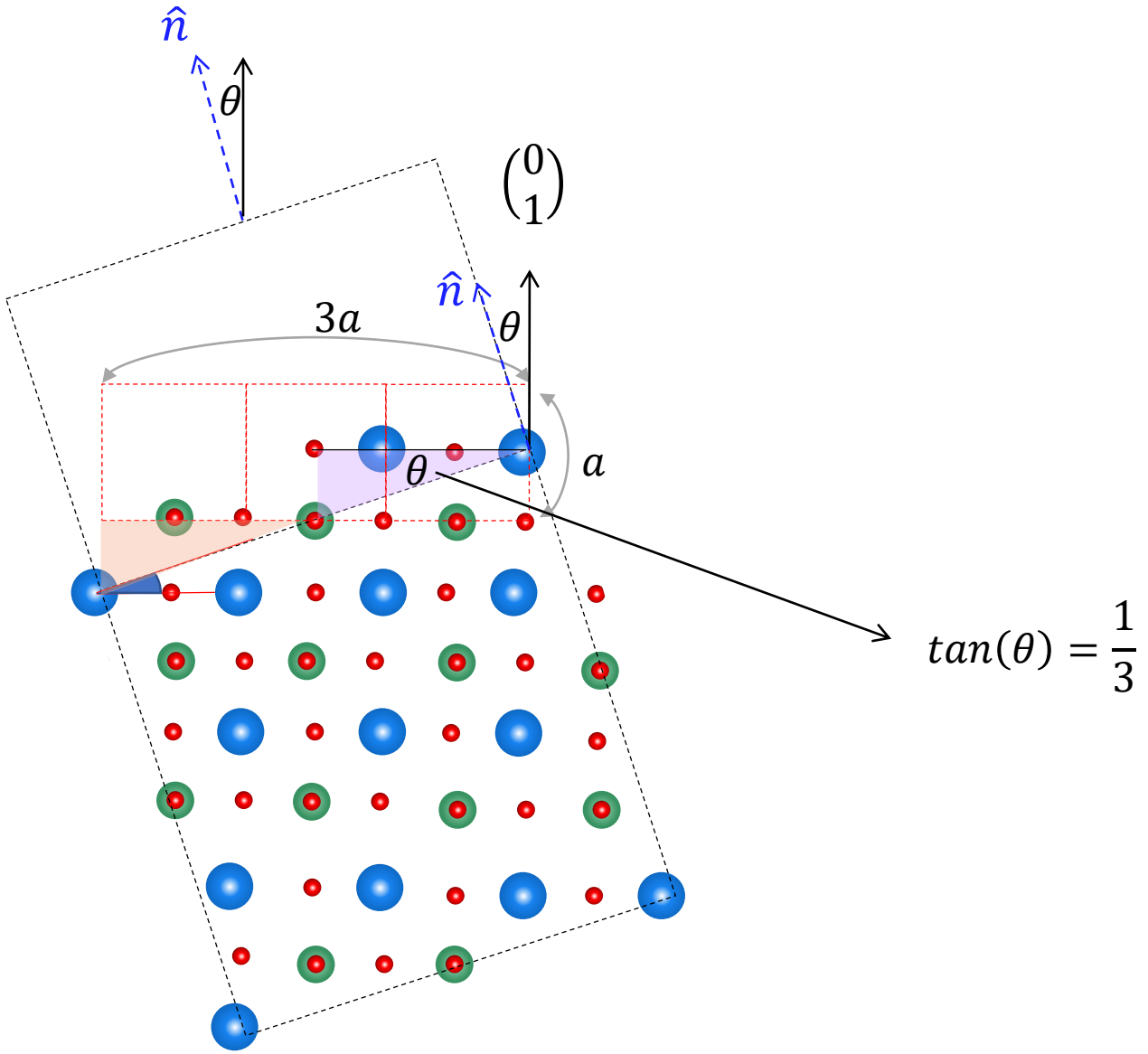

Computational Physics & Materials Design Lab.

$P\ \frac{1}{2}(3,\ 1)$

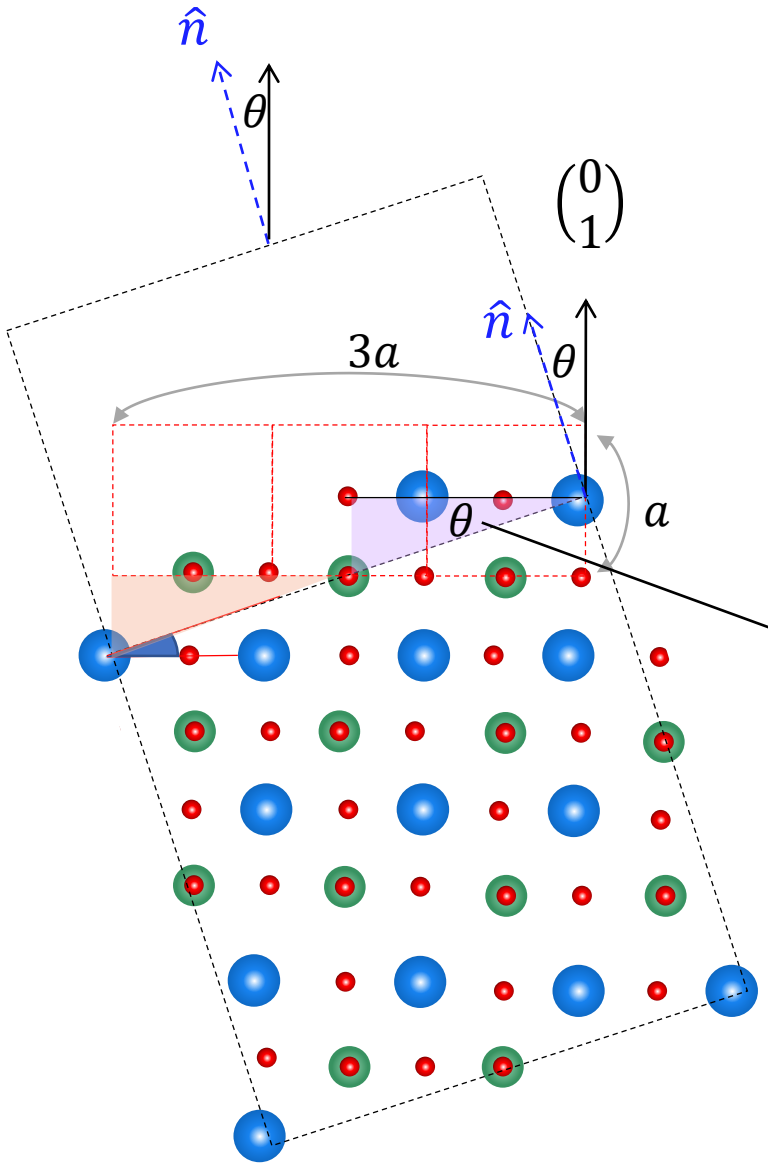

$$\begin{pmatrix}\cos(\theta) & -\sin(\theta)\\ \sin(\theta) & \cos(\theta)\end{pmatrix}\begin{pmatrix}0\\1\end{pmatrix}=\begin{pmatrix}-\sin(\theta)\\ \cos(\theta)\end{pmatrix}\hat{n}$$

$$tan(\theta)=\frac{1}{3}$$

Computational Physics & Materials Design Lab.

$P\ \frac{1}{2}(3,\ 1)$

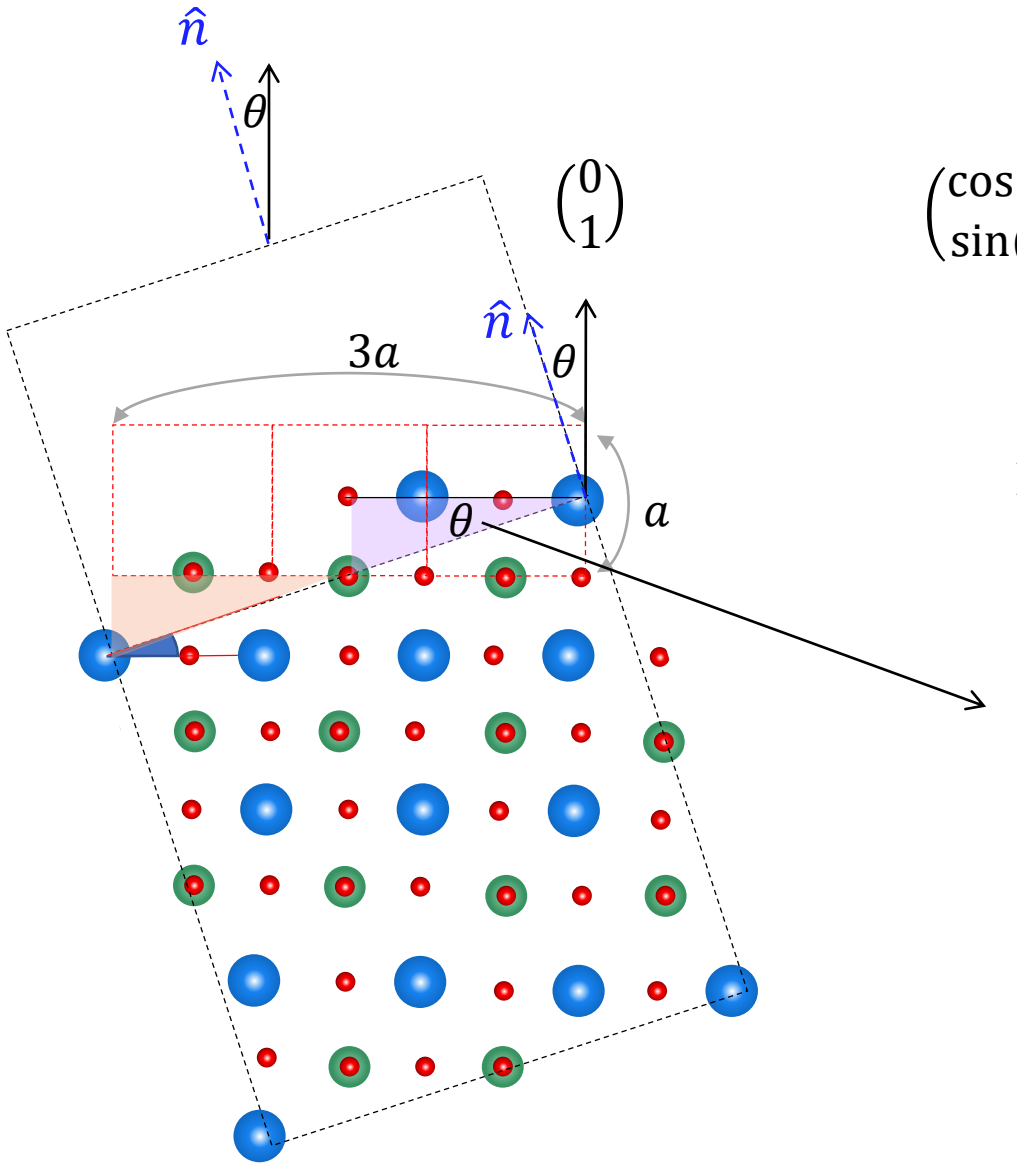

$$\begin{pmatrix}\cos(\theta) & -\sin(\theta)\\ \sin(\theta) & \cos(\theta)\end{pmatrix}\begin{pmatrix}0\\1\end{pmatrix}=\begin{pmatrix}-\sin(\theta)\\ \cos(\theta)\end{pmatrix}\ \hat{n}$$

$$\mathrm{P}\cdot n=\frac{1}{2}[\,-3\sin(\theta)+\cos(\theta)]$$

$$tan(\theta)=\frac{1}{3}$$

Computational Physics & Materials Design Lab.

$P\ \frac{1}{2}(3,\ 1)$

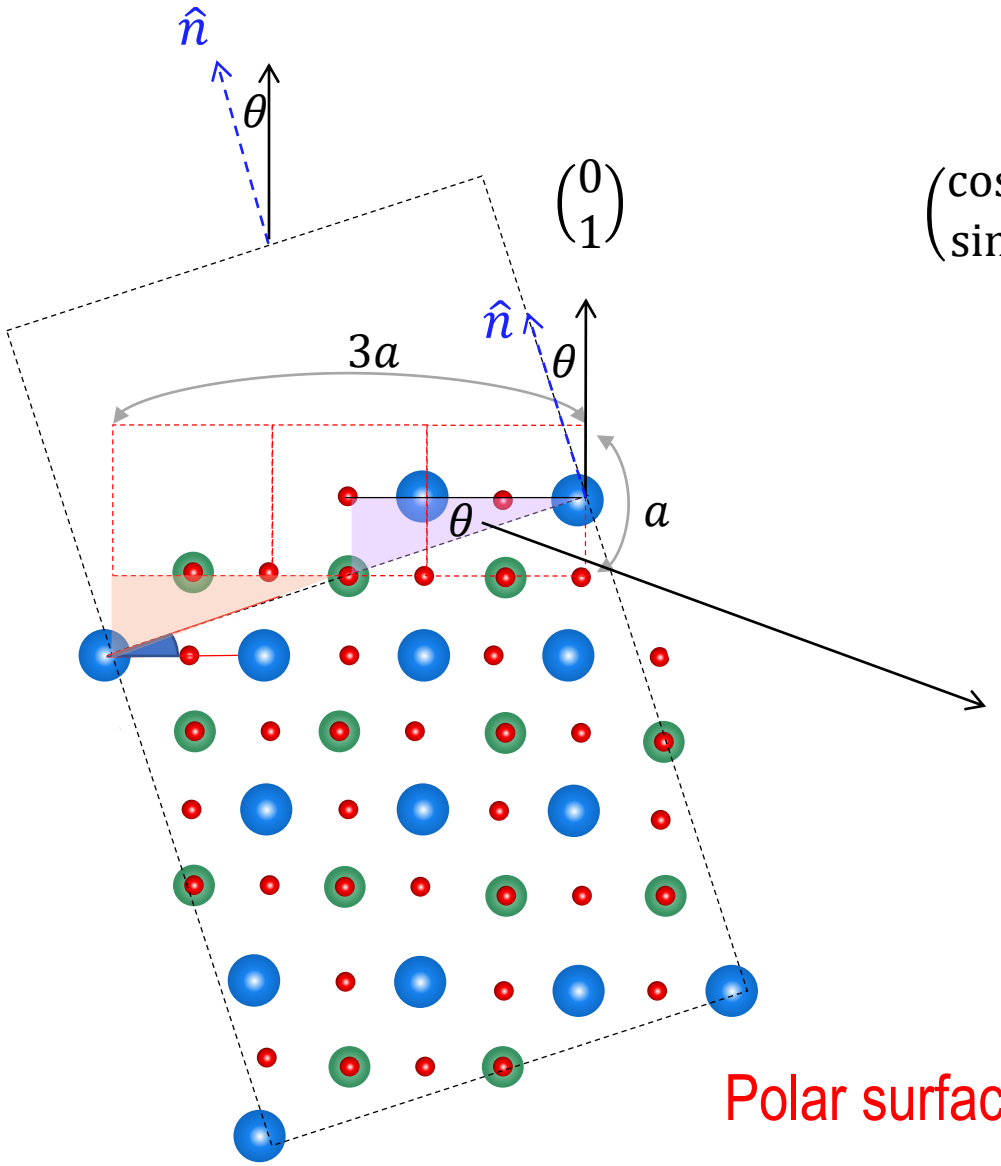

$$\begin{pmatrix}\cos(\theta) & -\sin(\theta)\\ \sin(\theta) & \cos(\theta)\end{pmatrix}\begin{pmatrix}0\\1\end{pmatrix}=\begin{pmatrix}-\sin(\theta)\\ \cos(\theta)\end{pmatrix}\ \hat{n}$$

$$\mathrm{P}\cdot n=\frac{1}{2}[\,-3\sin(\theta)+\cos(\theta)]$$

$$tan(\theta)=\frac{1}{3}$$

$$\mathrm{P}\cdot n=0$$

Polar surface stabilization without charge compensation

M. Stengel, *Phys. Rev. B* **84**, 205432 (2011)

P

$\frac{1}{2}(3, 1)$

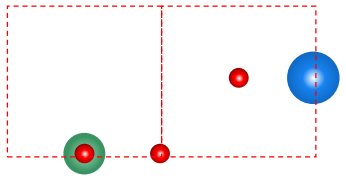

$tan(\theta)$:

1/3

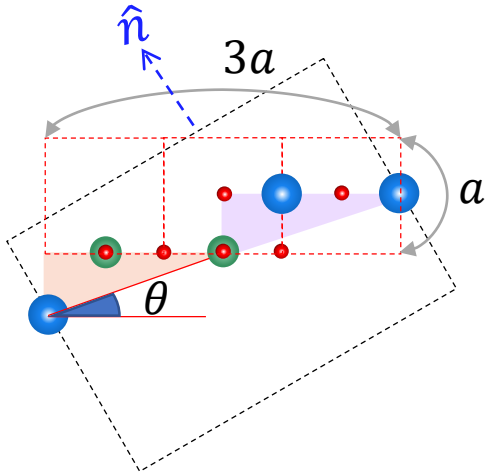

P

$\frac{1}{2}(3, 1)$

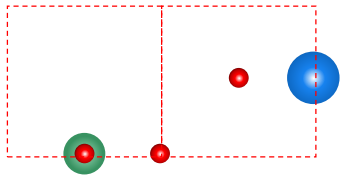

P

$\frac{1}{2}(5, 1)$

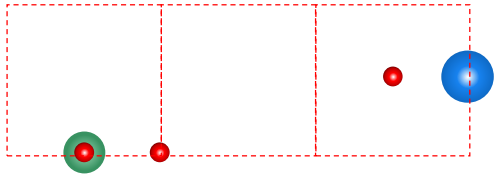

$tan(\theta)$:

1/3

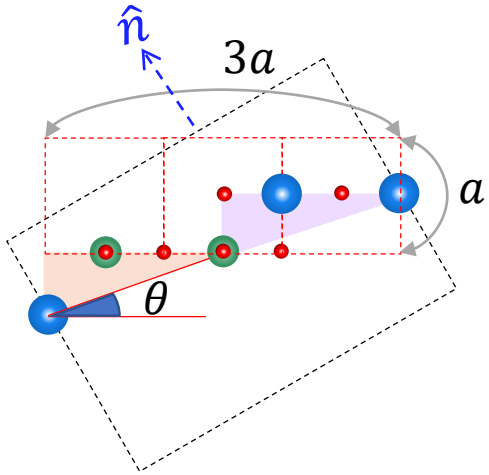

1/5

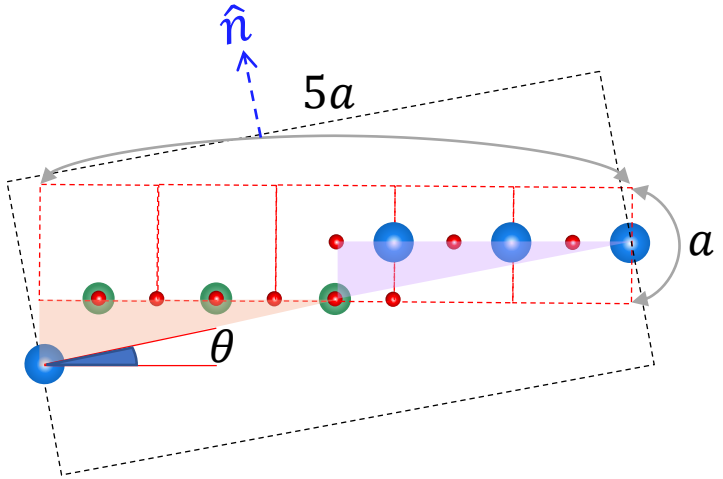

P

$\frac{1}{2}(3, 1)$

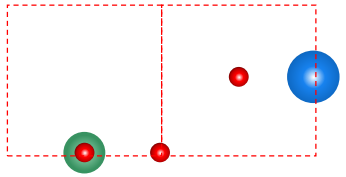

P

$\frac{1}{2}(5, 1)$

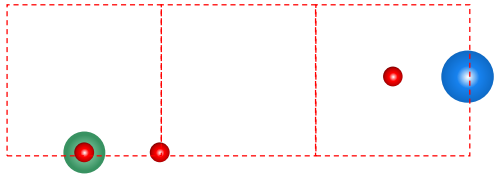

$\cdots$ $1/2\ (2k+1, 1)$

$$P \cdot n = 1/2\,[\,-(2k+1)\sin(\theta) + \cos(\theta)] = 0$$

$$tan(\theta) = \frac{1}{2k+1}$$

$tan(\theta)$:

$1/3$

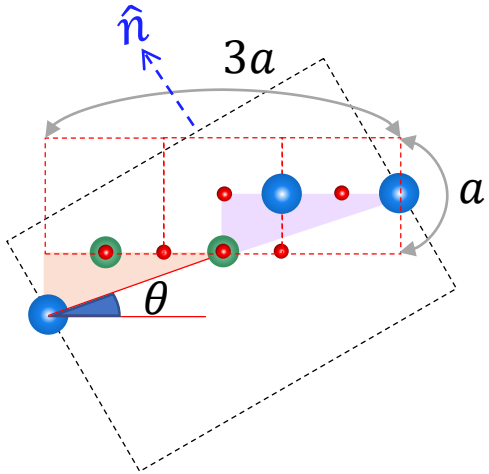

$1/5$ $\cdots$ $1/(2k+1)$

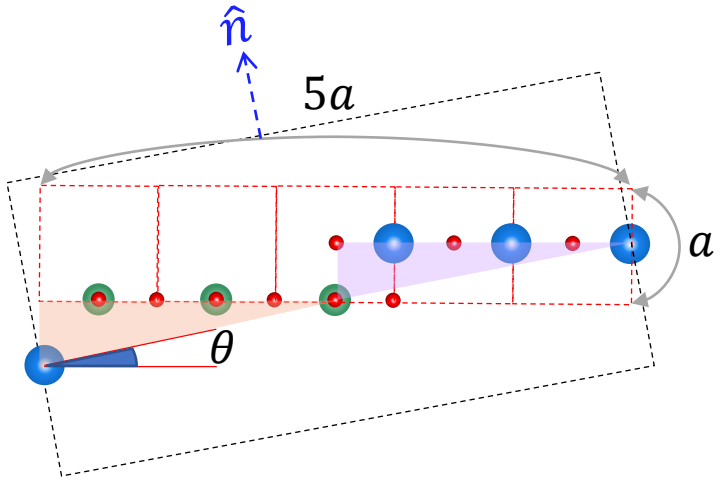

Stabilization of polarity without external charge in the vicinal surface structure

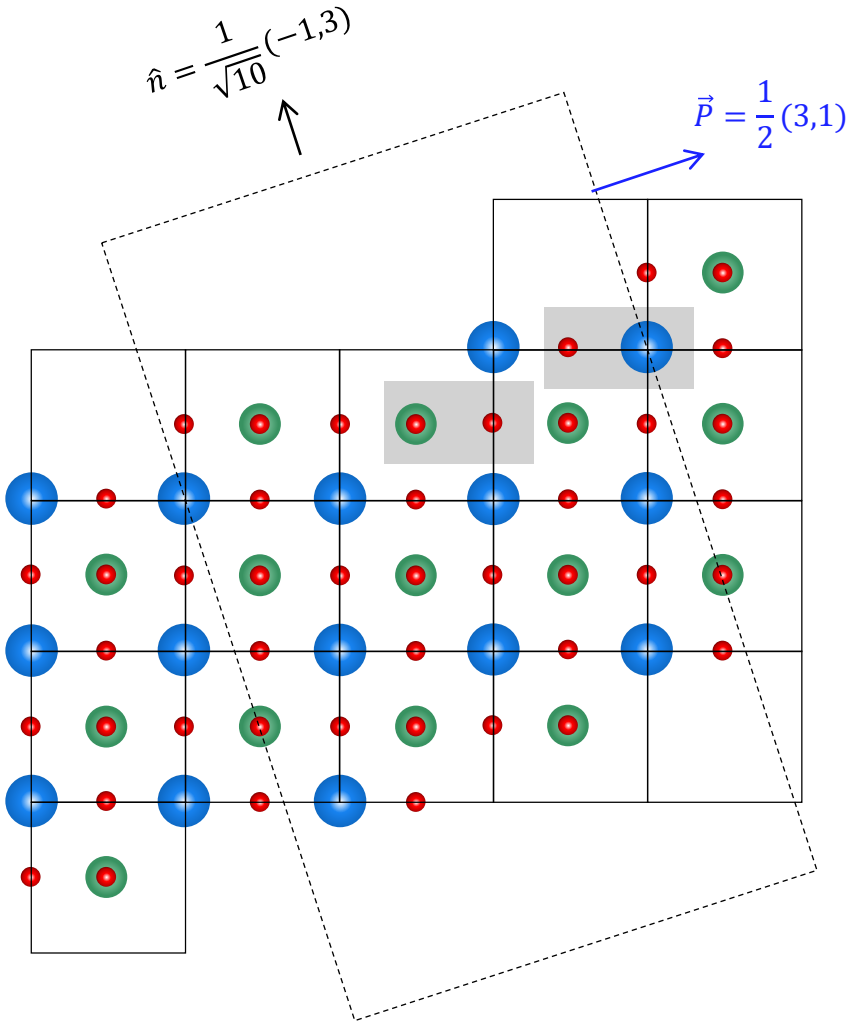

$$P_{LAO} \cdot \hat{n} = 0$$

Electrostatic potential calculation

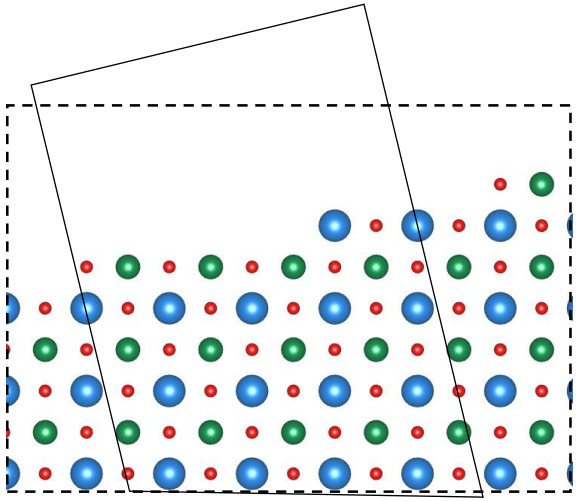

Fully relaxed
vicinal surface structure

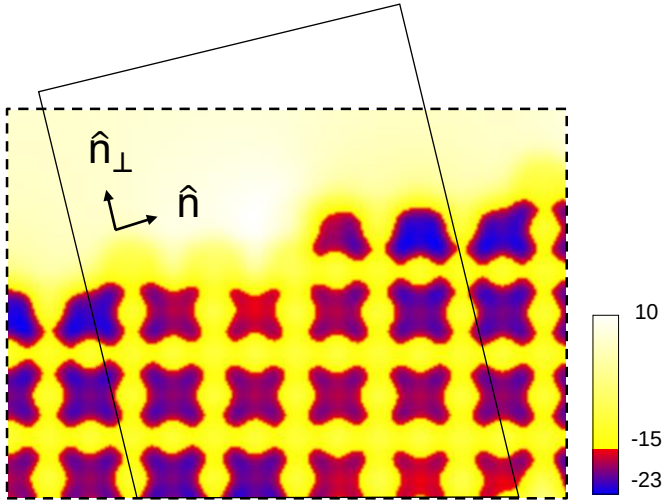

2D contour plot of
electrostatic potential

Line profile of electrostatic potential

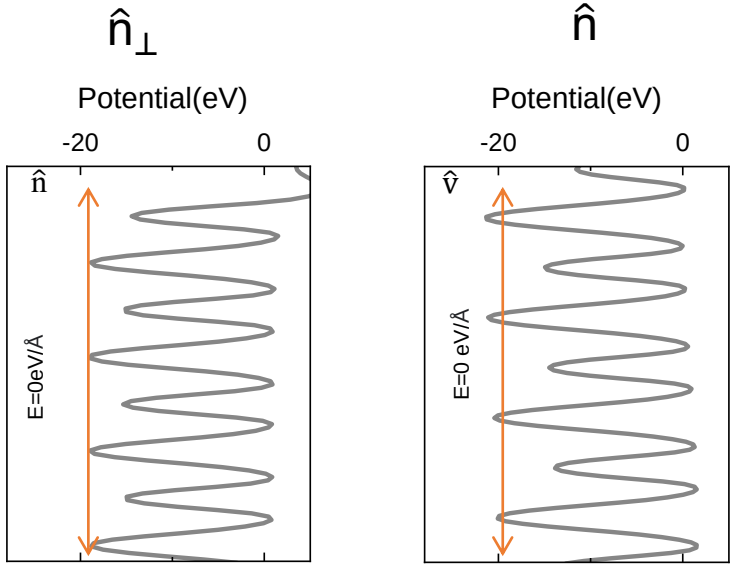

Vertical direction

Horizontal direction

$$V_{elect.}(x)$$

$$\left[-\frac{\hbar^2}{2m}\nabla^2 + e^2\int dx'\frac{\rho(x')}{|\mathbf{r}-\mathbf{r}'|} + u(x) + V_{\mathrm{XC}}(x) - \varepsilon_\alpha\right]\varphi_\alpha(x) = 0\ .$$

Magnetoelectric effect in FM/FE

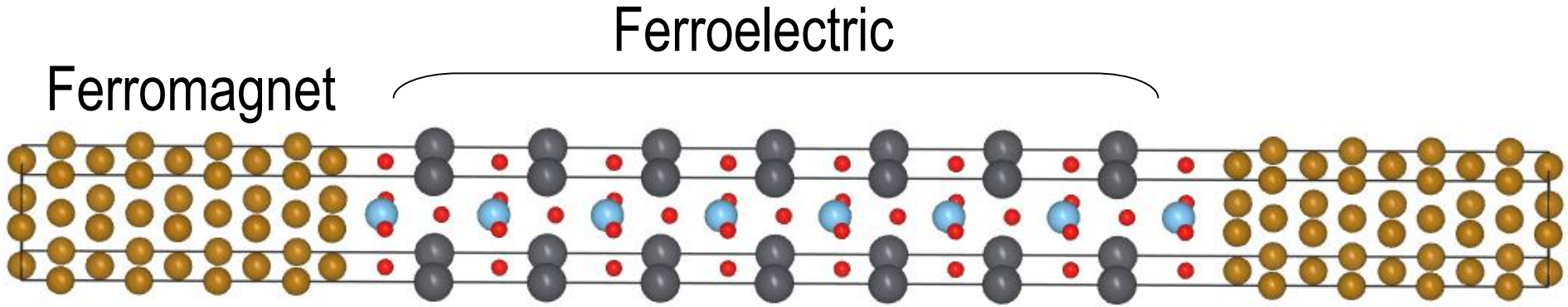

Jaekwang Lee
Dept. of Physics, PNU, Rep. of Korea

부산대학교
PUSAN NATIONAL UNIVERSITY

Magnetoelectric effect $\longrightarrow$ $\mu_0 M = \alpha E$

Ferroelectric (FE)



$P=\varepsilon_0 \chi_E E$

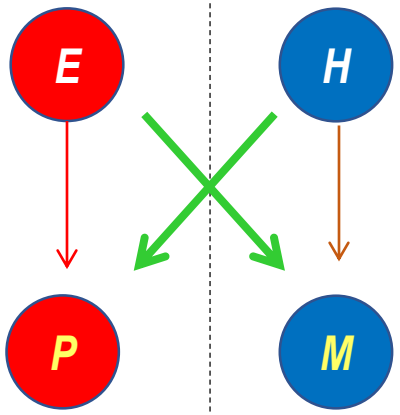

Ferromagnet (FM)

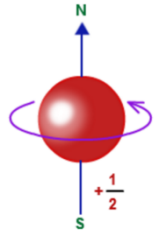

$M=\chi_M H$

$P=\varepsilon_0 \chi_E E+ \alpha H$

$\mu_0 M=\alpha E + \mu_0 \chi_M H$

: cross coupled response to electric and magnetic fields

Weak FE-FM coupling: Physics

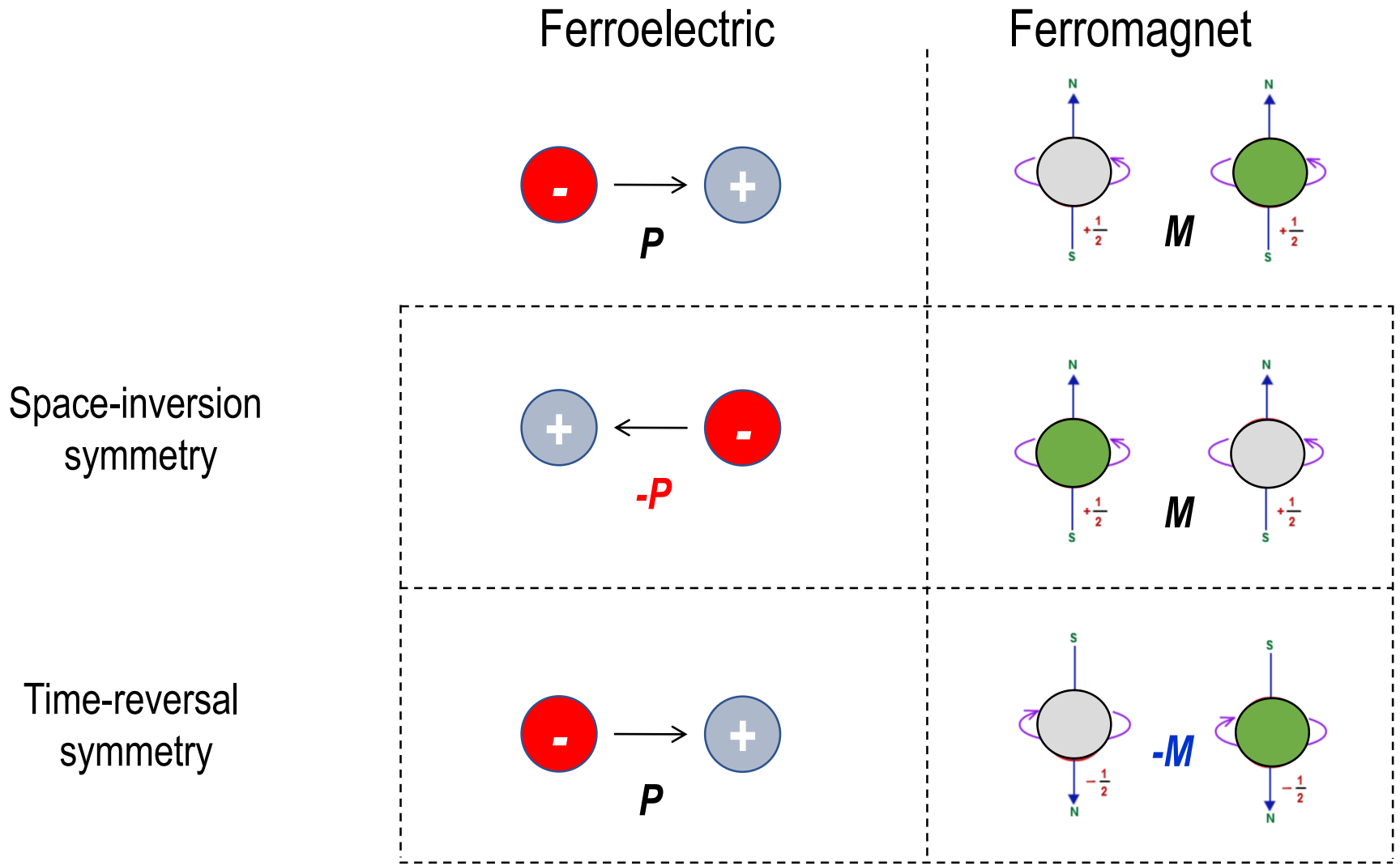

Weak FE-FM coupling: Chemistry

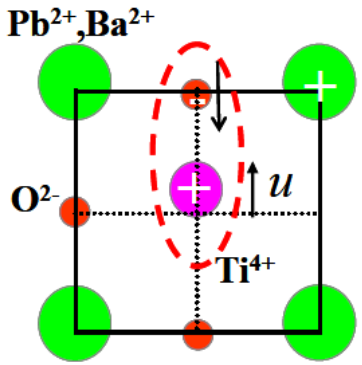

$$\delta E \sim -\left(\frac{\left(t_{pd}\left(1+gu\right)\right)^2}{\Delta} + \frac{\left(t_{pd}\left(1-gu\right)\right)^2}{\Delta} \right) + \frac{2t_{pd}^2}{\Delta} = -\frac{2t_{pd}^2\left(gu\right)^2}{\Delta}$$

$$\delta E_{elastic} \sim Bu^2$$

d^0-rule

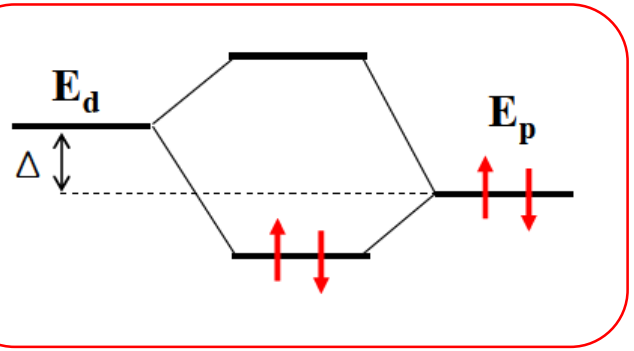

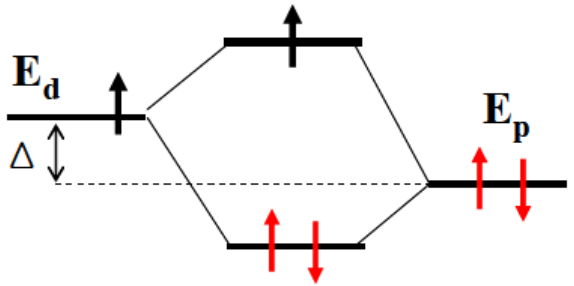

Hill, N.A., *Why Are There so Few Magnetic Ferroelectrics?* The Journal of Physical Chemistry B, 2000. **104**(29): p. 6694-6709.

Strong FE-FM coupling in heterostructure ?

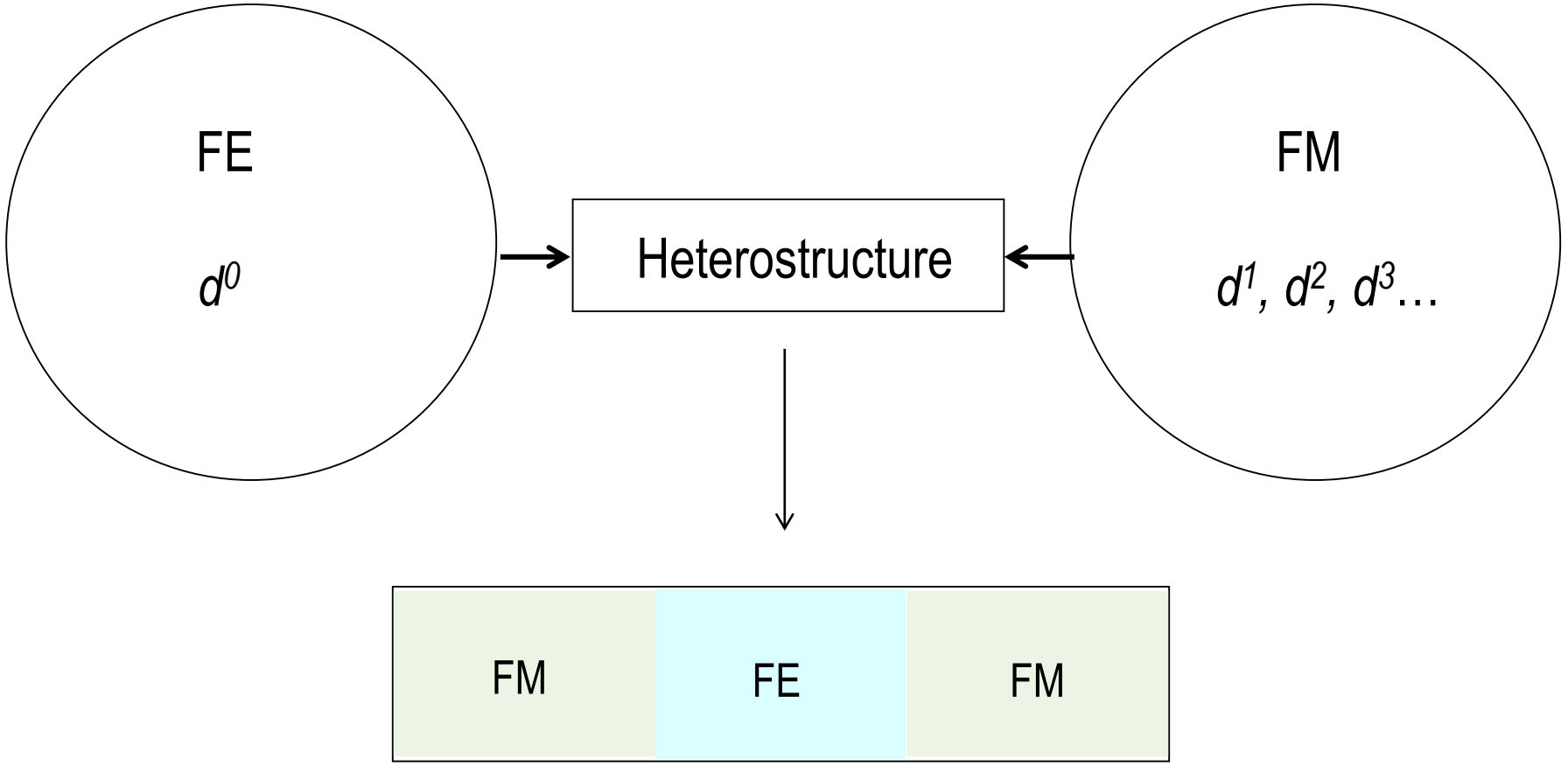

Magnetoelectric effect in oxide superlattice

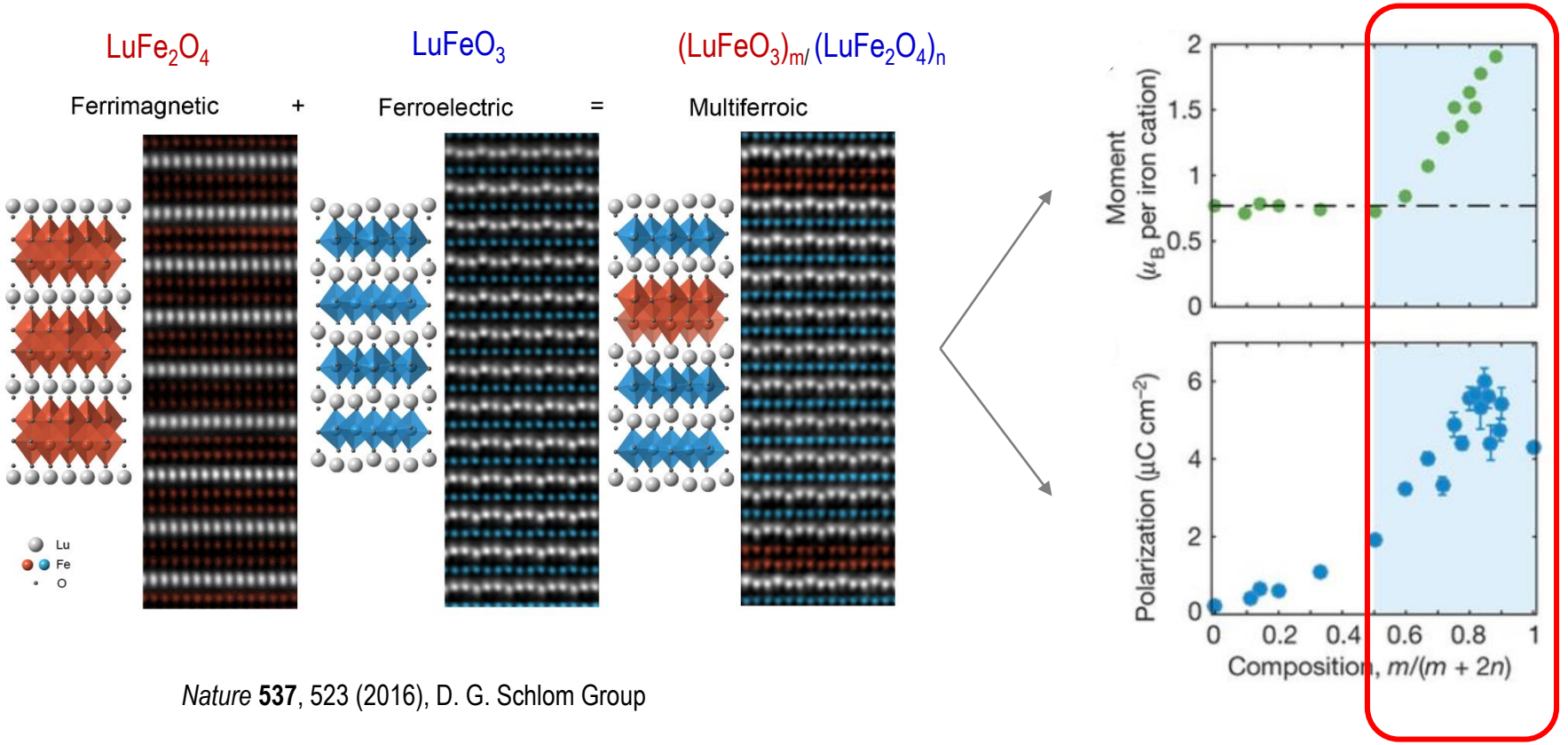

Nature **537**, 523 (2016), D. G. Schlom Group

Science **347**, 420 (2015): M. J. Rosseinsky Group

Nature **523**, 363 (2015): M. J. Rosseinsky Group

Nature **516**, 370 (2014): D. G. Schlom Group

Advances in magnetoelectric multiferroics

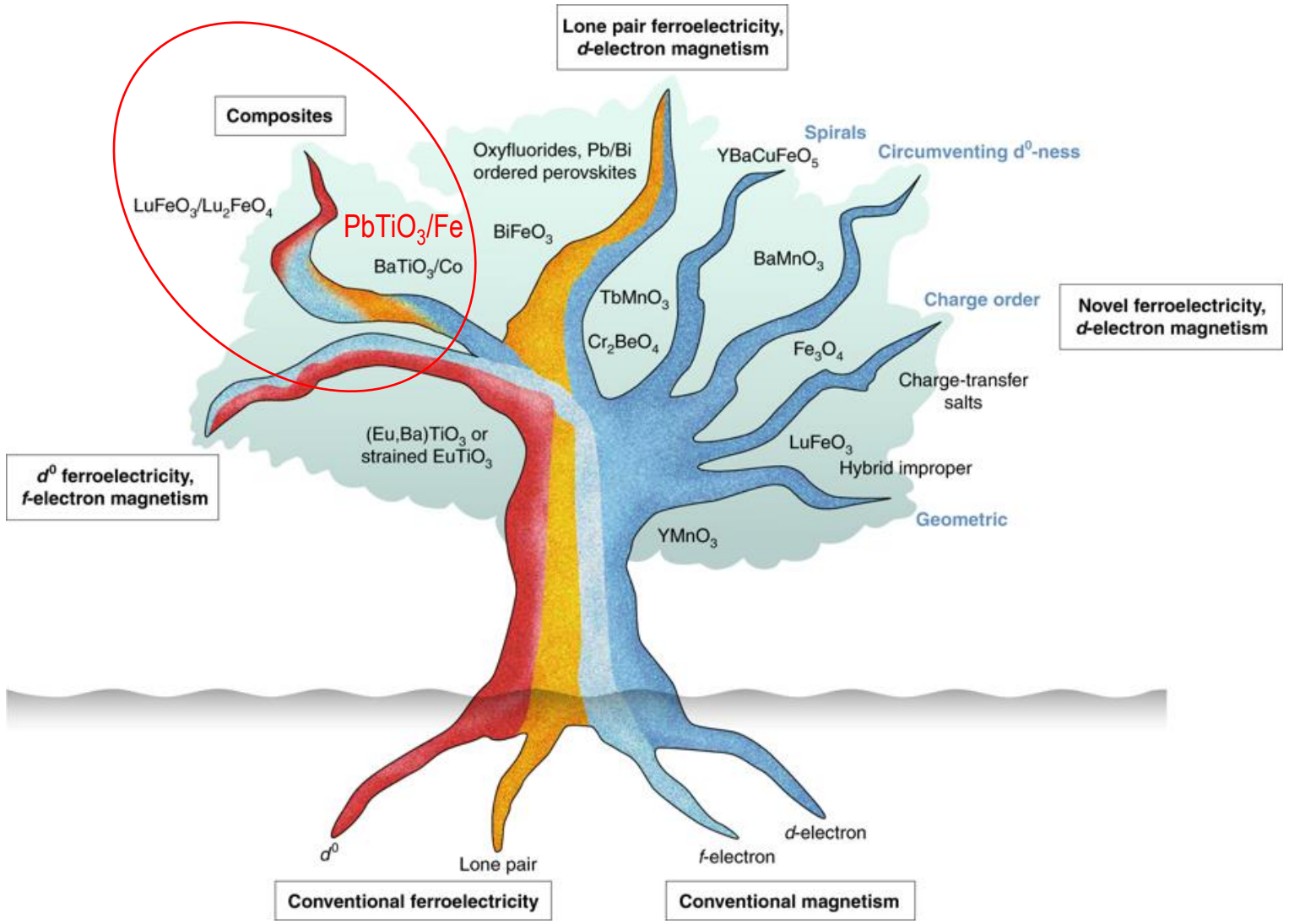

N. A. Spaldin, R. Ramesh, Nature materials **18**, 203 (2019)

Depolarizing field (E_d)

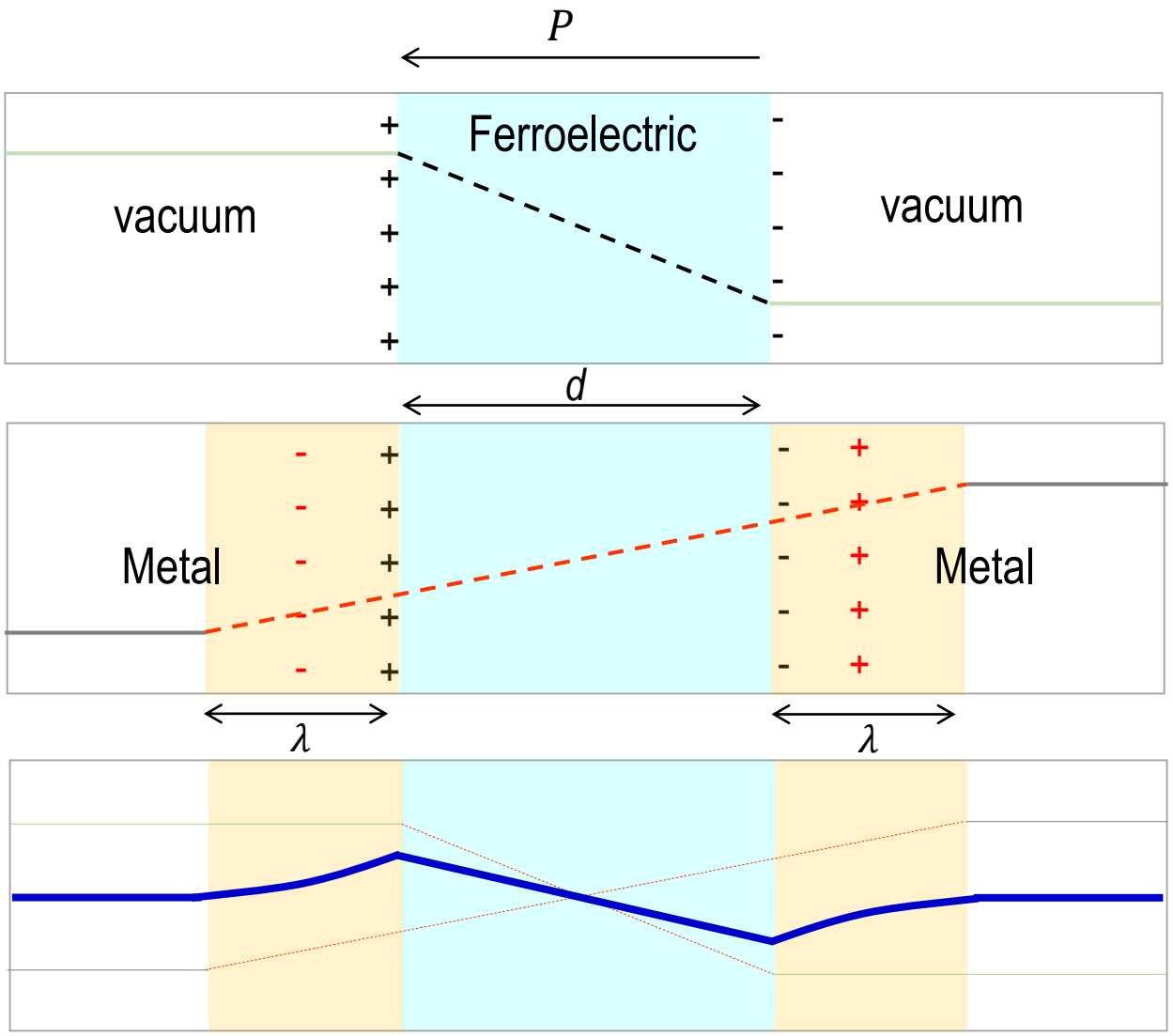

$$D=\varepsilon_0 E^{bare}+P=0$$

$$E^{bare}=-\left(\frac{P}{\varepsilon_0}\right)$$

$$E^{bare}d+E^{com}(d+2\lambda)=0$$

$$E^{com}=\frac{d}{d+2\lambda}\left(\frac{P}{\varepsilon_0}\right)$$

$$E_d=E^{bare}+E^{com}$$

Depolarizing field (E_d)

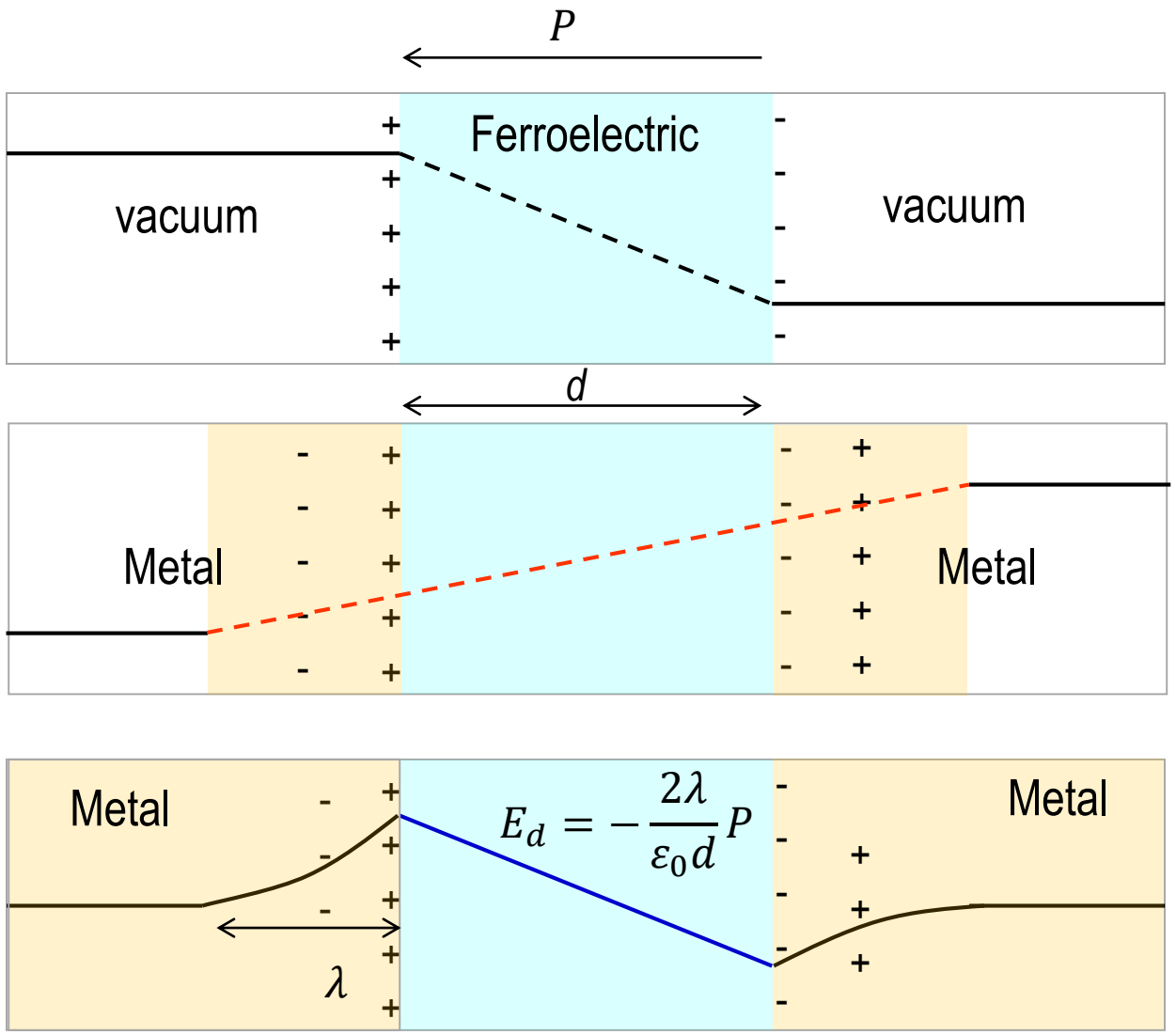

$$E^{bare} = -\left(\frac{P}{\varepsilon_0}\right)$$

$$E^{com} = \frac{d}{d + 2\lambda}\left(\frac{P}{\varepsilon_0}\right)$$

$$E_d = E^{bare} + E^{com}$$

$$= -\frac{2\lambda}{\varepsilon_0 d} P$$

E_d=0 for perfect screening

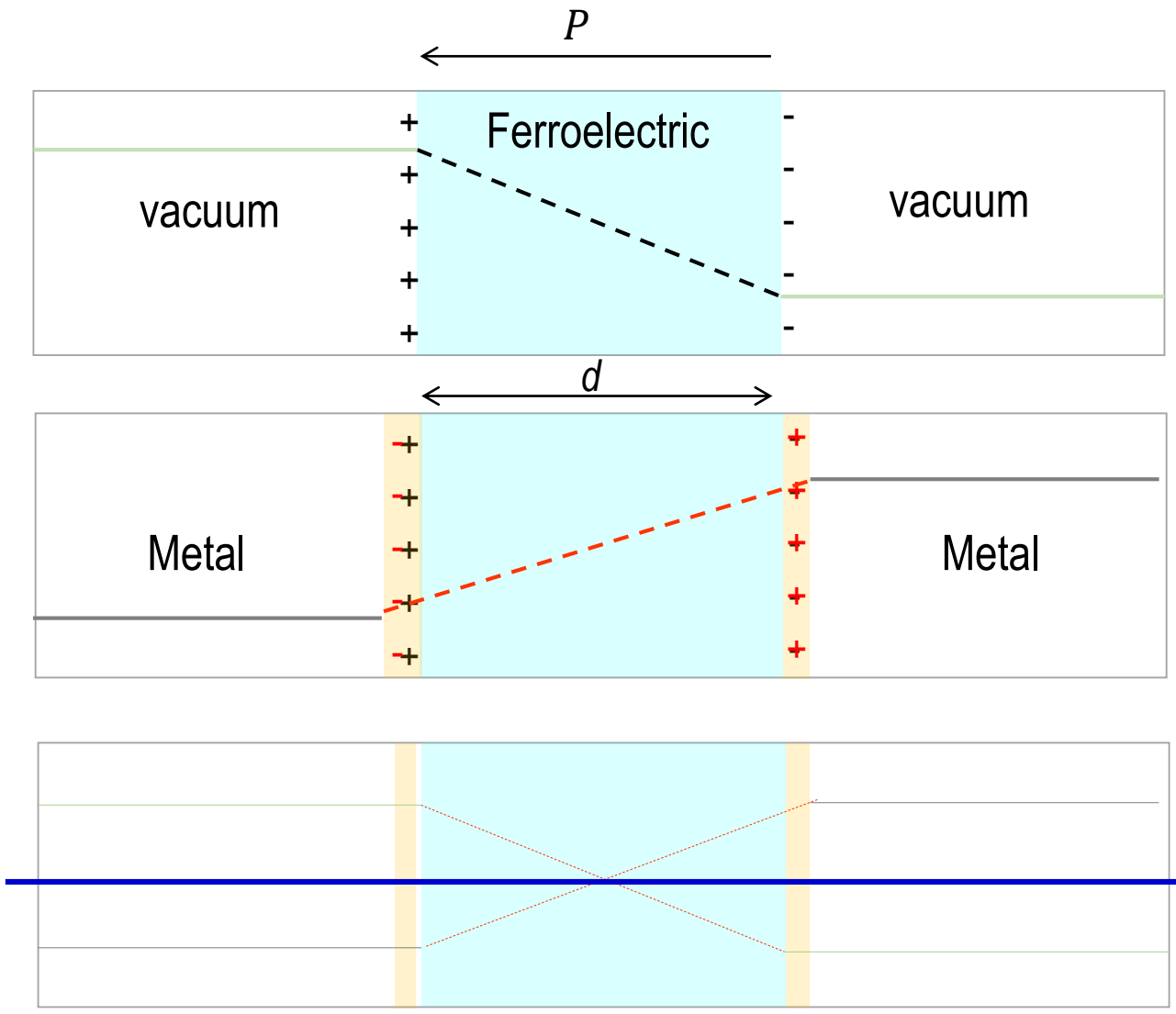

$$D=\varepsilon_0 E^{bare}+P=0$$

$$E^{bare}=-\left(\frac{P}{\varepsilon_0}\right)$$

$$E^{bare}d+E^{com}d=0$$

$$E^{com}=-E^{bare}$$

$$E^{bare}+E^{com}=0$$

Magnetoelectric effect in FM/FE/FM heterostructure

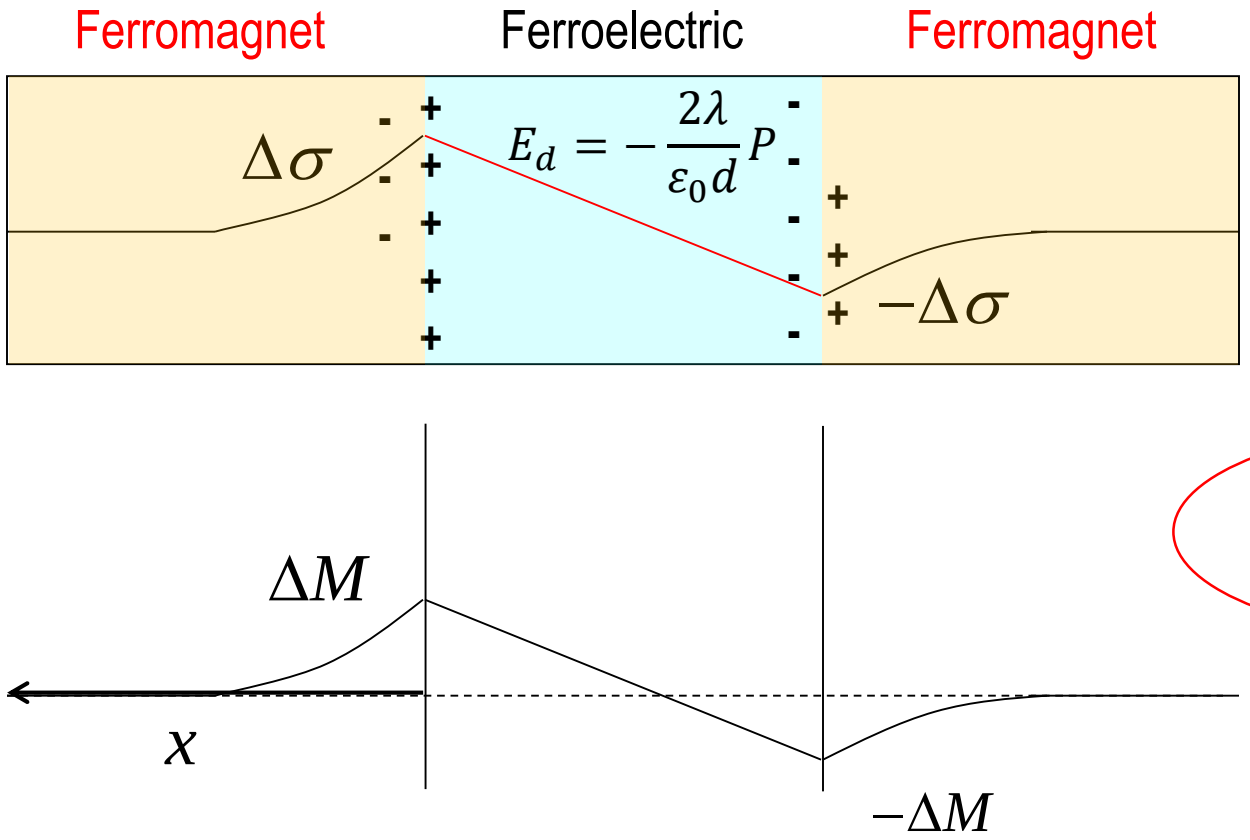

$$\mu_0 \Delta M = \alpha E_d$$

At the interface between FM and FE, the electron screening is spin dependent and therefore simultaneously induce magnetization ΔM, -ΔM on each surface

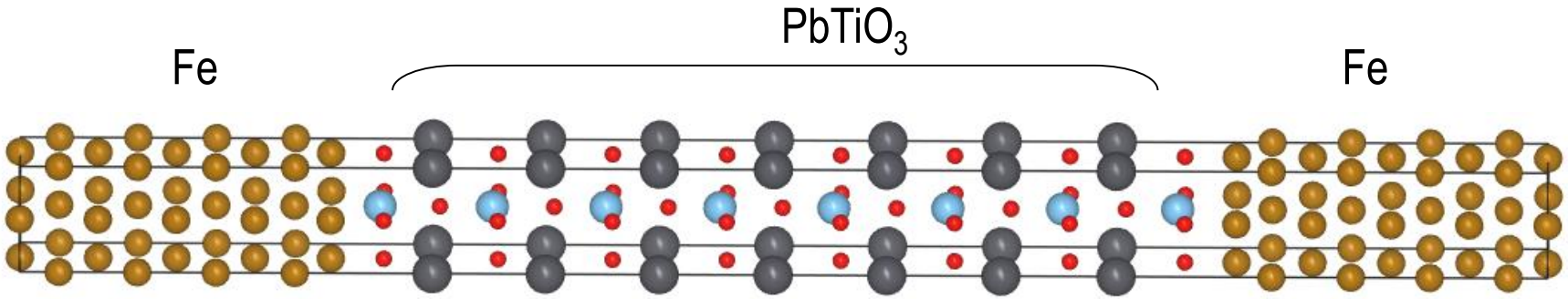

$\mu_0 \Delta M = \alpha E_d$

E_d : depolarizing field

ΔM : magnetization change

Free energy across the FE phase transition

$$f(P,T) = f(-P,T) = \frac{1}{2} g_2 P^2 + \frac{1}{4} g_4 P^4$$

$$g_2 = \frac{(T - T_c)}{C}, \quad g_4 > 0$$

even power series of *P*

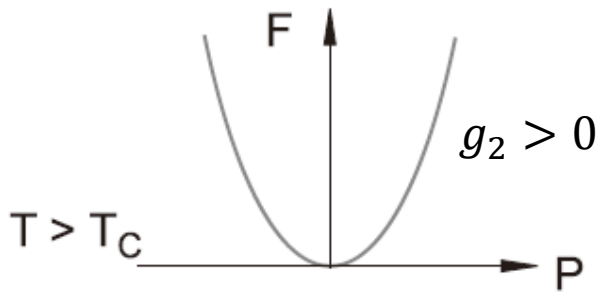

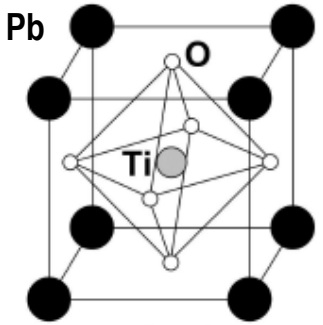

Paraelectric

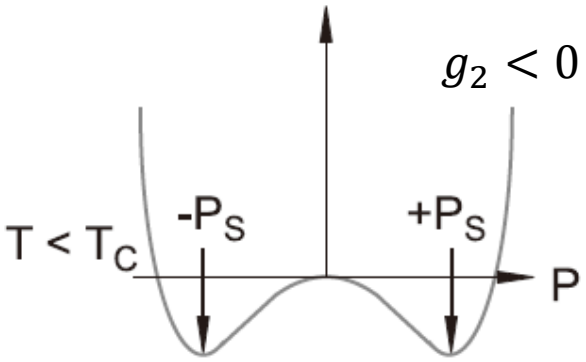

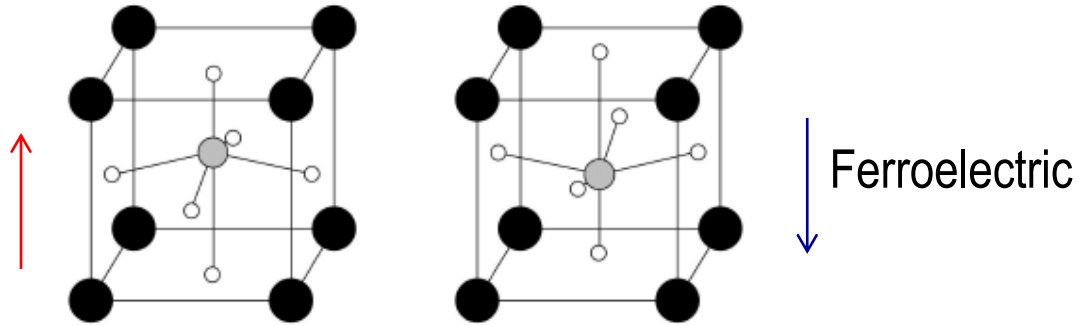

$P = +P_s$ $P = -P_s$

Ferroelectric

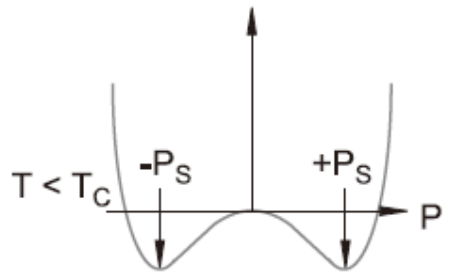

$$f(P,T)=\frac{1}{2}g_2P^2+\frac{1}{4}g_4P^4$$

$$\frac{\partial f}{\partial P}=P\left(g_2+g_4P^2\right)=0$$

$$P_s=\sqrt{-\frac{g_2}{g_4}} \qquad g_4P_s^2=-g_2$$

$$f(P,T)=-\frac{1}{2}g_4P_s^2P^2+\frac{1}{4}g_4P^4$$

$$=\frac{1}{4}g_4\left(-2P_s^2P^2+P^4\right)$$

$$\frac{P}{P_s}=\xi \quad P=P_s\xi \qquad (0\le\xi\le1)$$

$$f(\xi)=\frac{1}{4}g_4P_s^4(\xi^4-2\xi^2)=f_0(\xi^4-2\xi^2)$$

Simplified free energy expression for FE phase

FE thickness dependent free energy under the E_d

$$g(P,T) = \frac{1}{2}g_2P^2 + \frac{1}{4}g_4P^4 - \int E_d P dV$$

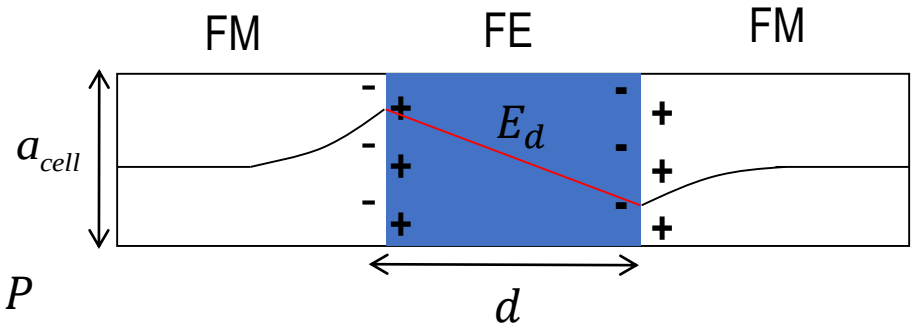

$$E_d = -\frac{2\lambda}{\varepsilon_0 d}P$$

$$\downarrow$$

$$g(P,T) = \frac{1}{4}g_4P^4 + \frac{1}{2}g_2P^2 + V\frac{2\lambda}{\varepsilon_0 d}P^2$$

$$\downarrow$$

$$g(\xi,T) = c\left(\xi^4 - 2\xi^2 + \frac{2m_c}{m}\xi^2\right)$$

$$P = P_s\xi$$

$$m_c = \frac{\lambda P_s^2 a_{cell}^2}{f_0\varepsilon_0}$$

$$g(\xi) = mf(\xi) - \int E_d P d\,V$$

$$g(\xi) = mf(\xi) + \frac{2\lambda P^2}{\varepsilon_0 d} V$$

$$P = P_s \xi, \quad V = d a_{cell}^2$$

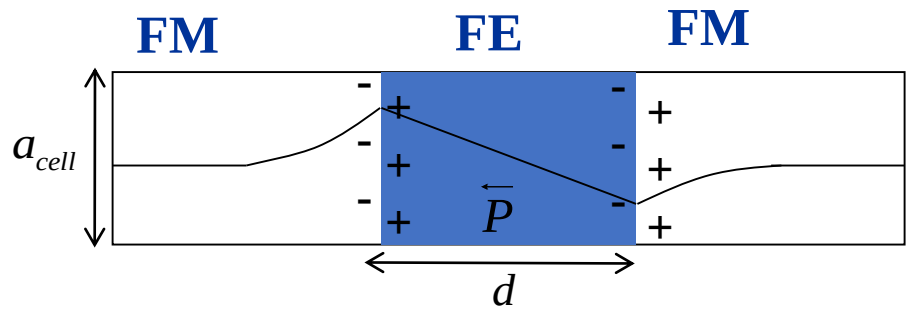

$$E_d = -\frac{2\lambda}{\varepsilon_0 d} P$$

$$g(\xi) = mf_0(\xi^4 - 2\xi^2) + \left(\frac{2\lambda P_s^2 a_{cell}^2}{\varepsilon_0}\right)\xi^2$$

$$g(\xi) = c\left(\xi^4 - 2\xi^2 + \frac{2}{m}\frac{\lambda P_s^2 a_{cell}^2}{f_0 \varepsilon_0}\xi^2\right)$$

$$g(\xi) = c\left(\xi^4 - 2\xi^2 + \frac{2m_c}{m}\xi^2\right) \qquad m_c = \frac{\lambda P_s^2 a_{cell}^2}{f_0 \varepsilon_0}$$

FE thickness dependent free energy (m_c=2)

$$: \xi^4 - 2\xi^2 + \frac{2m_c}{m}\xi^2$$

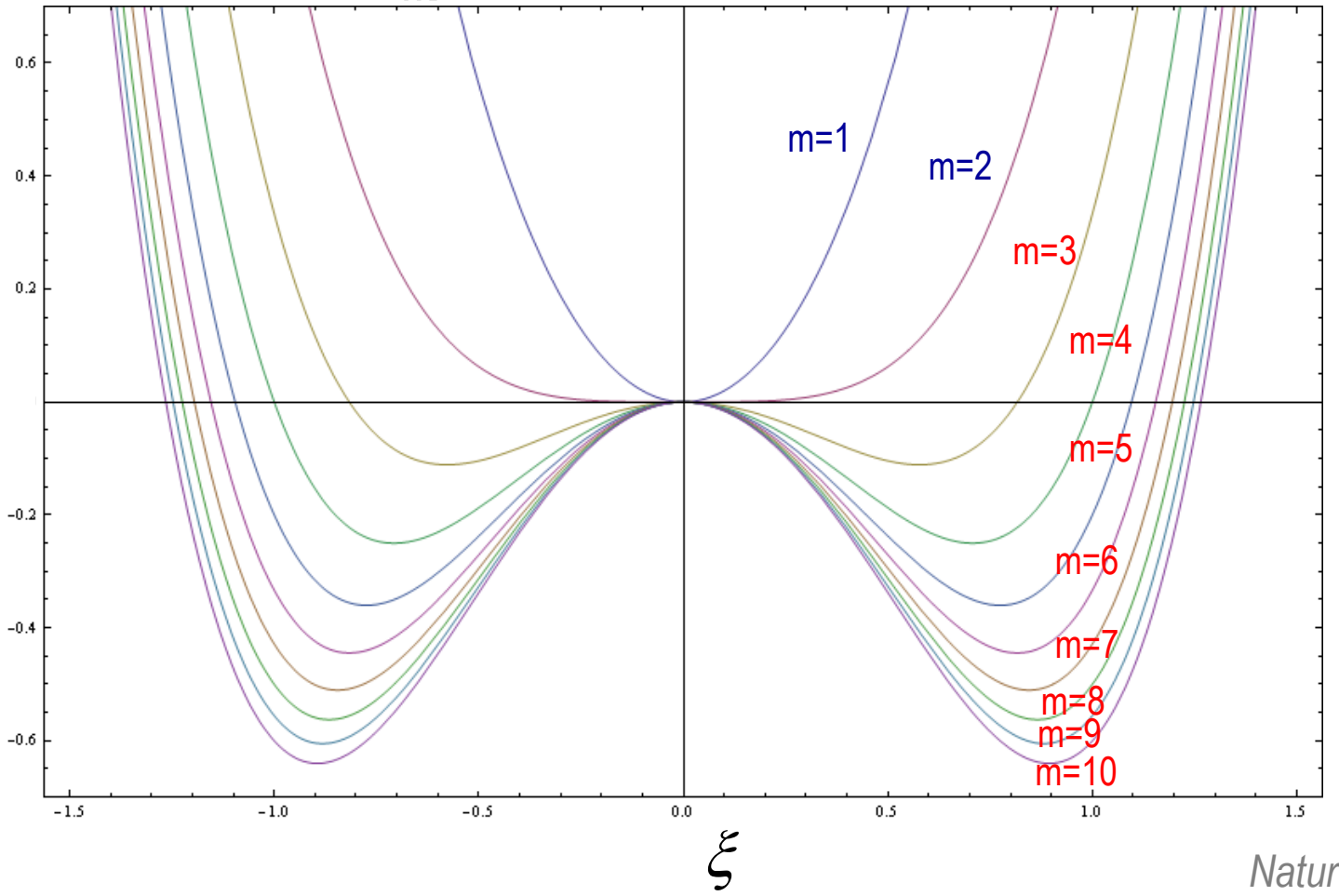

$m \leq m_c$

PE

FE

$m > m_c$

Nature **422**, 506-509

$$m_c = 6$$

$$: \xi^4 - 2\xi^2 + \frac{2m_c}{m}\xi^2$$

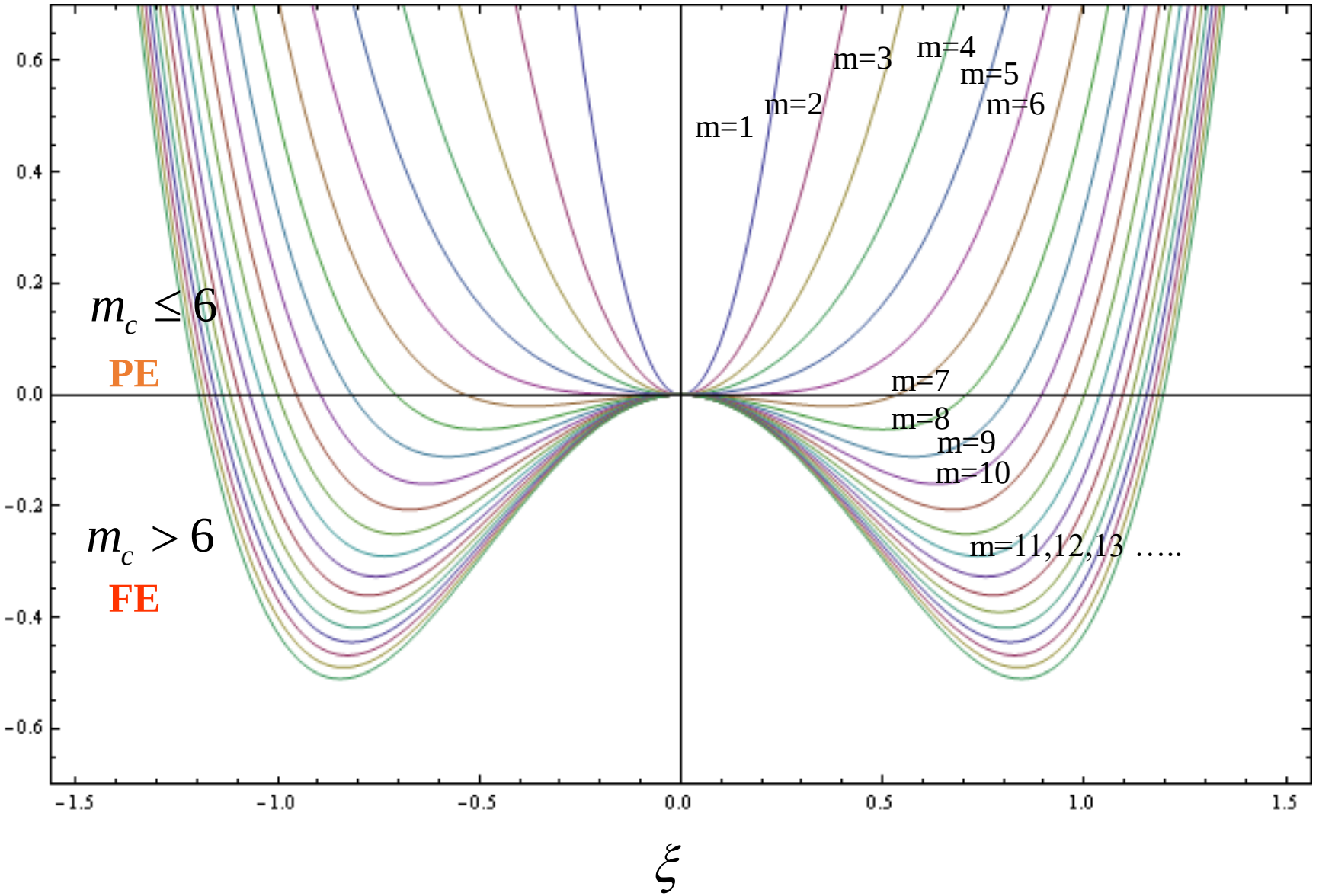

The free energy minimum

$$u(\xi) = \xi^4 - 2\xi^2 + \frac{2m_c}{m}\xi^2$$

$$u'(\xi) = 4\xi^3 - 4\xi + \frac{4m_c}{m}\xi$$

$$= 4\xi(\xi^2 - 1 + \frac{m_c}{m}) = 0$$

$$\xi = \pm\sqrt{1 - \frac{m_c}{m}}$$

FE thickness dependent free energy minima (m_c=2)

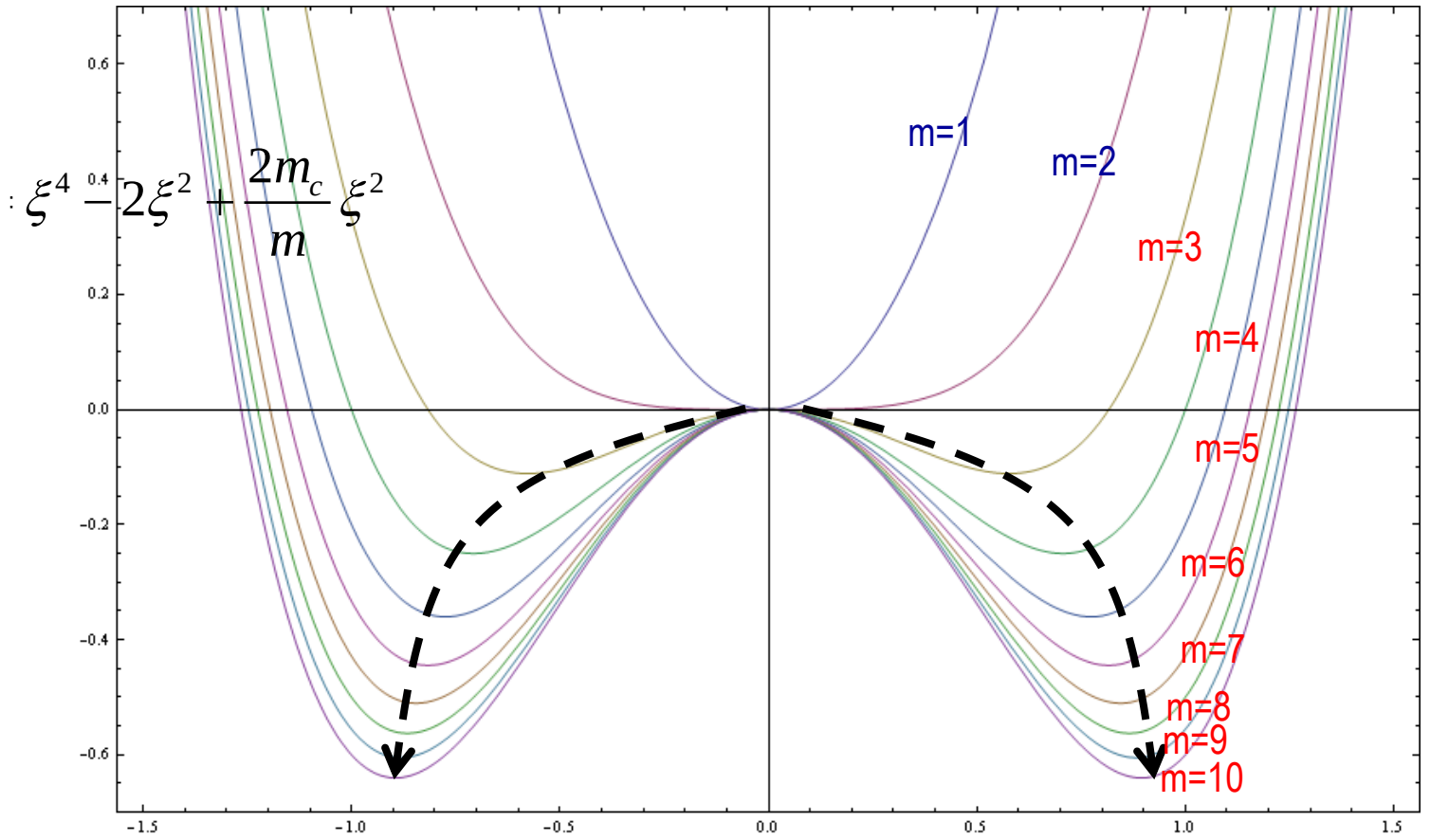

$m \leq m_c$

PE

FE

$m > m_c$

$$\xi = -\sqrt{1 - \frac{m_c}{m}} \qquad \xi = +\sqrt{1 - \frac{m_c}{m}}$$

Nature **422**, 506-509

$$E_d = -\frac{2\lambda P}{\varepsilon_0 d} = -\left(\frac{2\lambda P_s}{\varepsilon_0 a_{cell}}\right)\frac{\xi}{m} = \frac{\Delta}{m}\sqrt{1-\frac{m_c}{m}} \qquad \Delta = \left(\frac{2\lambda P_s}{\varepsilon_0 a_{cell}}\right)$$

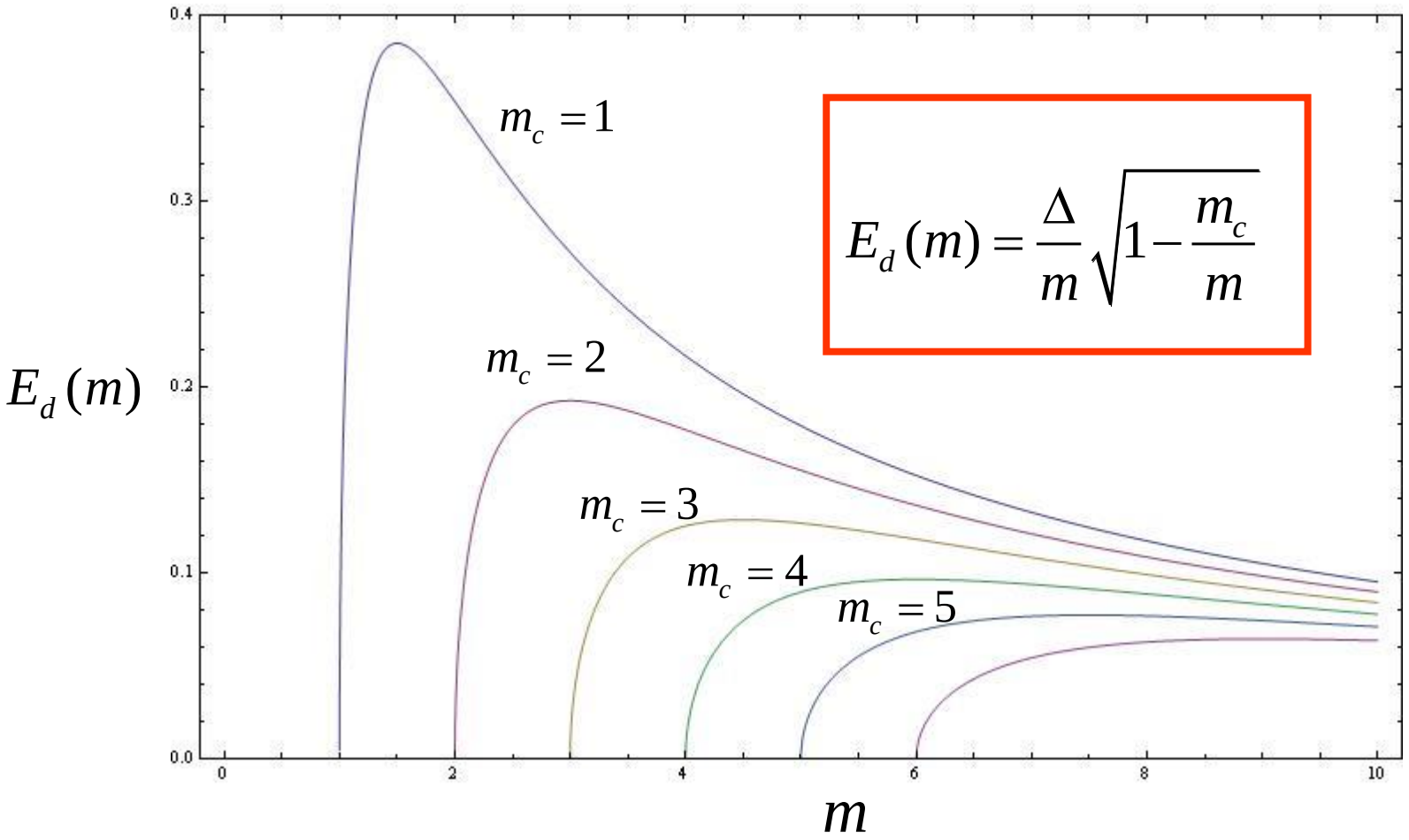

E_d calculation in Fe/PTO heterostructure

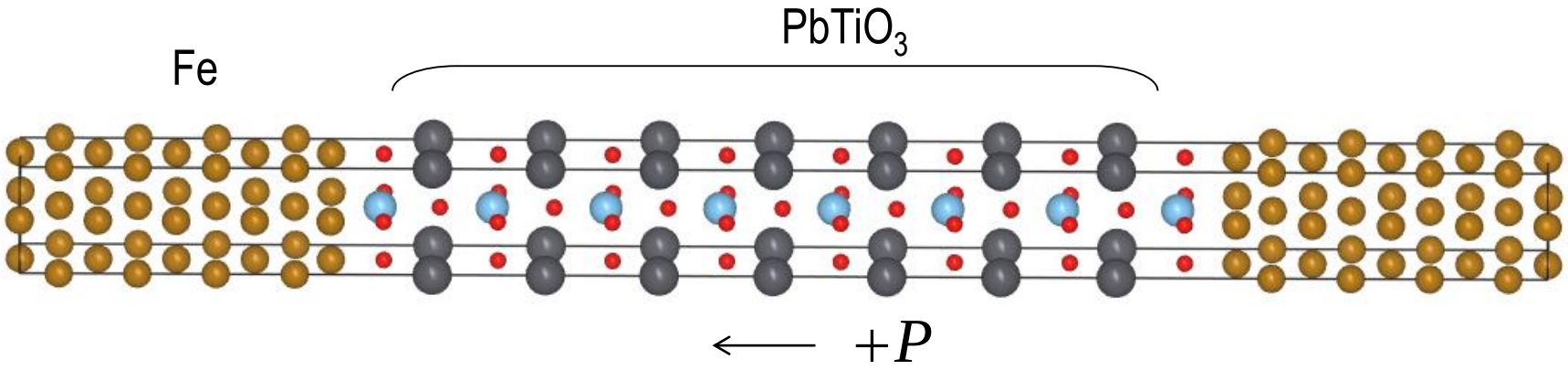

$$\left(-\frac{\hbar^2}{2m}\nabla^2 + v_{\text{ext}}(\mathbf{r}) + v^e_{\text{coul}}(\mathbf{r}) + v_{\text{xc}}(\mathbf{r})\right)\psi_{n\mathbf{k}}(\mathbf{r}) = \epsilon_{n\mathbf{k}}\psi_{n\mathbf{k}}(\mathbf{r})$$

Electrostatic potential

E_d in Fe/PTO heterostructure

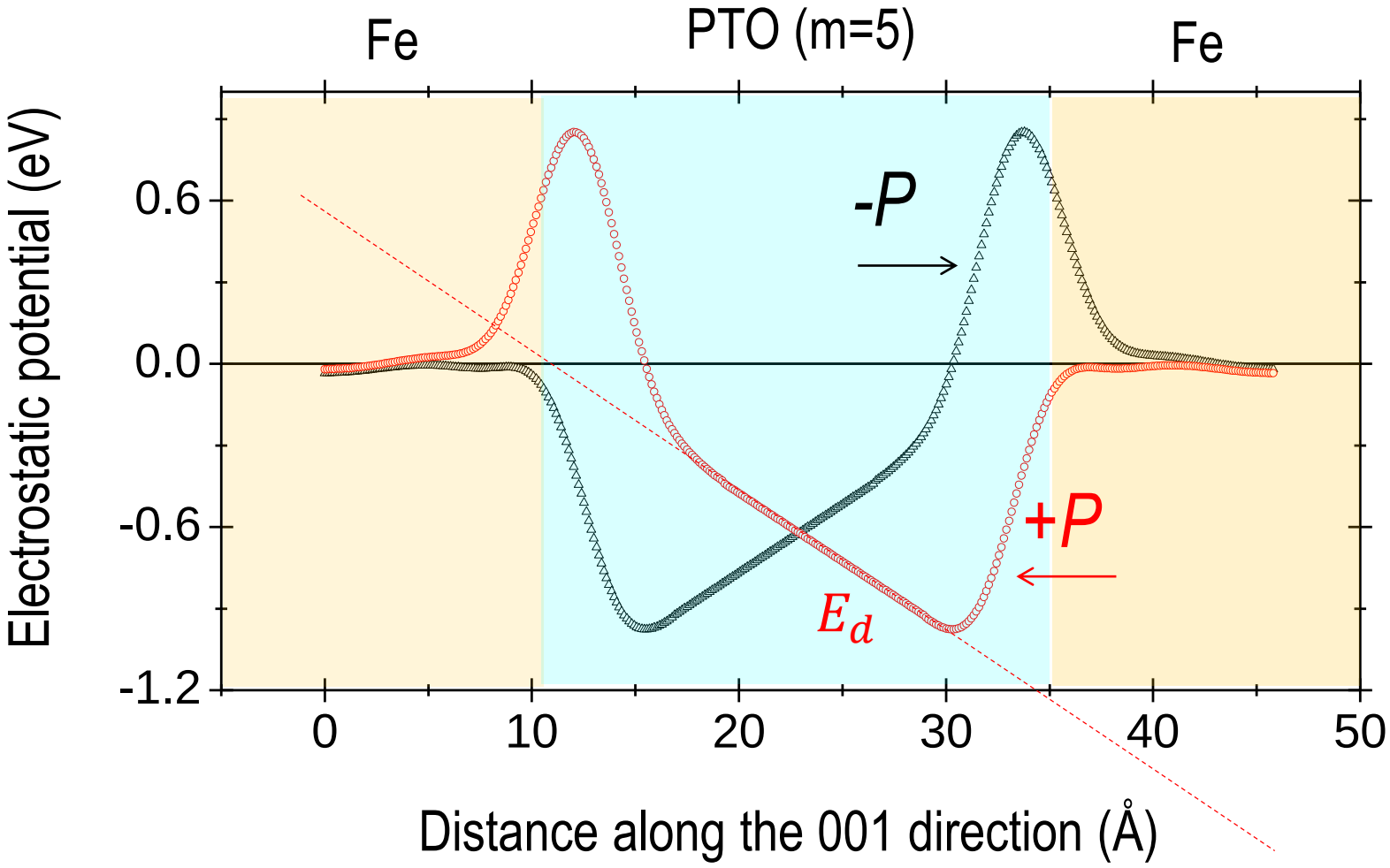

$E_d(m)$ in $Fe/(PTO)_m$ heterostructure

$$E_d = 0.32\frac{1}{m}\sqrt{1-\frac{2}{m}}$$

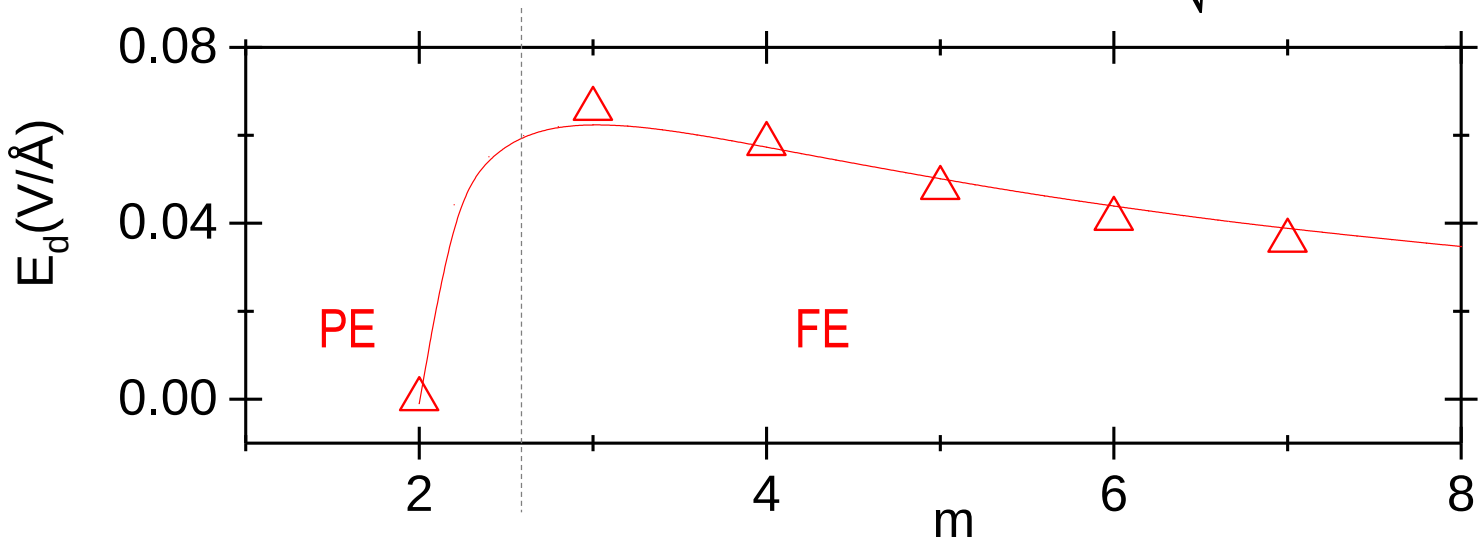

Critical thickness

Critical thickness of PTO in Fe/PTO/Fe

$$m_c = \frac{\lambda P_s^2 a_{cell}^2}{f_0 \varepsilon_0}$$

$\lambda \sim 0.24\text{Å}$

$P_s \sim \frac{0.6\ e}{a_{cell}{}^2}$ $\quad a_{cell} \sim 4\text{Å}$

$f_0 \approx 0.4\ eV$

$m_c = 2.4$

$m_c = 4.5$ $\quad$ $Fe/BaTiO_3/Fe$

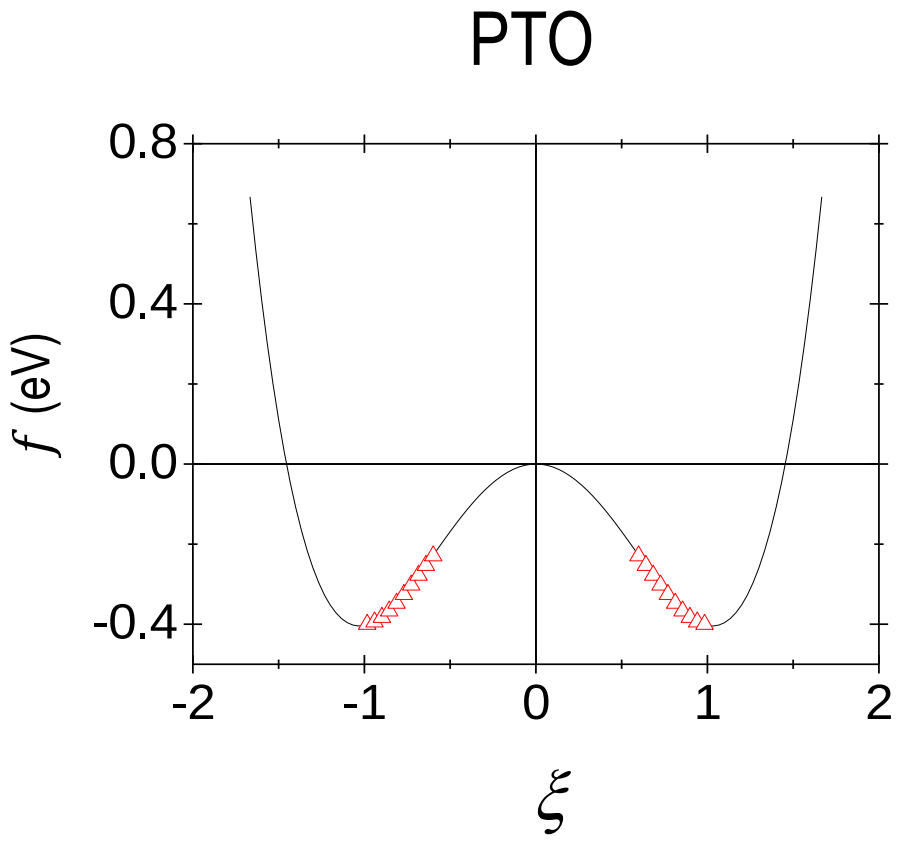

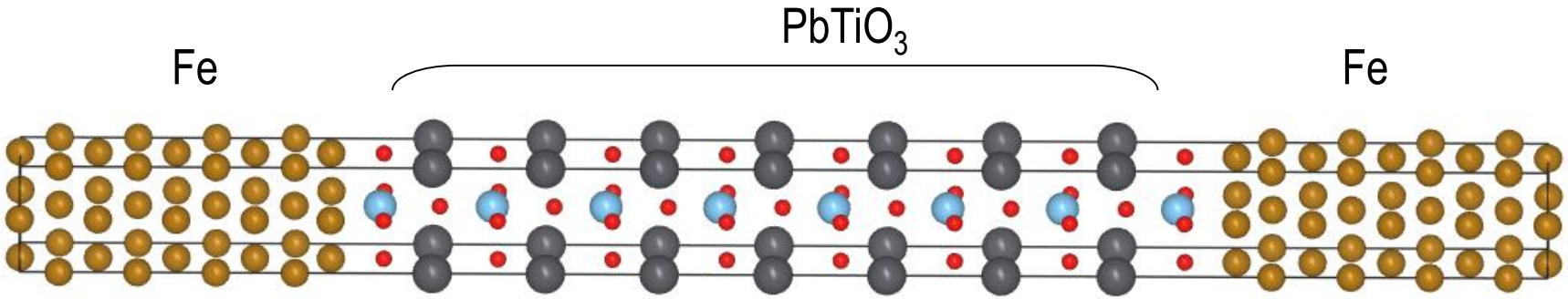

$\mu_0 \Delta M = \alpha E_d$

E_d : *depolarizing field*

ΔM : *magnetization change*

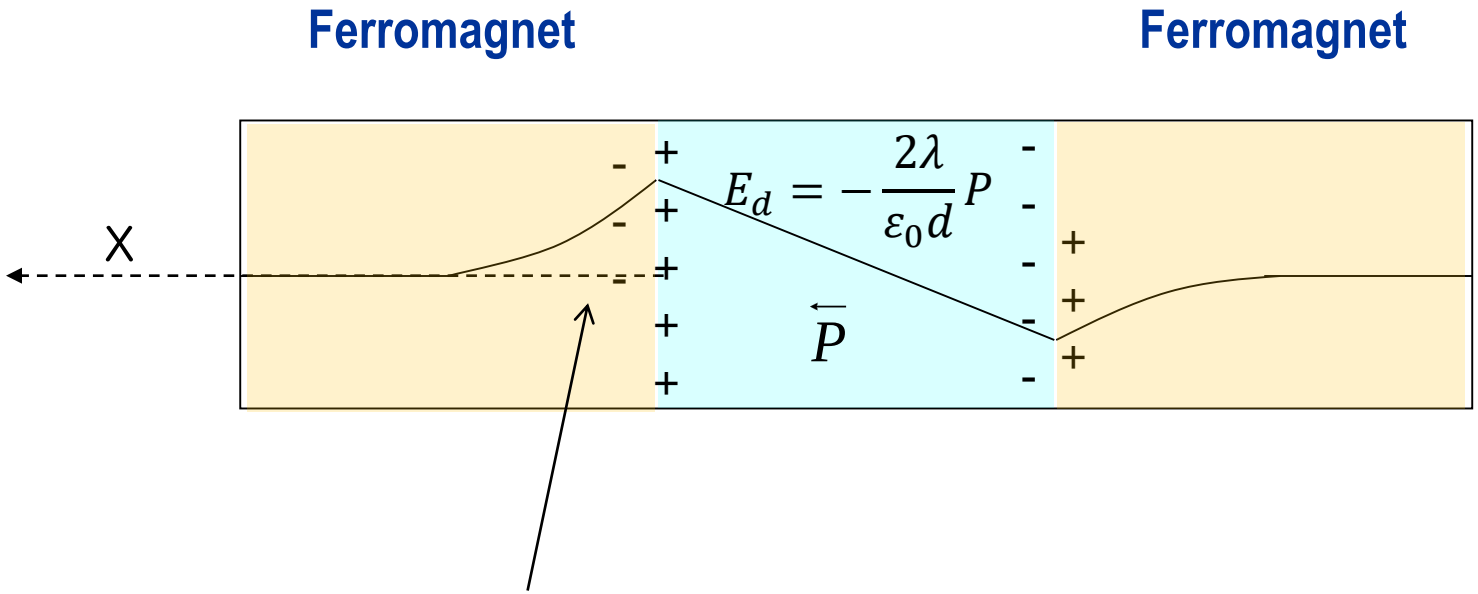

Induced charge density $\Delta n(x)$

charge density in the absence of the electric field n_0

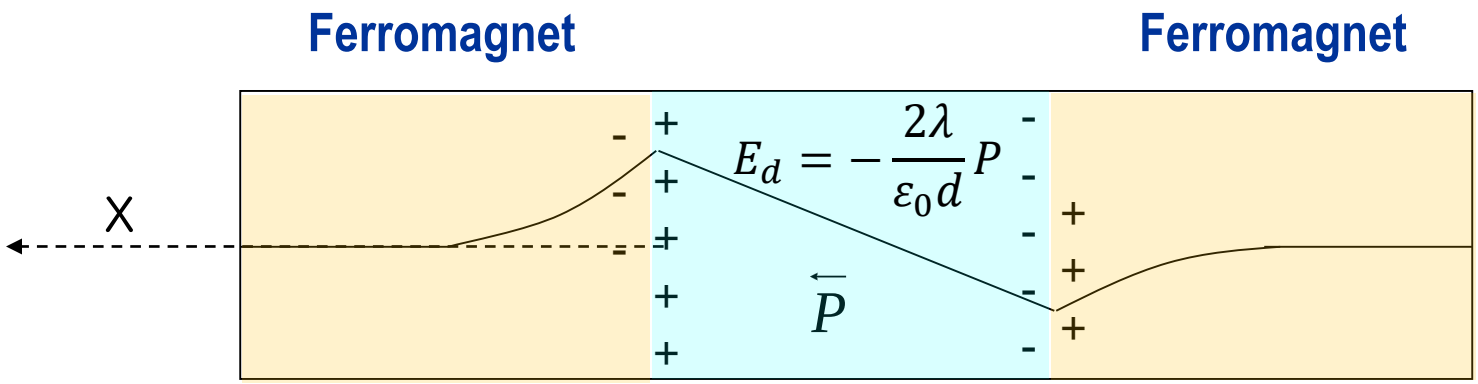

$$\Delta n(x) = \Delta n^{\uparrow}(x) + \Delta n^{\downarrow}(x)$$

$$W_c = \frac{e^2}{8\pi\varepsilon_0} \int \frac{\left[\Delta n^{\uparrow}(x) + \Delta n^{\downarrow}(x)\right] \cdot \left[\Delta n^{\uparrow}(x') + \Delta n^{\downarrow}(x')\right]}{|x - x'|} dx dx'$$

Coulomb energy contribution

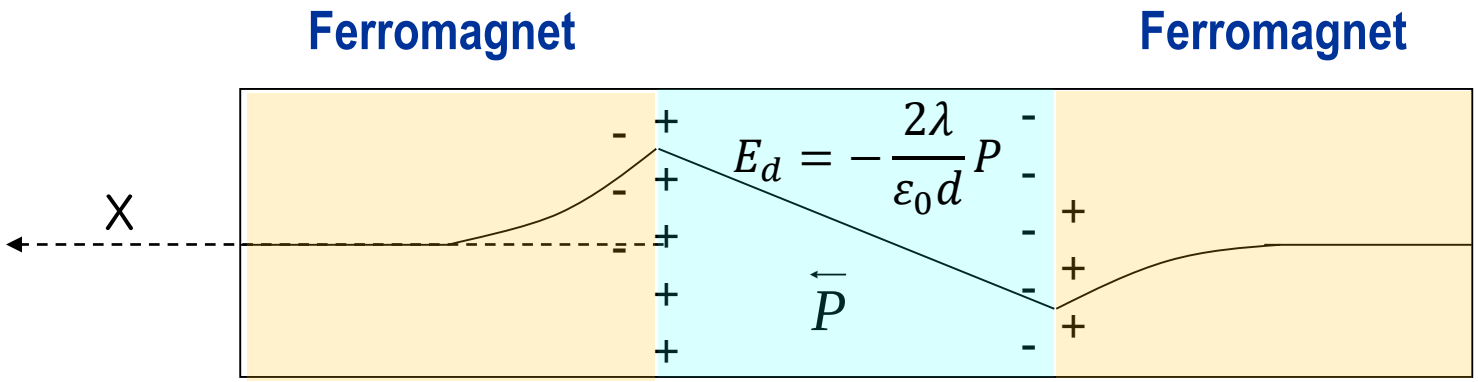

$$\Delta M = \left(\Delta n^{\uparrow}(x) - \Delta n^{\downarrow}(x)\right)\mu_B$$

$$H_{eff} = JM/\mu_B^2$$

$$M = M_0 + \Delta M$$

$$W_e = \frac{J}{2}(M_0 + \Delta M) \cdot \Delta M/\mu_B^2$$

Exchange energy contribution

$$W_c = \frac{e^2}{8\pi\varepsilon_0}\int \frac{\left[\Delta n^{\uparrow}(x) + \Delta n^{\downarrow}(x)\right]\cdot\left[\Delta n^{\uparrow}(x') + \Delta n^{\downarrow}(x')\right]}{|x - x'|}\,dx dx'$$

Coulomb energy contribution

$$W_e = \frac{J}{2}\left[\left(n_0^{\uparrow} - n_0^{\downarrow}\right)\left[\Delta n^{\uparrow}\,(x) - \Delta n^{\downarrow}\,(x)\right]\right] + \frac{J}{2}\left[\Delta n^{\uparrow}\,(x) - \Delta n^{\downarrow}\,(x)\right]^2$$

Exchange energy contribution

$$W_c = \frac{e^2}{8\pi\varepsilon_0}\int \frac{\left[\Delta n^{\uparrow}(x) + \Delta n^{\downarrow}(x)\right]\cdot\left[\Delta n^{\uparrow}(x') + \Delta n^{\downarrow}(x')\right]}{|x - x'|}\,dxdx'$$

$$W_e = \frac{J}{2}\left[\left(n_0^{\uparrow} - n_0^{\downarrow}\right)\left[\Delta n^{\uparrow}\,(x) - \Delta n^{\downarrow}\,(x)\right]\right] + \frac{J}{2}\left[\Delta n^{\uparrow}\,(x) - \Delta n^{\downarrow}\,(x)\right]^2$$

$$\frac{\partial(W_c+W_e)}{\partial\Delta n^{\sigma}(x)} = eV^{\sigma}(x)$$

$$= E_0^{\sigma} + eV_c(x) + J[\Delta n^{\sigma}\,(x) - \Delta n^{-\sigma}(x)] \qquad \sigma = \uparrow,\downarrow$$

$$\frac{J}{2}[(n_0^{\sigma} - n_0^{-\sigma})]$$

Spin dependent Potential $\qquad V^{\sigma}(x) = \frac{E_0^{\sigma}}{e} + V_c(x) + \frac{J}{e}[\Delta n^{\sigma}\,(x) - \Delta n^{-\sigma}(x)] \qquad \sigma = \uparrow,\downarrow$

S. Zhang, PRL **83** 640

J. Lee et al., PRB **81** 144425

$$V^{\sigma}(x) \sim V_c(x) + \frac{J}{e}[\Delta n^{\sigma}(x) - \Delta n^{-\sigma}(x)] \qquad \sigma = \uparrow, \downarrow$$

DOS at the Fermi energy

$$\Delta n^{\sigma}(x) = -eD^{\sigma}(E_F)V^{\sigma}(x) \quad \sigma = \uparrow, \downarrow$$ Linearized Thomas Fermi equation

$$\frac{d^2V_c(x)}{dx^2} = \frac{1}{\lambda^2}V_c(x)$$ Poisson's equation

$$\left(\Delta n^{\uparrow}(x) - \Delta n^{\downarrow}(x)\right) \sim \Delta M(x) = -\frac{D^{\uparrow}(E_F) - D^{\downarrow}(E_F)}{1 + J\left(D^{\uparrow}(E_F) + D^{\downarrow}(E_F)\right)} eV_c(x)$$

$$\left(\Delta n^{\uparrow}(x) + \Delta n^{\downarrow}(x)\right) = -\left(D^{\uparrow}(E_F) + D^{\downarrow}(E_F)\right) eV_c(x) - J\left(D^{\uparrow}(E_F) - D^{\downarrow}(E_F)\right)\left(\Delta n^{\uparrow}(x) - \Delta n^{\downarrow}(x)\right)$$

$$\Delta M_{tot} \sim \int \left(\Delta n^{\uparrow}(x) - \Delta n^{\downarrow}(x)\right) dx \sim \int \left(\Delta n^{\uparrow}(x) + \Delta n^{\downarrow}(x)\right) dx \sim P \sim E_d$$

ΔM in Fe/PTO heterostructure

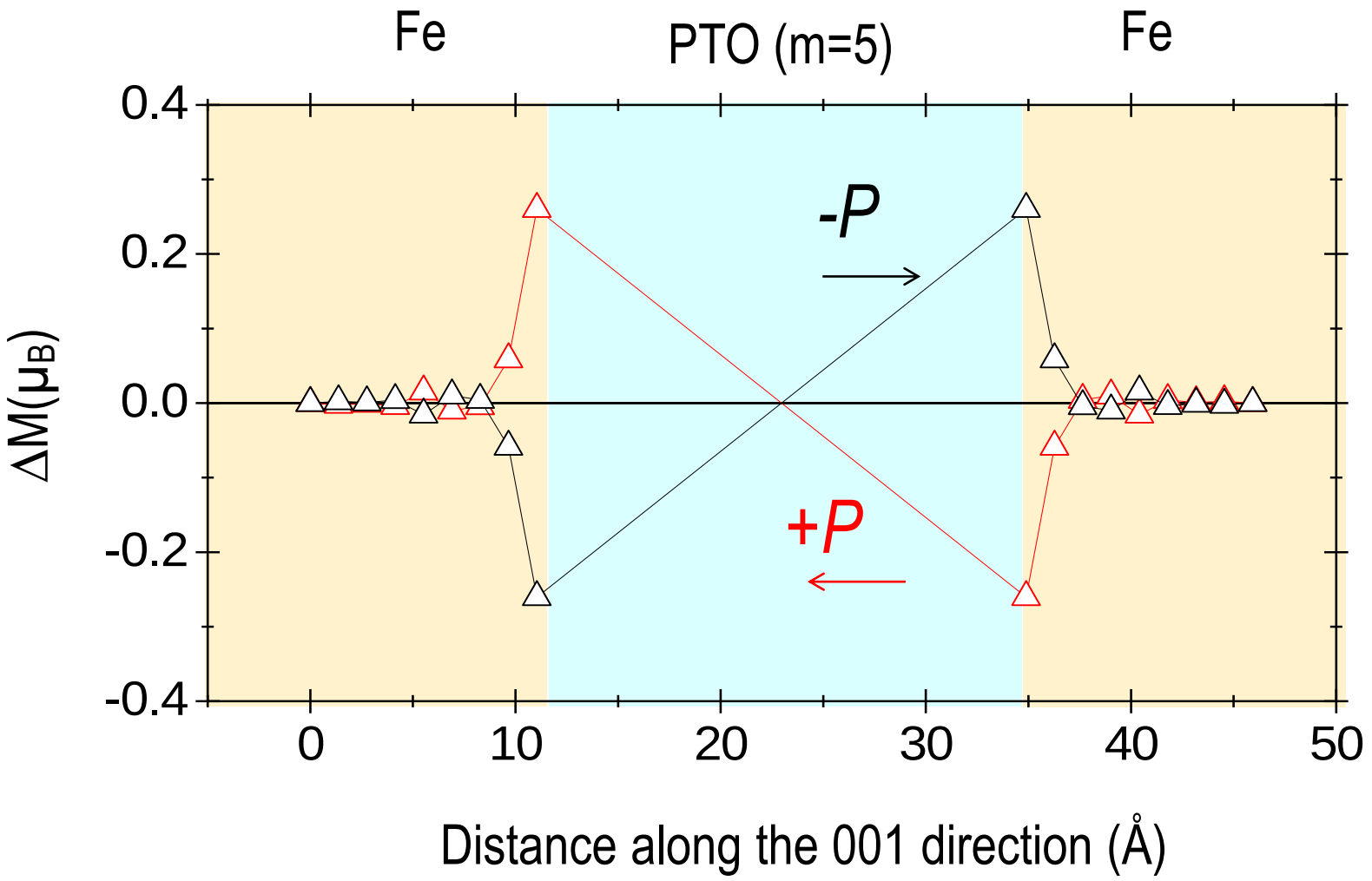

$E_d(m)$, $\Delta M(m)$ in $Fe/(PTO)_m$

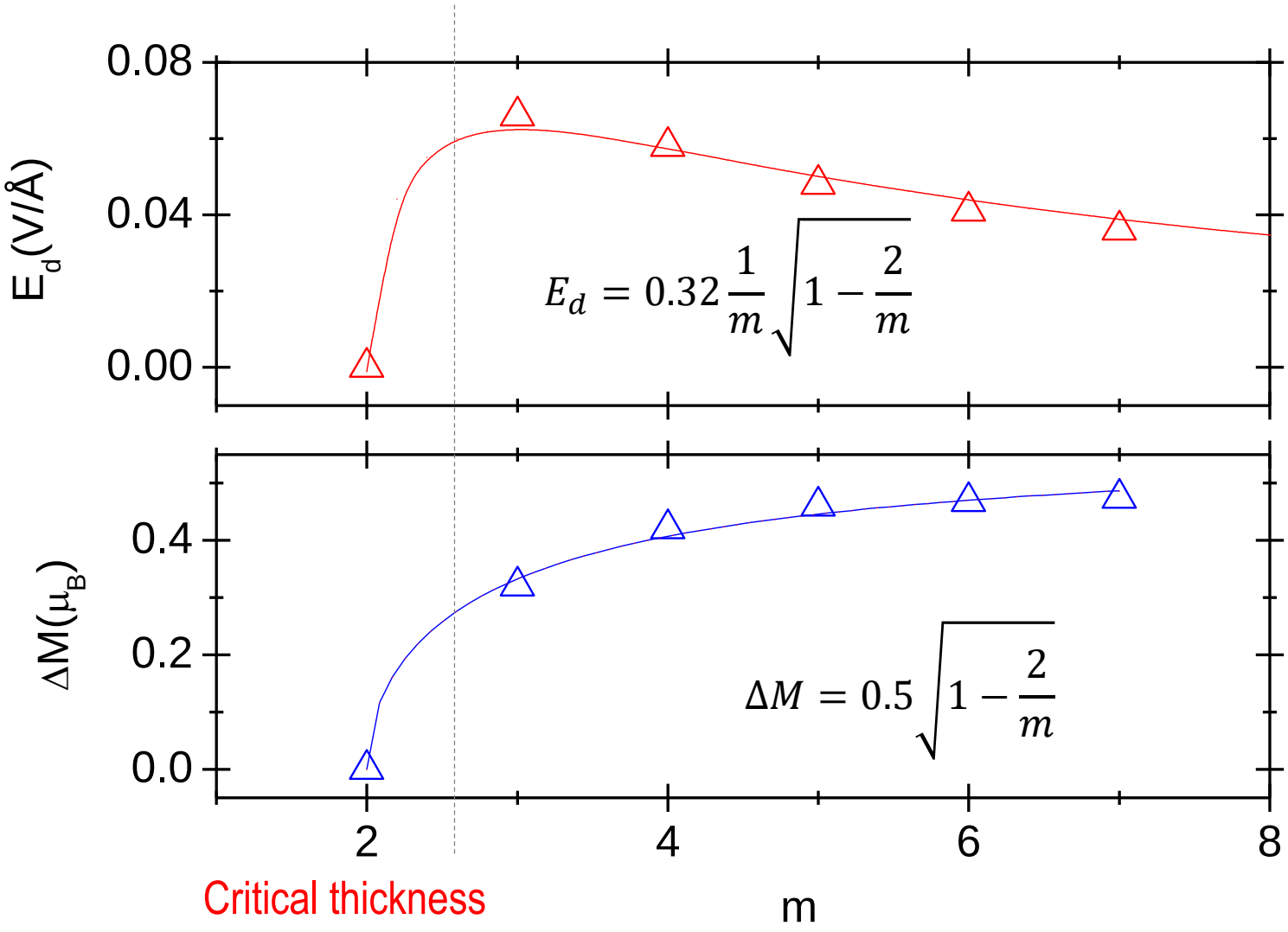

Summary

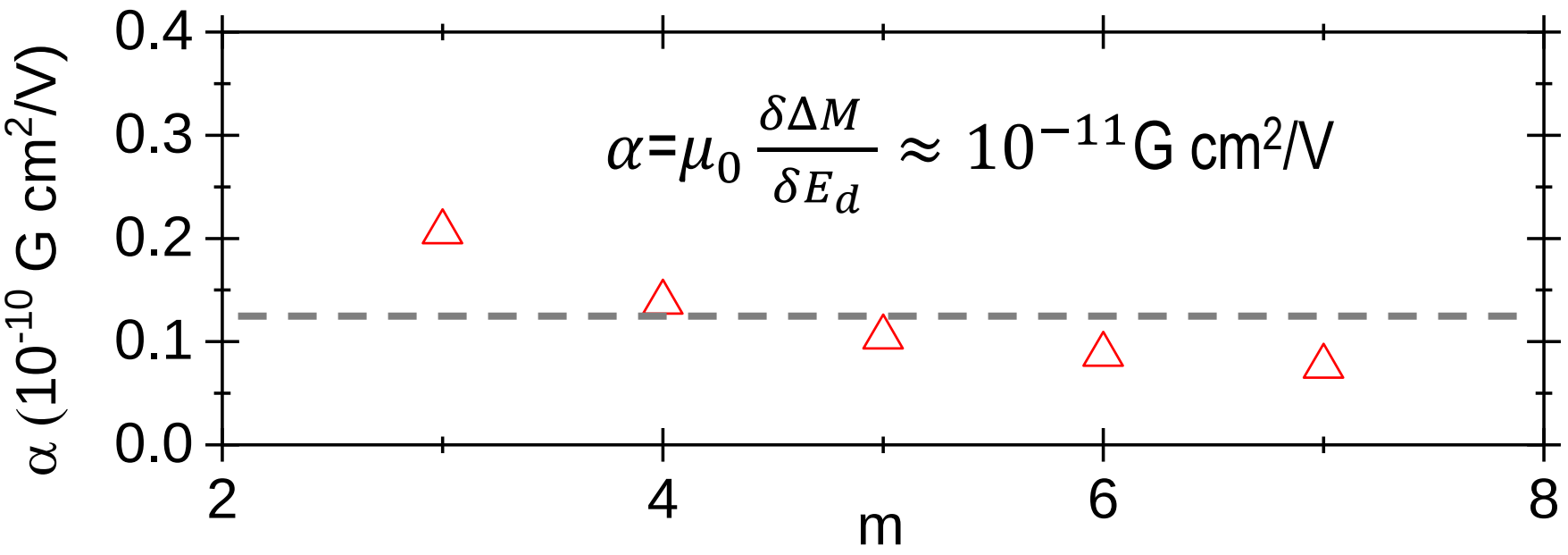

$E_c \approx 100$ KV/cm → $\alpha \approx 4 \times 10^{-10}$ G cm²/V

ME coupling constant in Fe/PTO/Fe

Ferroelectric tunnel junction

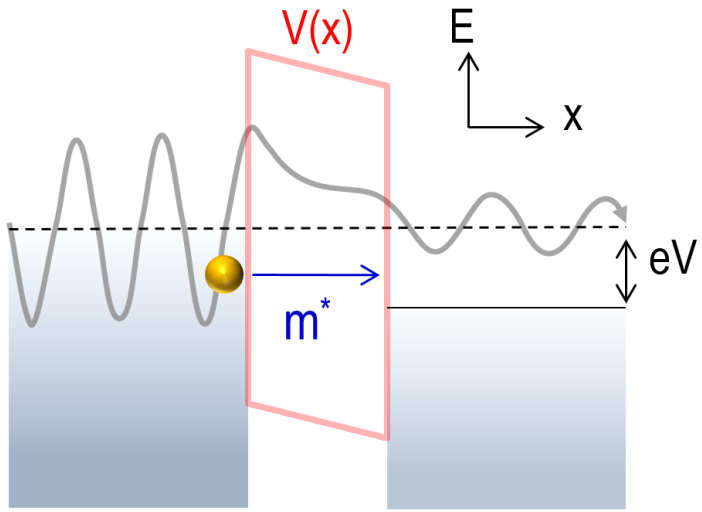

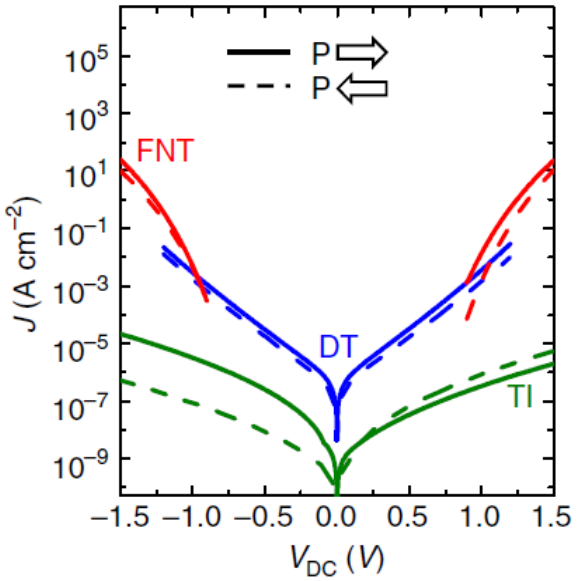

Jaekwang Lee
Dept. of Physics, PNU, Rep. of Korea

부산대학교
PUSAN NATIONAL UNIVERSITY

Tunneling barrier is dependent on *P* direction

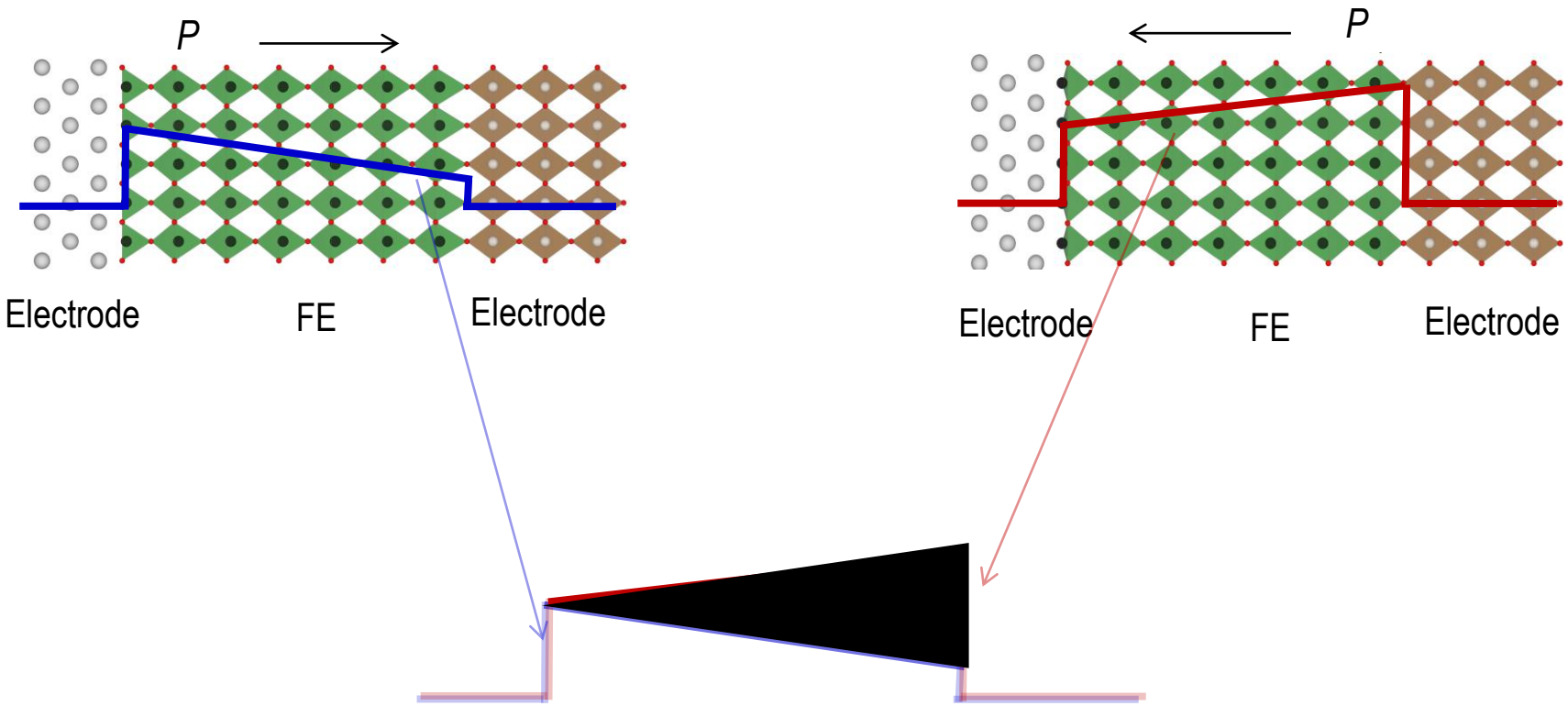

Tunneling current is dependent on *P* direction

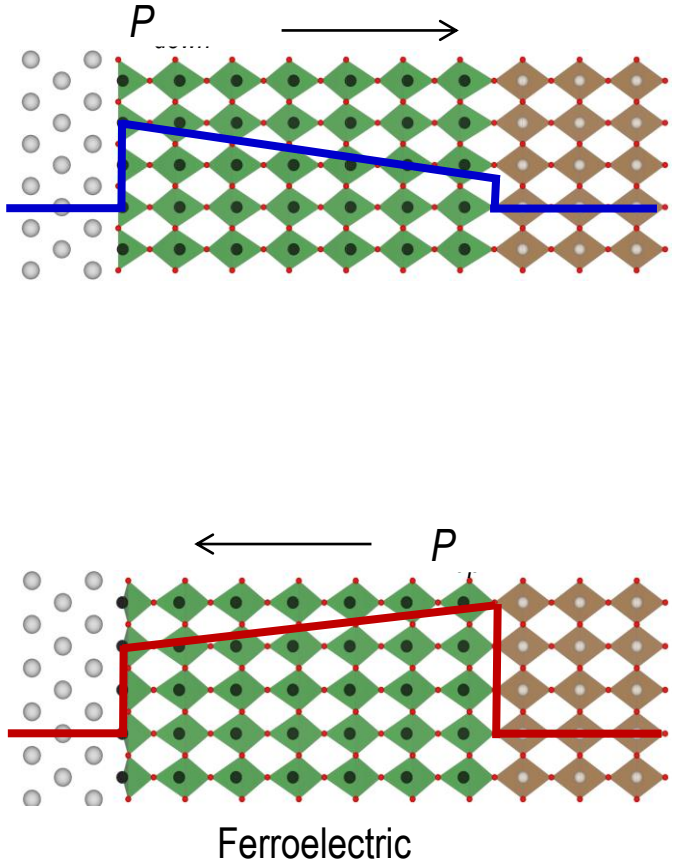

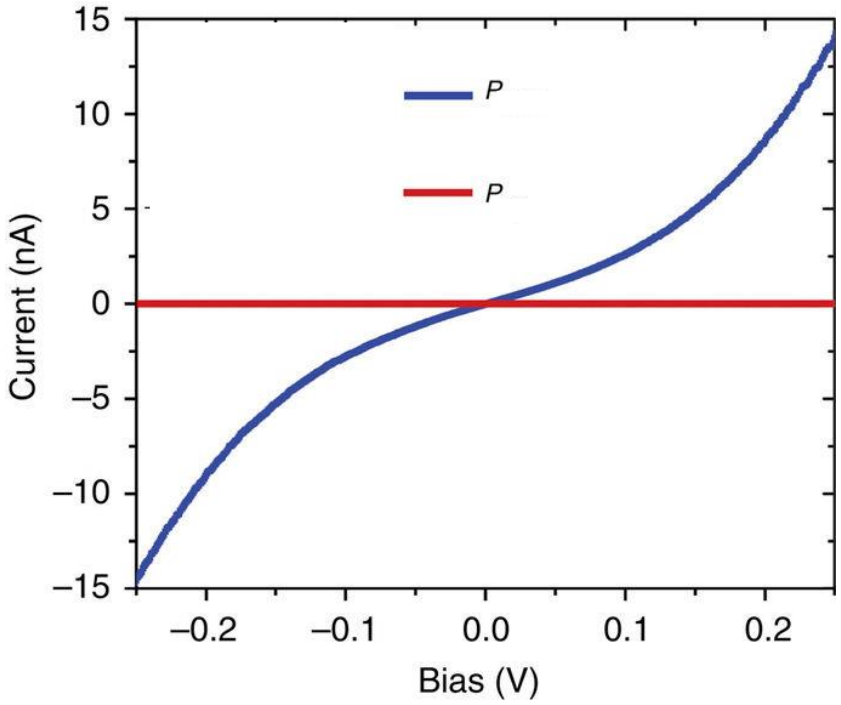

Li *et al.*, *Adv. Mater.* (2014)

Ferroelectric Tunneling Junction (FTJ)

Advantage of FTJ device

Device	NAND/NOR	ReRAM	PCM	MTJ	FTJ
Visual (Red and blue boxes are two different states in time)	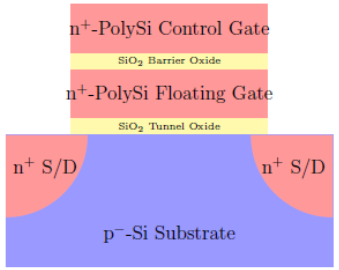	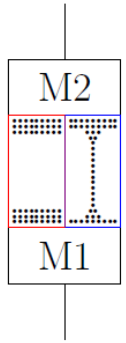	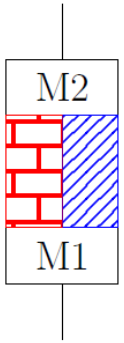	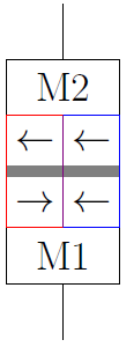	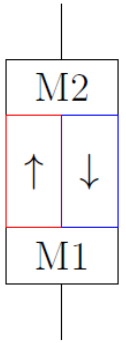
Mechanism	Vt Shift	O_2 Vac./ Filamentary	Phase change	e^- Spin (Mag)	Polarization
Speed (s)	400u [27]	500n	50n	30n [27]	10n
Power (J)	15u [28]	250n	6p	1.4u	30f
Cell Area	$4F^2$ or $10F^2$ [29]	$25F^2$	$16F^2$	$1.3F^2$	$22F^2$
Material	Si	Ag, a-Si, W	$Ge_2Sb_2Te_5$	MgO(mag)	$BaTiO_2$ (now HfO_2)

Tunneling mechanism

Direct tunneling

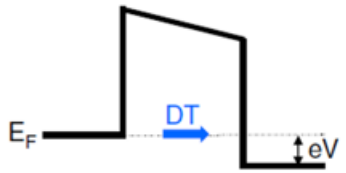

$$j_{DT} = C \frac{\exp\left[\alpha\left\{\left(\Phi_{B,2} - \frac{eV}{2}\right)^{3/2} - \left(\Phi_{B,1} + \frac{eV}{2}\right)^{3/2}\right\}\right]}{\alpha^2\left[\sqrt{\Phi_{B,2} - \frac{eV}{2}} - \sqrt{\Phi_{B,1} + \frac{eV}{2}}\right]^2} \times \sinh\left[\frac{3eV}{4}\alpha\left\{\sqrt{\Phi_{B,2} - \frac{eV}{2}} - \sqrt{\Phi_{B,1} + \frac{eV}{2}}\right\}\right]$$

Thermionic injection

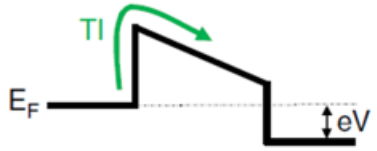

$$j_{Schottky} = A^{**}T^2 \exp\left[-\frac{1}{k_B T}\left(\Phi_B - \sqrt{\frac{e^3 E}{4\pi\varepsilon_0\varepsilon_{ifl}}}\right)\right]$$

Fowler-Nordheim tunneling

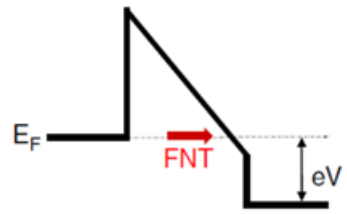

$$j_{FN} = \frac{e^3 m_e}{8\pi h m_{e,ox}\Phi_B} E^2 \exp\left[-\frac{8\pi\sqrt{2m_{e,ox}}}{3he}\frac{\Phi_B^{3/2}}{E}\right]$$

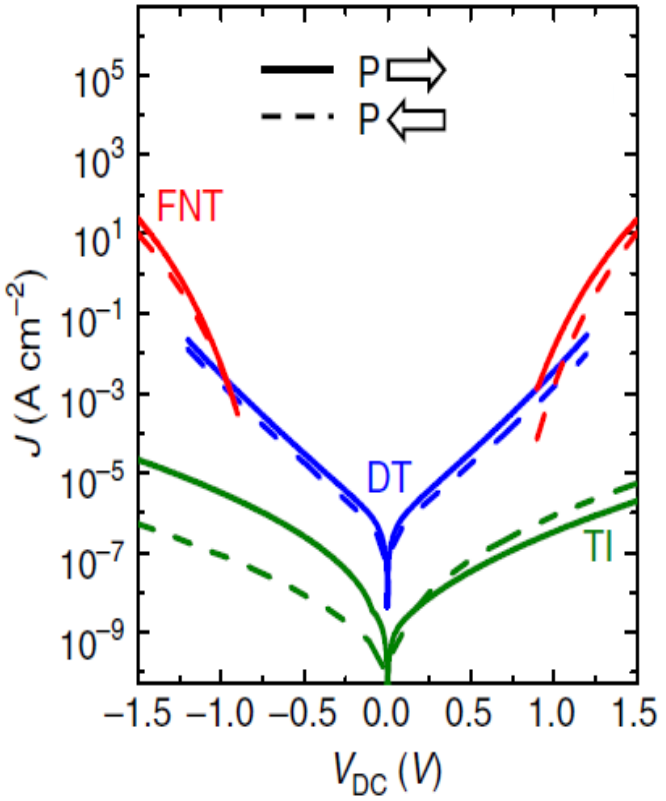

D. Pantel and M. Alexe *PRB 82 134105 (2010)*

J-V prediction of FTJ

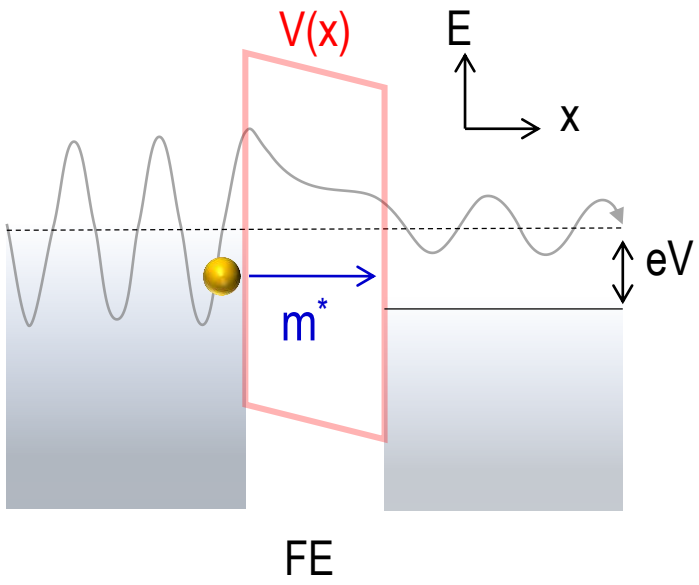

V(x)

$$\left(-\frac{\hbar^2}{2m}\nabla^2 + v_{\text{ext}}(\mathbf{r}) + v^e_{\text{coul}}(\mathbf{r}) + v_{\text{xc}}(\mathbf{r})\right)\psi_{n\mathbf{k}}(\mathbf{r}) = \epsilon_{n\mathbf{k}}\psi_{n\mathbf{k}}(\mathbf{r})$$

↓ 1. DFT calculation

$$T(E) = \exp\left(-\frac{2}{\hbar}\int_0^d \sqrt{2m^*\,(V(x) - E)}\,dx\right)$$

↓ 2. Numerical calculation

$$J = \left(\frac{4\pi me}{h^3}\right)\int_0^\infty T(E)\int_0^\infty [f(E - eV) - f(E)]\,dE$$

Transfer Matrix Approach

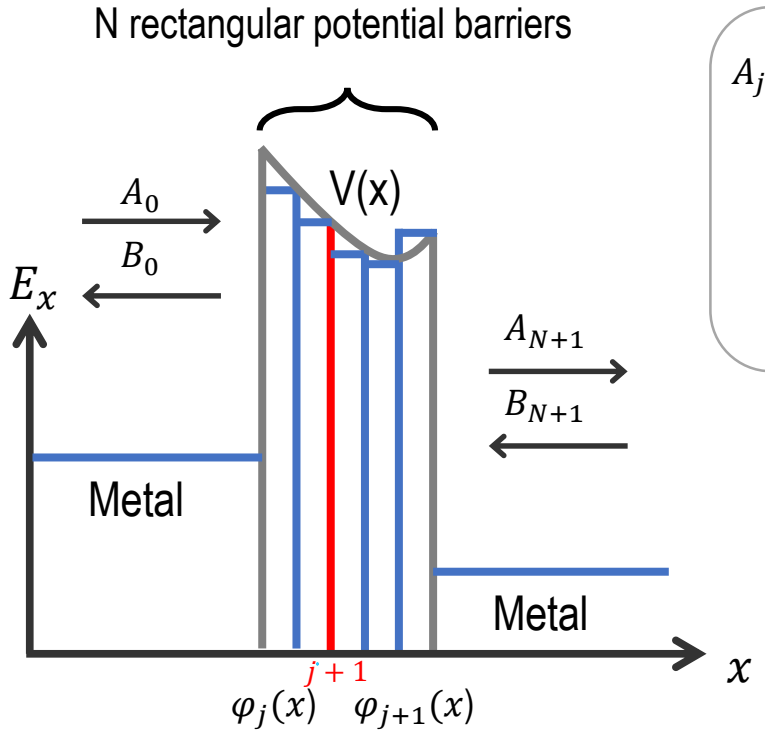

$$A_{j+1} + B_{j+1} = A_j \exp\left(ik_j(x_{j+1} - x_j)\right) + B_j \exp\left(-ik_j(x_{j+1} - x_j)\right)$$

$$A_{j+1} + B_{j+1} = A_j \exp(ik_j \Delta x) + B_j \exp(-ik_j \Delta x)$$
$$ik_{j+1}(A_{j+1} - B_{j+1}) = ik_j A_j \exp(ik_j \Delta x) - ik_j B_j \exp(-ik_j \Delta x)$$

$$\begin{pmatrix} A_{j+1} \\ B_{j+1} \end{pmatrix} = \begin{pmatrix} \frac{k_{j+1}+k_j}{2k_{j+1}} e^{ik_j \Delta x} & \frac{k_{j+1}-k_j}{2k_{j+1}} e^{-ik_j \Delta x} \\ \frac{k_{j+1}-k_j}{2k_{j+1}} e^{ik_j \Delta x} & \frac{k_{j+1}+k_j}{2k_{j+1}} e^{-ik_j \Delta x} \end{pmatrix} \begin{pmatrix} A_j \\ B_j \end{pmatrix}$$

$$\varphi_j(x) = A_j \exp\left(ik_j(x - x_j)\right) + B_j \exp\left(-ik_j(x - x_j)\right)$$

$$\varphi_{j+1}(x) = A_{j+1} \exp\left(ik_{j+1}(x - x_{j+1})\right) + B_{j+1} \exp\left(-ik_{j+1}(x - x_{j+1})\right)$$

C. Jirauscheck, *IEEE J. Quantum Electron. 45 1059 (2009)*

Transfer Matrix Approach

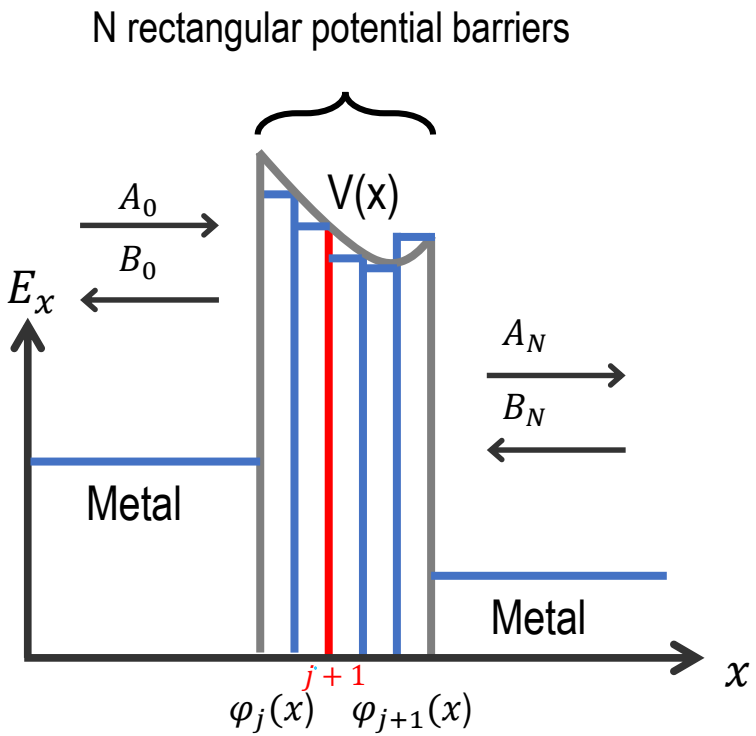

$$\begin{pmatrix} A_{j+1} \\ B_{j+1} \end{pmatrix} = \begin{pmatrix} \frac{k_{j+1}+k_j}{2k_{j+1}} e^{ik_j\Delta x} & \frac{k_{j+1}-k_j}{2k_{j+1}} e^{-ik_j\Delta x} \\ \frac{k_{j+1}-k_j}{2k_{j+1}} e^{ik_j\Delta x} & \frac{k_{j+1}+k_j}{2k_{j+1}} e^{-ik_j\Delta x} \end{pmatrix} \begin{pmatrix} A_j \\ B_j \end{pmatrix}$$

$$\downarrow$$

$$\begin{pmatrix} A_j \\ B_j \end{pmatrix} = \begin{pmatrix} \frac{k_{j+1}+k_j}{2k_j} e^{-ik_j dx} & \frac{k_j-k_{j+1}}{2k_j} e^{-ik_j dx} \\ \frac{k_j-k_{j+1}}{2k_j} e^{ik_j dx} & \frac{k_{j+1}+k_j}{2k_j} e^{ik_j dx} \end{pmatrix} \begin{pmatrix} A_{j+1} \\ B_{j+1} \end{pmatrix}$$

$$\begin{pmatrix} A_j \\ B_j \end{pmatrix} = T_{j,j+1} \begin{pmatrix} A_{j+1} \\ B_{j+1} \end{pmatrix}$$

$$\begin{pmatrix} A_0 \\ B_0 \end{pmatrix} = T_{1,0} T_{2,1} \cdots T_{N,N-1} \begin{pmatrix} A_N \\ B_N \end{pmatrix} = \begin{pmatrix} T_{11} & T_{12} \\ T_{21} & T_{22} \end{pmatrix} \begin{pmatrix} A_N \\ B_N \end{pmatrix}$$

$$T(E) = |A_N/A_0|^2 = |1/T_{11}|^2$$

C. Jirauscheck, *IEEE J. Quantum Electron. 45 1059 (2009)*

Tunneling probability from WKB

N rectangular potential barriers

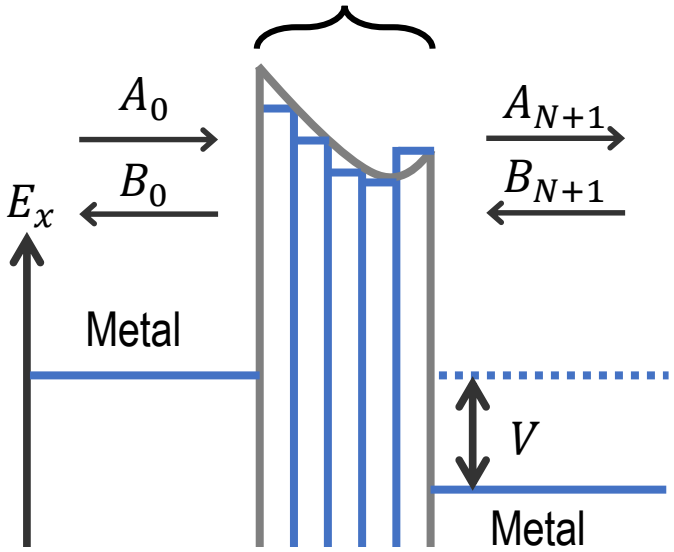

$$\begin{pmatrix} A_0 \\ B_0 \end{pmatrix} = T_{1,0}T_{2,1}\cdots T_{N,N-1}\begin{pmatrix} A_N \\ B_N \end{pmatrix} = \begin{pmatrix} T_{11} & T_{12} \\ T_{21} & T_{22} \end{pmatrix}\begin{pmatrix} A_N \\ B_N \end{pmatrix}$$

$$T_{j,j+1} = \begin{pmatrix} \frac{k_j + k_{j+1}}{2k_j} e^{-ik_j dx} & \frac{k_j - k_{j+1}}{2k_j} e^{-ik_j dx} \\ \frac{k_j - k_{j+1}}{2k_j} e^{ik_j dx} & \frac{k_j + k_{j+1}}{2k_j} e^{ik_j dx} \end{pmatrix}$$

```
def tunneling(self, E):
    k = [self.reduced_mass * csqrt(2. * (E - v)) / hbar for v in self.potential]
    matrix = identity(2, dtype=np.complex128)
    for n in range(0, self.N - 1):
        if k[n].__abs__() < 1e-5:
            continue
        T11 = (k[n] + k[n + 1]) / 2 / k[n] * cexp(-1j * k[n] * self.dx)
        T12 = (k[n] - k[n + 1]) / 2 / k[n] * cexp(-1j * k[n] * self.dx)
        T21 = (k[n] - k[n + 1]) / 2 / k[n] * cexp(1j * k[n] * self.dx)
        T22 = (k[n] + k[n + 1]) / 2 / k[n] * cexp(1j * k[n] * self.dx)
        matrix = dot(matrix, [[T11, T12], [T21, T22]])
    return matrix[0][0].__abs__() ** -2
```

Tunneling current formula in tunnel junction

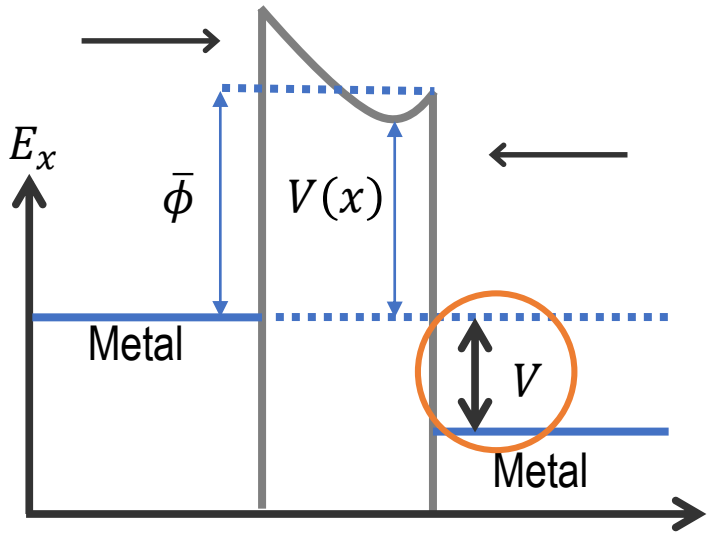


```
def current(self, V, result):
    self.gen_pot(V)
    constants = 4. * pi * m * e / h ** 3
    i_tot = 0.
    dn = 0.003
    E_x = Ef + 0.6
    Em = 0.6
    if V > 0:
        E_x += V
    else:
        Em -= V
    while E_x > Ef - Em:
        i_tot += self.density(E_x, V) * \
                 self.tunneling(E_x) * dn
        E_x -= dn
    result.put(constants * i_tot)
```

```
def density(self, e_x, v):
    a = quad(self.fermi, e_x, np.inf)
    b = quad(self.fermi, e_x + v, np.inf)
    return b[0] - a[0]
```

$$J = \frac{4\pi me}{h^3}\int_0^{E_m} T(E_x)dE_x \times \int_0^{E_m} f(E) - f(E+eV)dE_{y,z}$$

Effective mass is determined from the complex band structure

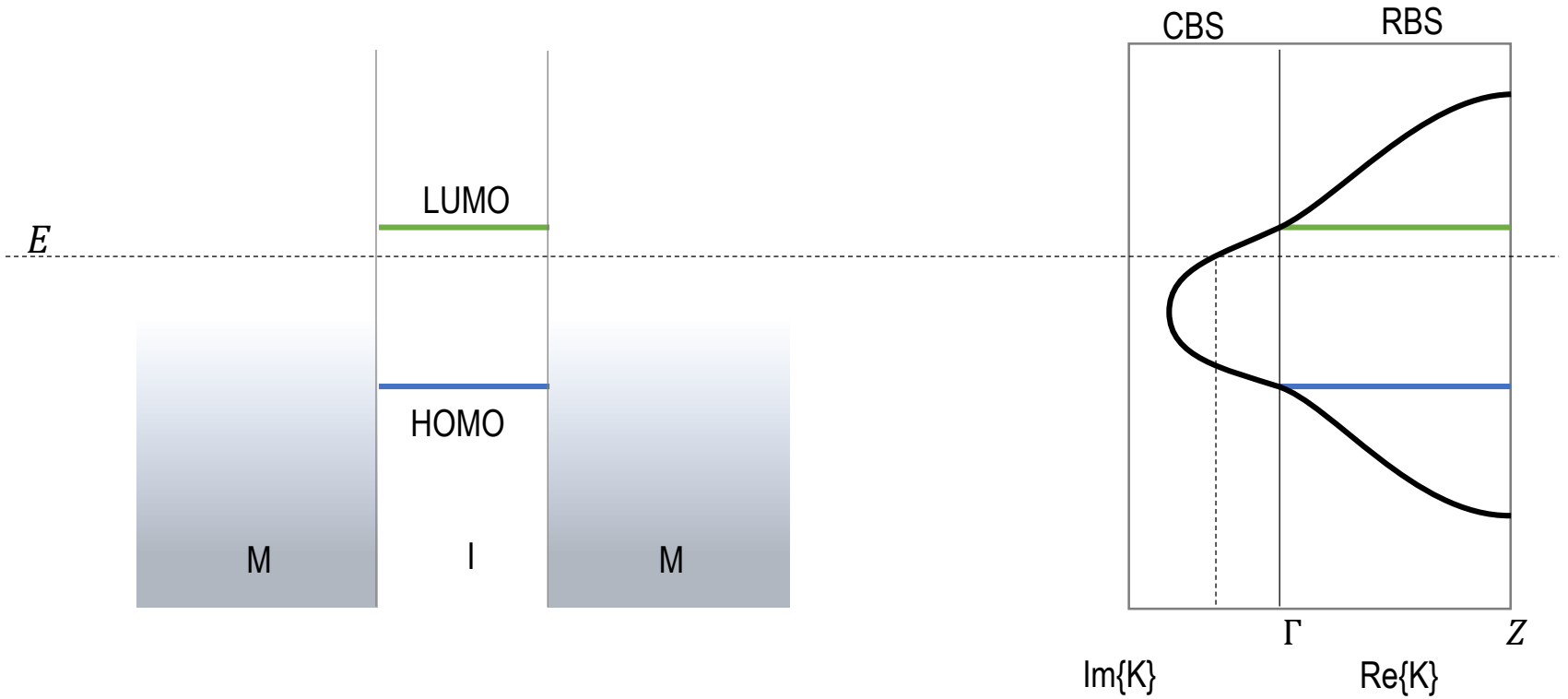

Complex band structure of HfO_2

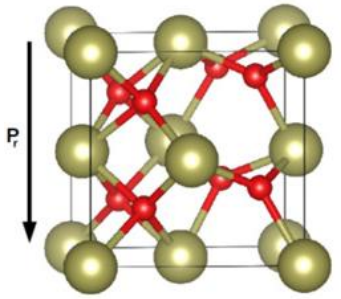

Complex band structure

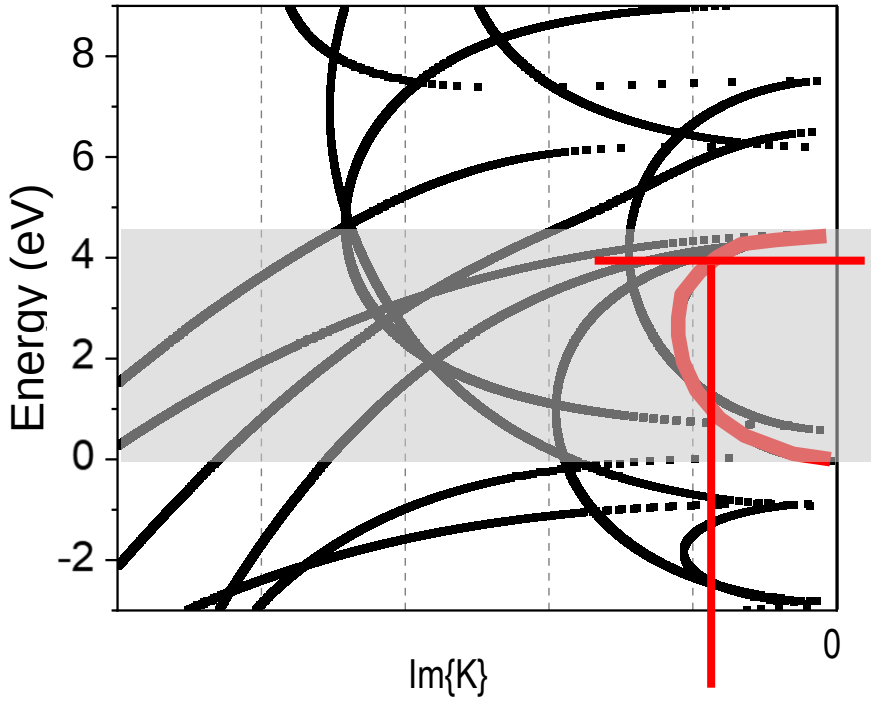

$m^*=0.09\ m_e$

Real band structure

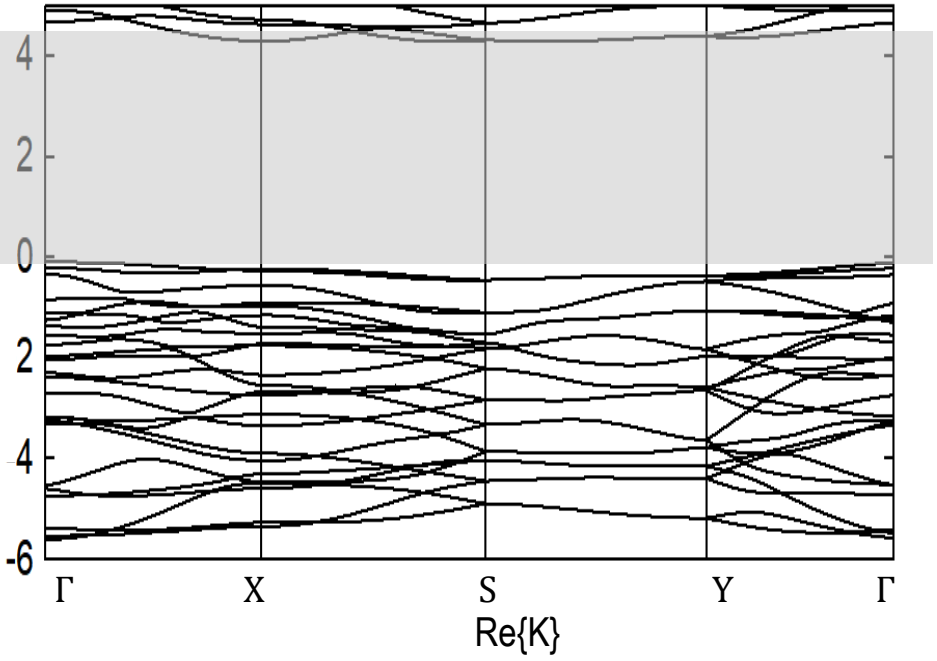

Tunneling current modeling: $Pt/PbTiO_3/SRuO_3$ FTJ

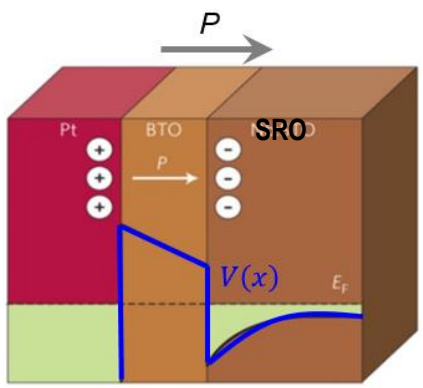

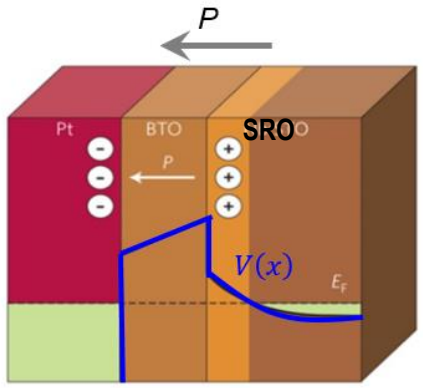

Experiment

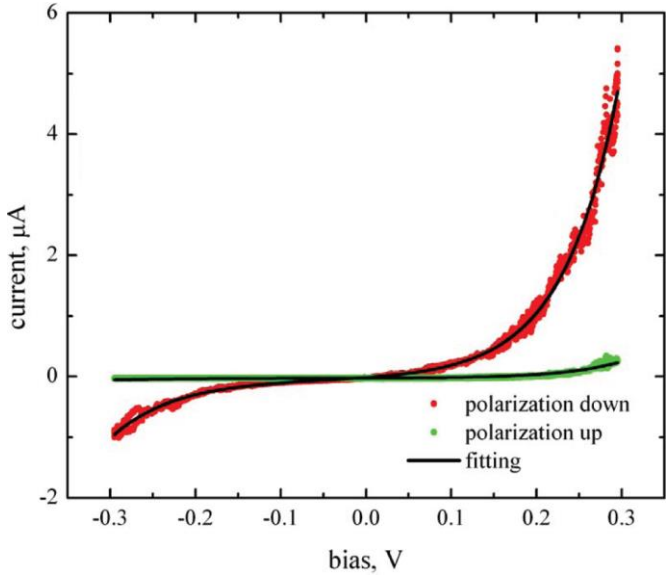

Our modeling

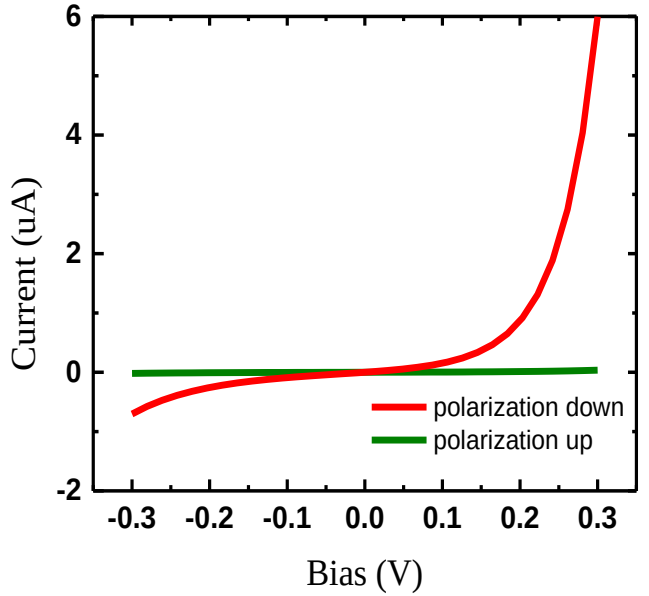

Nano letters (2009)

Tunneling current modeling: TiN/YHO/SiOx/Si FTJ

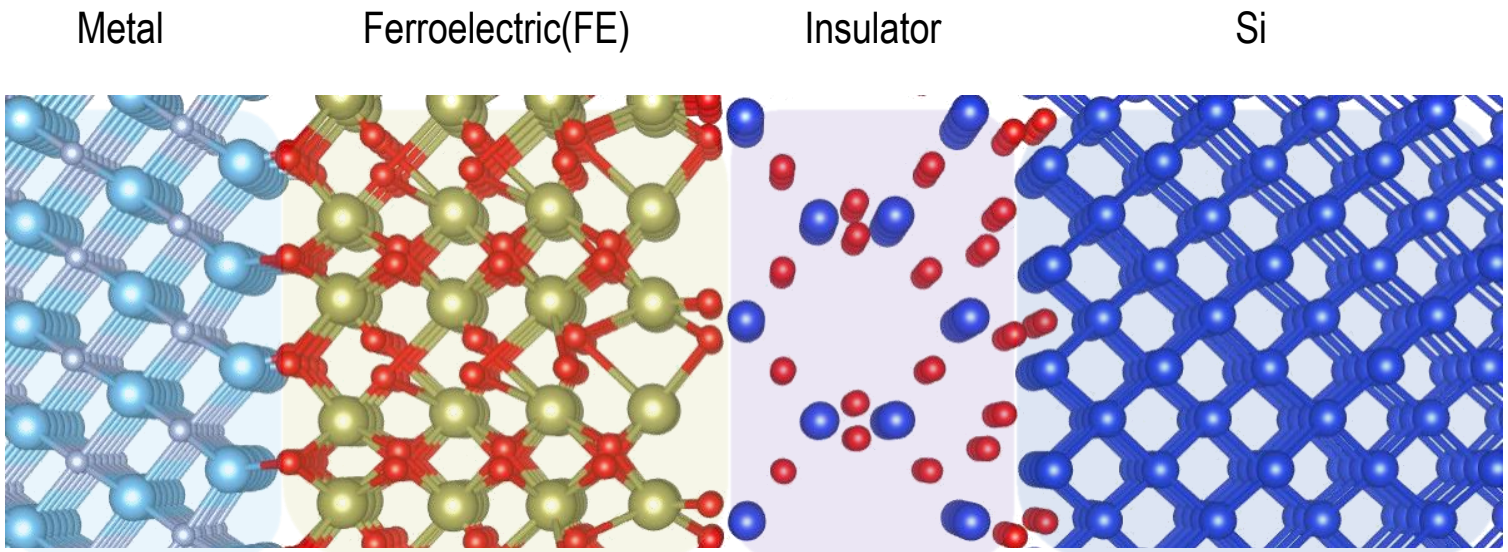



Tunneling potential profile

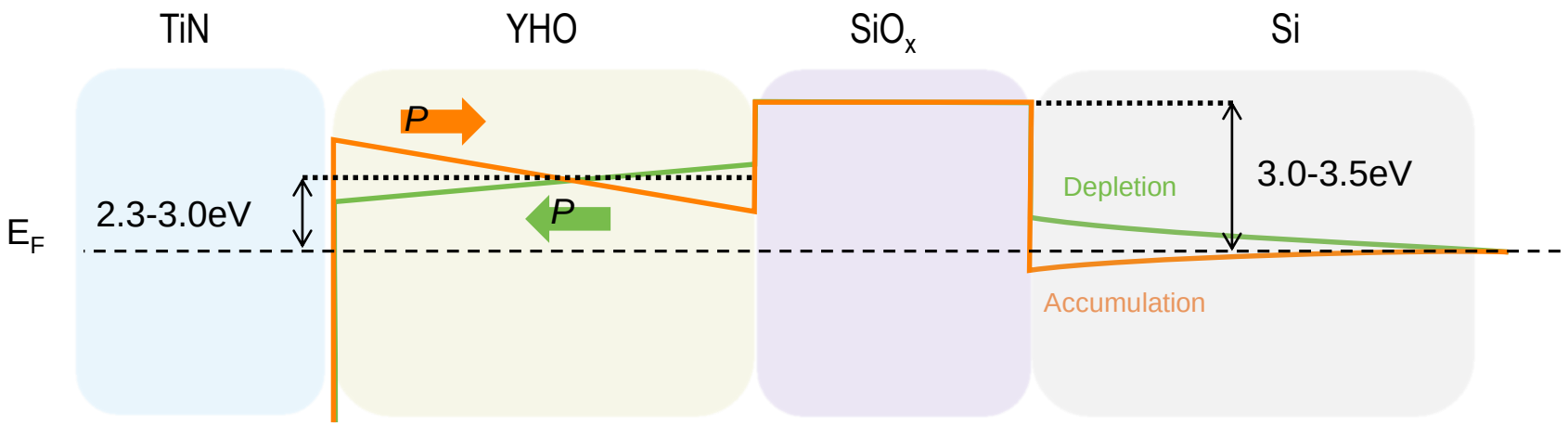

10^6 on/off ratio in $TiN/HfO_2/SiOx/Si$

Theory

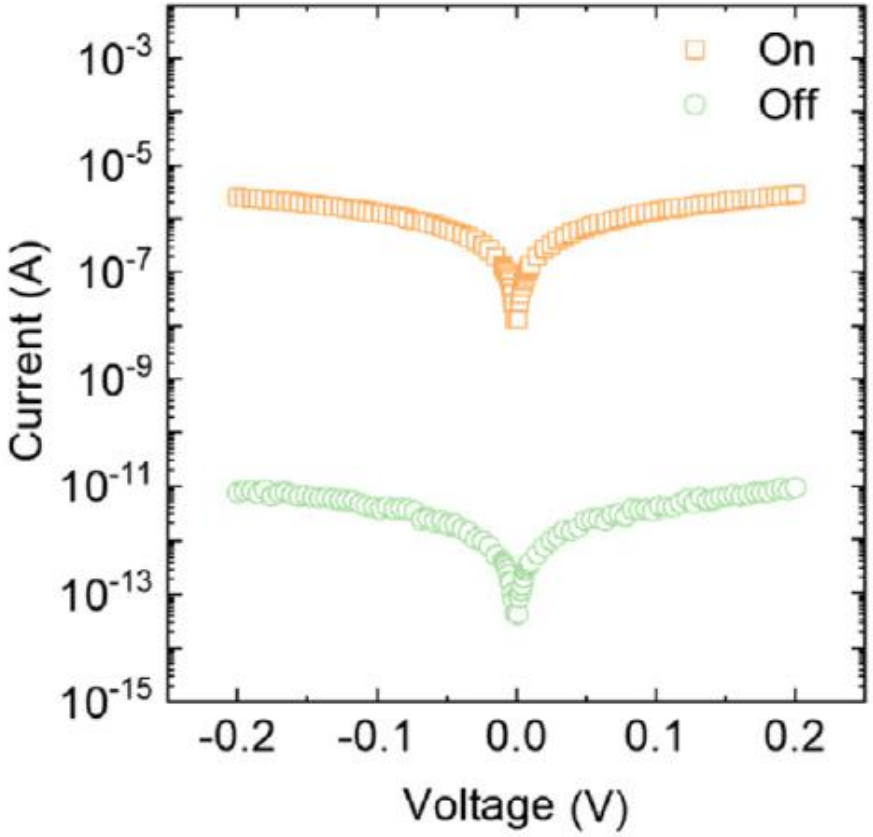

Experiment (Prof. Chae's group, SNU)

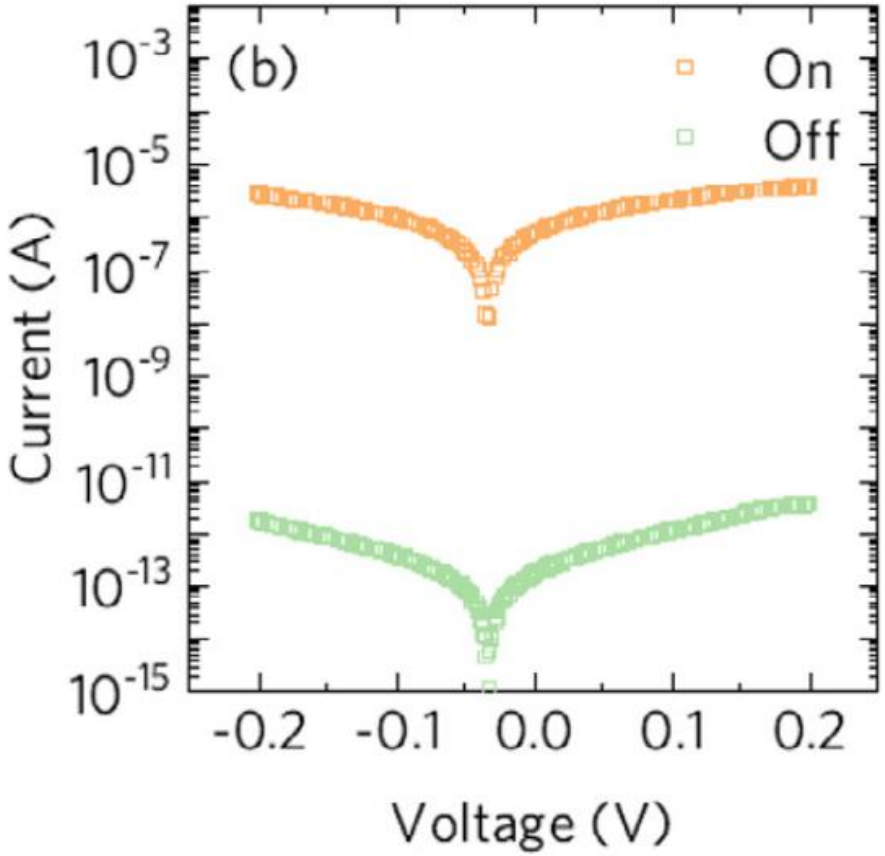

Applied Materials Today (2022), https://doi.org/10.1016/j.apmt.2021.101308

Tunneling potential model

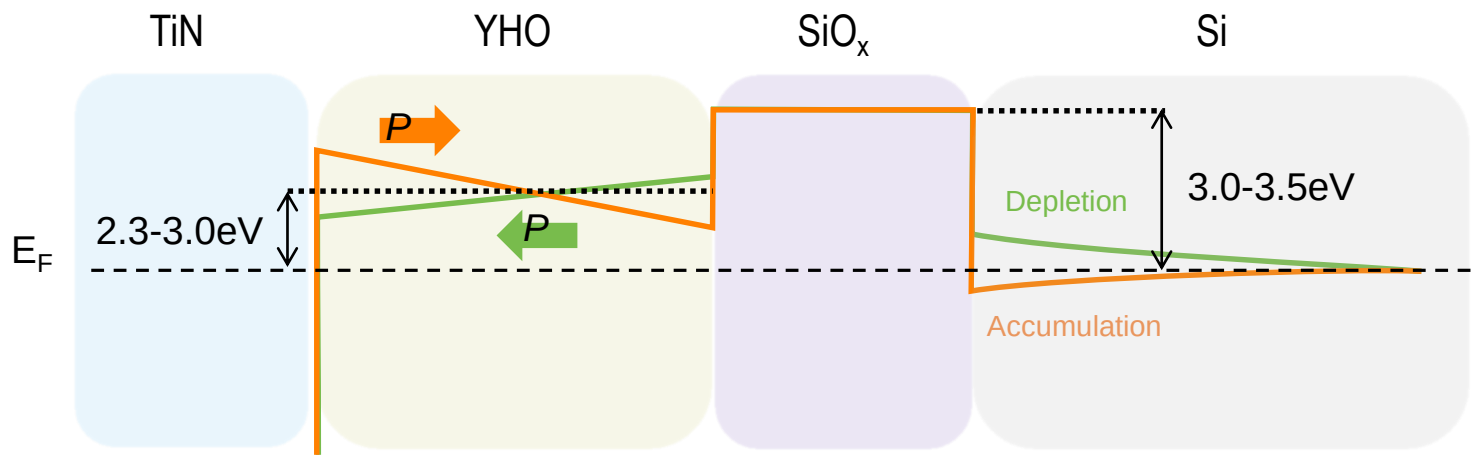

Tunneling parameter

	YHO	SiOx	Depletion layer (Si)
Layer thickness	1.2nm	1.3nm	5.3nm
Average barrier height	2.7eV [1]	3.5eV [2]	0.27eV
Effective mass	0.12m_0	0.43m_0	0.38m_0

FTJ code

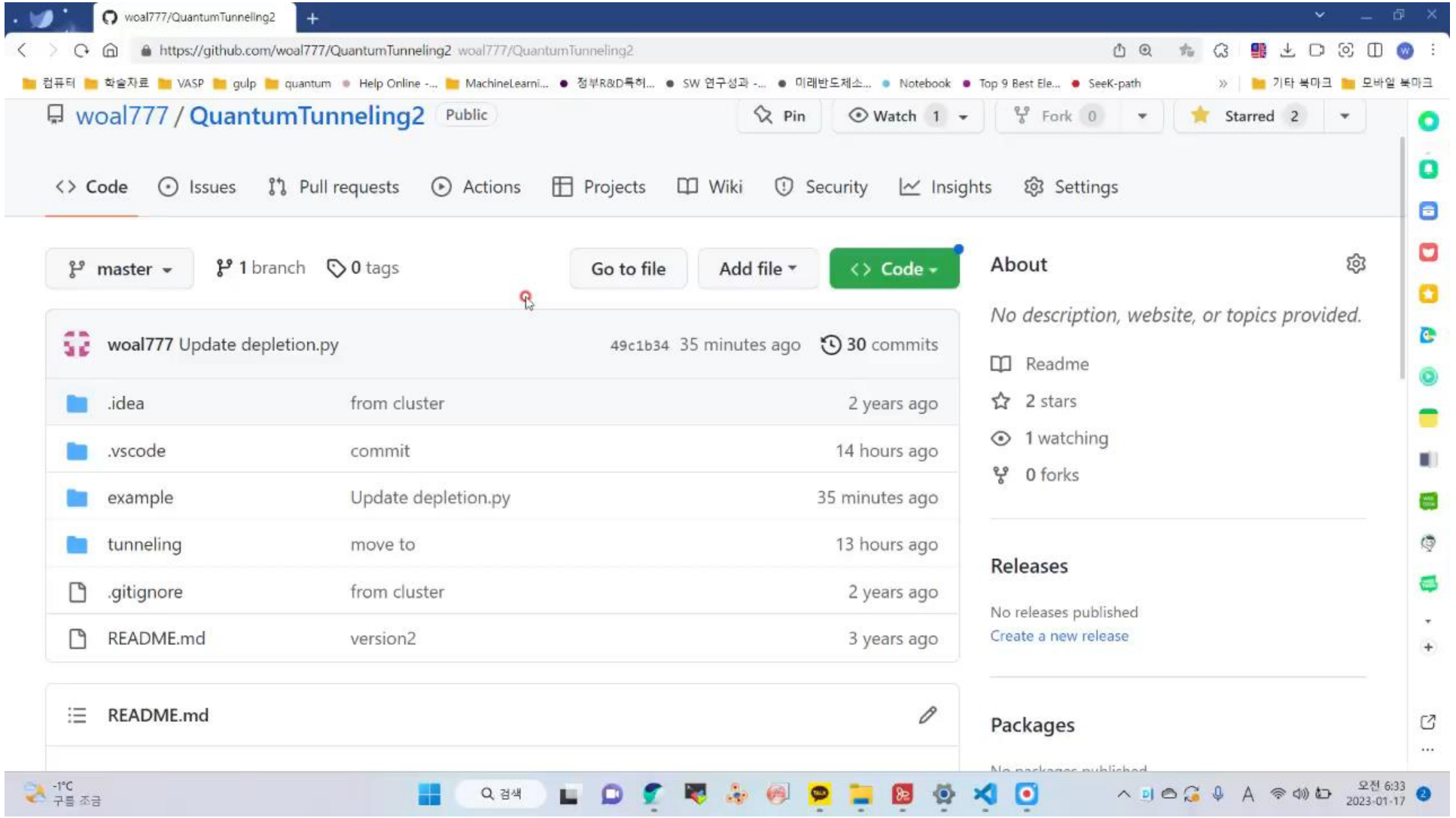

https://github.com/woal777/QuantumTunneling2

Recent issue in HfO2-based FTJ

Sneak paths problem in HfO_2-based FTJ due to its low nonlinearity

1: Off state
2: On state
3: On state
4: On state

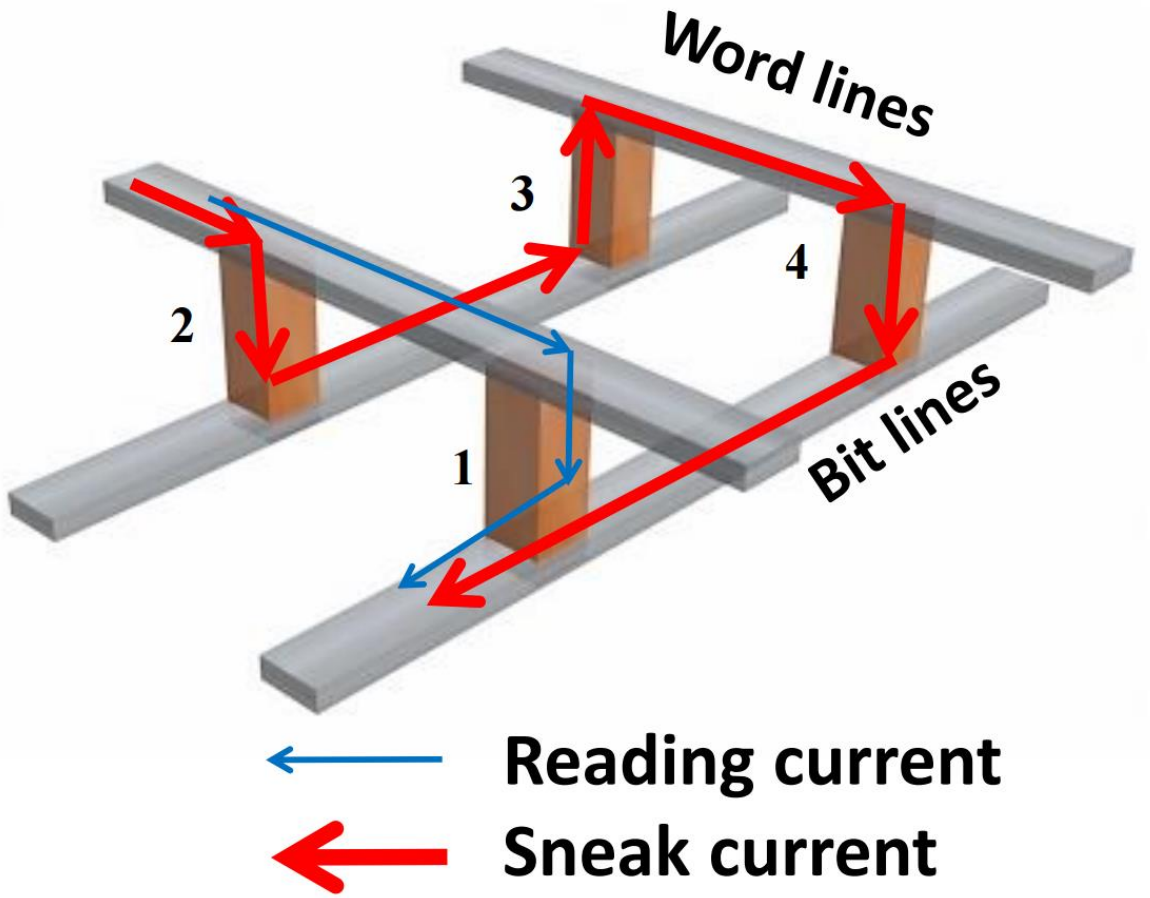

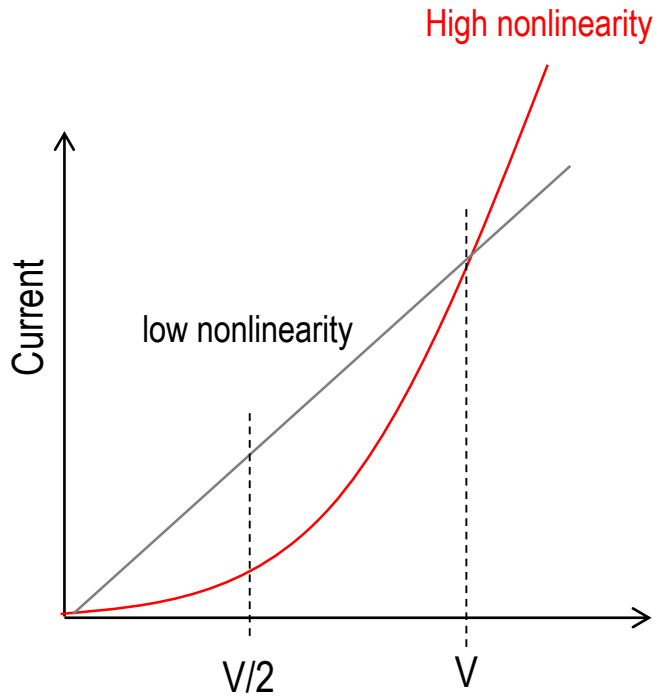

Luo Q. *et al., Nanoscale* (2016)

Modeling of tunneling current through various potential

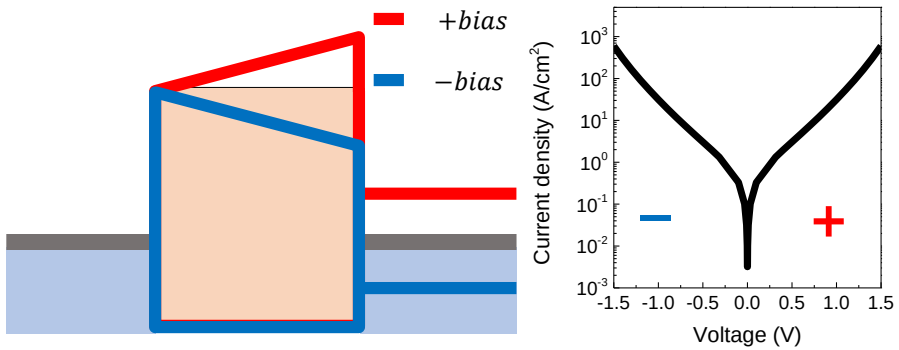

rectangular shape

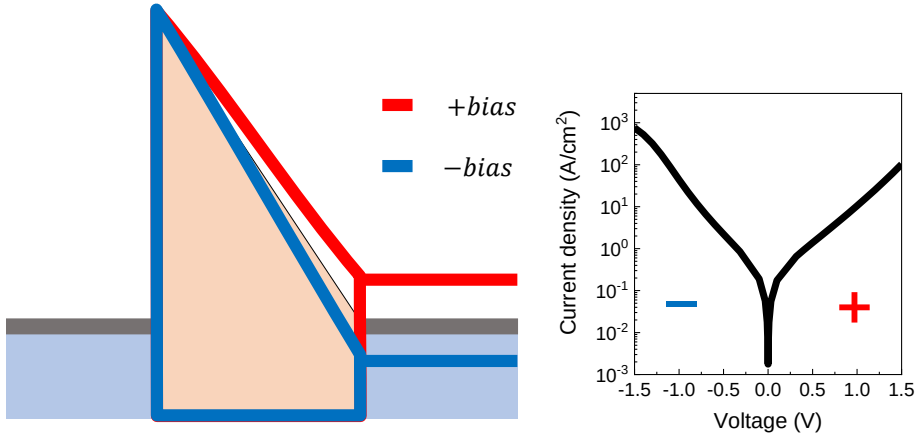

triangular shape

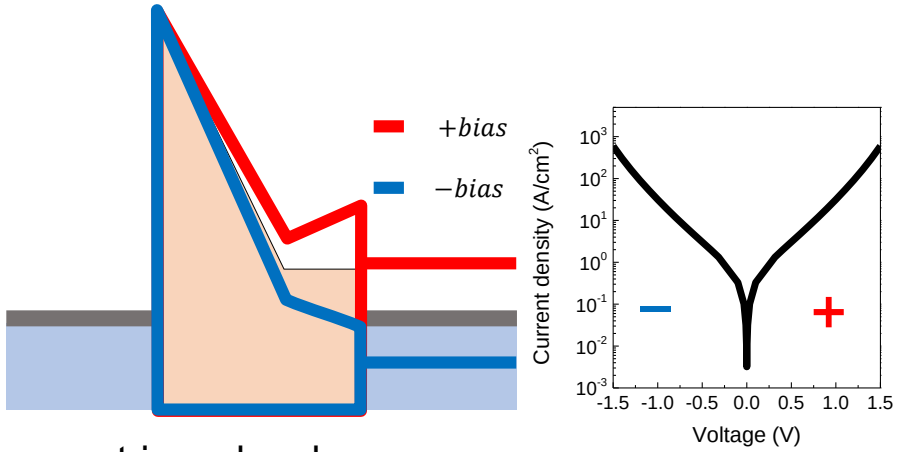

triangular shape
with flat region

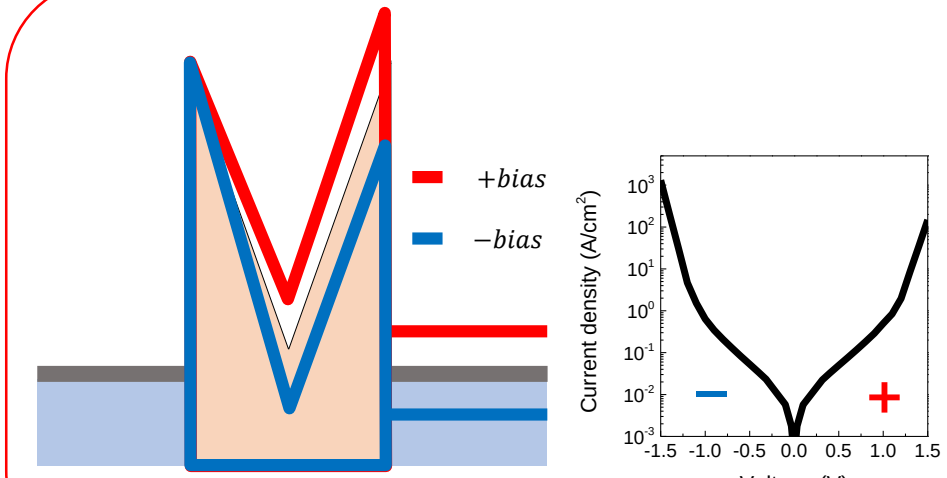

two triangular shape

Giant nonlinearity in two triangular shape potential

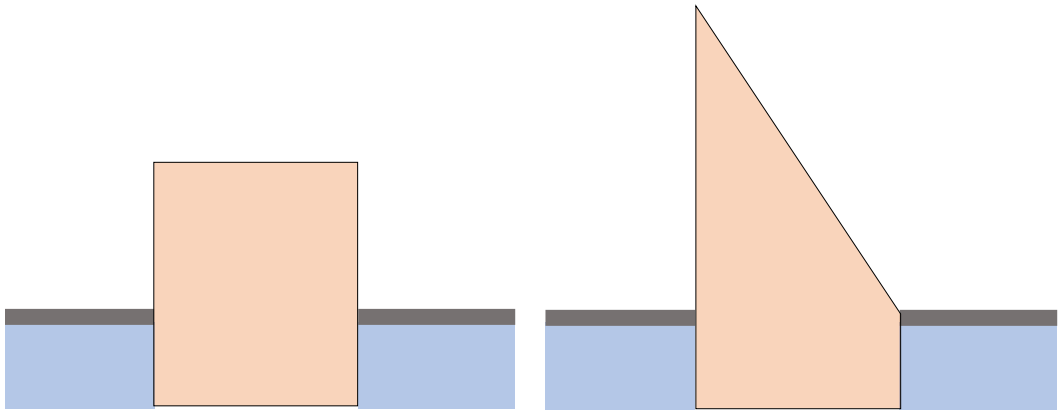

1: rectangular shape

2: triangular shape

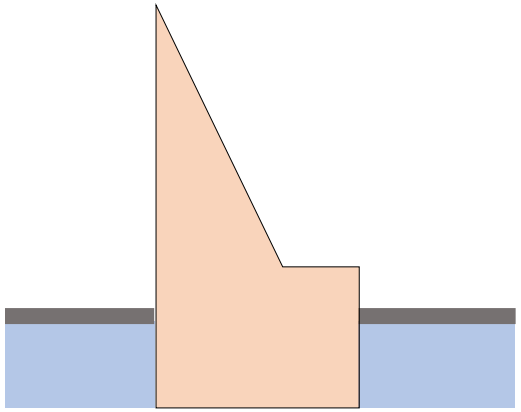

3: triangular shape
with flat region

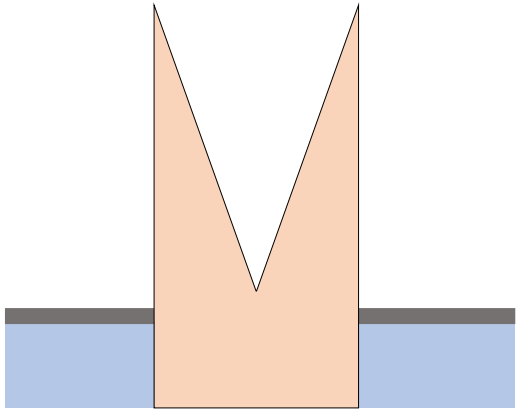

4: two triangular shape

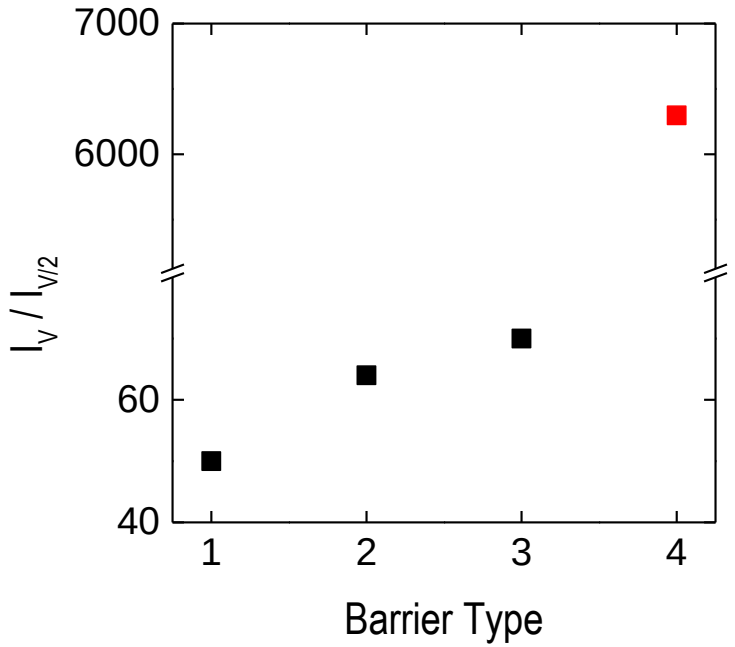

100 times higher nonlinearity in two triangular shape potential

Defect-Assisted Tunneling Electroresistance in Ferroelectric Tunnel Junctions

Konstantin Klyukin,[1,‡] L. L. Tao,[2,‡] Evgeny Y. Tsymbal,[2,3,*] and Vitaly Alexandrov[1,3,†]

[1]*Department of Chemical and Biomolecular Engineering, University of Nebraska, Lincoln, Nebraska 68588, USA*

[2]*Department of Physics and Astronomy, University of Nebraska, Lincoln, Nebraska 68588, USA*

[3]*Nebraska Center for Materials and Nanoscience, University of Nebraska, Lincoln, Nebraska 68588, USA*

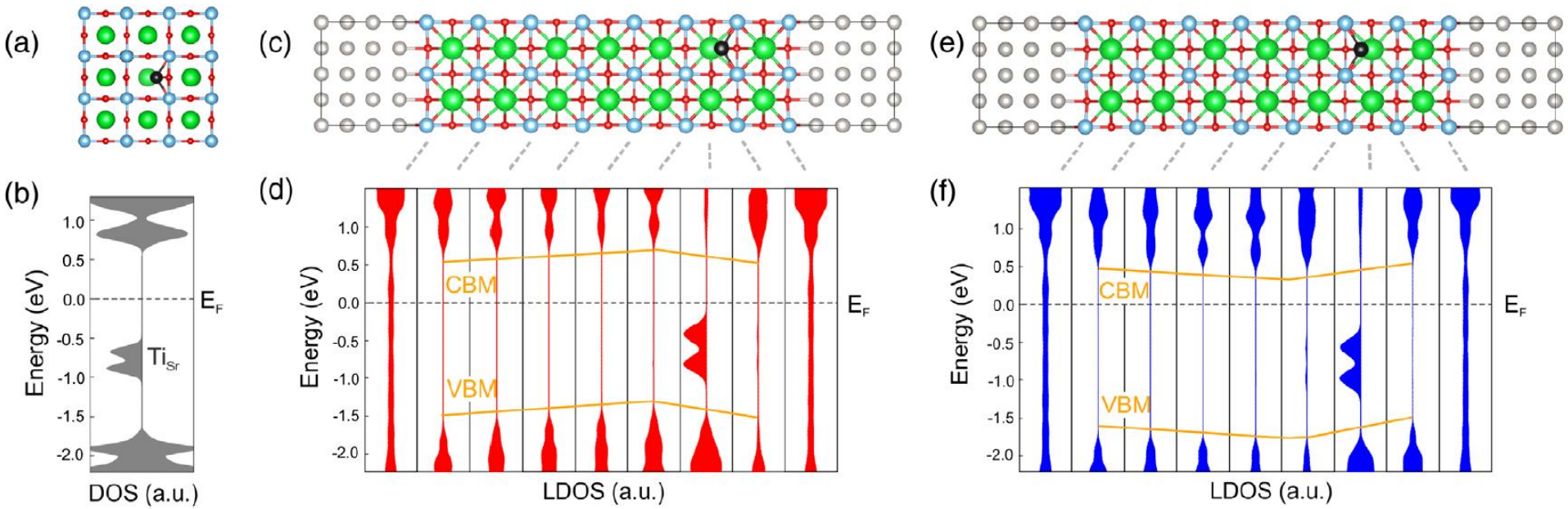

This article may be downloaded for personal use only. Any other use requires prior permission of the author and AIP Publishing. The following article appeared in Applied Physics Letters (Vol.108, Issue 25) and may be found at http://dx.doi.org/10.1063/1.4954714.

Hafnium carbide formation in oxygen deficient hafnium oxide thin films

C. Rodenbücher,[1] E. Hildebrandt,[2] K. Szot,[1,3] S. U. Sharath,[2] J. Kurian,[2] P. Komissinskiy,[2] U. Breuer,[4] R. Waser,[1, 5] and L. Alff [2]

[1)]Forschungszentrum Jülich GmbH, Peter Grünberg Institute (PGI-7), JARA-FIT, 52425 Jülich, Germany
[2)]Technische Universität Darmstadt, Institute of Materials Science, 64287 Darmstadt, Germany
[3)]University of Silesia, A. Chełkowski Institute of Physics, 40-007 Katowice, Poland
[4)]Forschungszentrum Jülich GmbH, Central Institute for Engineering, Electronics and Analytics (ZEA-3), 52425 Jülich, Germany
[5)]RWTH Aachen, Institute of Electronic Materials (IWE 2), 52056 Aachen, Germany

On highly oxygen deficient thin films of hafnium oxide (hafnia, HfO_{2-x}) contaminated with adsorbates of carbon oxides the formation of hafnium carbide (HfC_x) at the surface during vacuum annealing at temperatures as low as 600 °C is reported. Using X-ray photoelectron spectroscopy the evolution of the HfC_x surface layer related to a transformation from insulating into metallic state is monitored in situ. In contrast, for fully stoichiometric HfO_2 thin films prepared and measured under identical conditions, the formation of HfC_x was not detectable suggesting that the enhanced adsorption of carbon oxides on oxygen deficient films provides a carbon source for the carbide formation. This shows that a high concentration of oxygen vacancies in carbon contaminated hafnia lowers considerably the formation energy of hafnium carbide. Thus the presence of a sufficient amount of residual carbon in resistive random access memory devices might lead to a similar carbide formation within the conducting filaments due to Joule heating.

AFE configuration is stabilized by defect

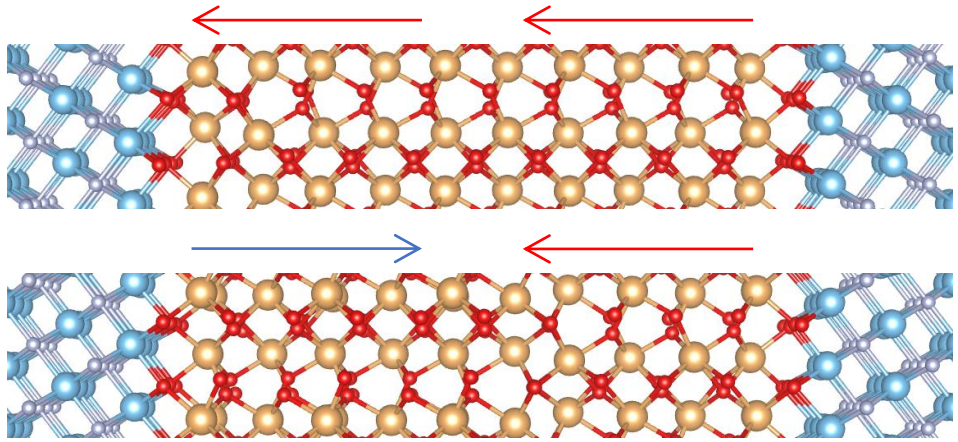

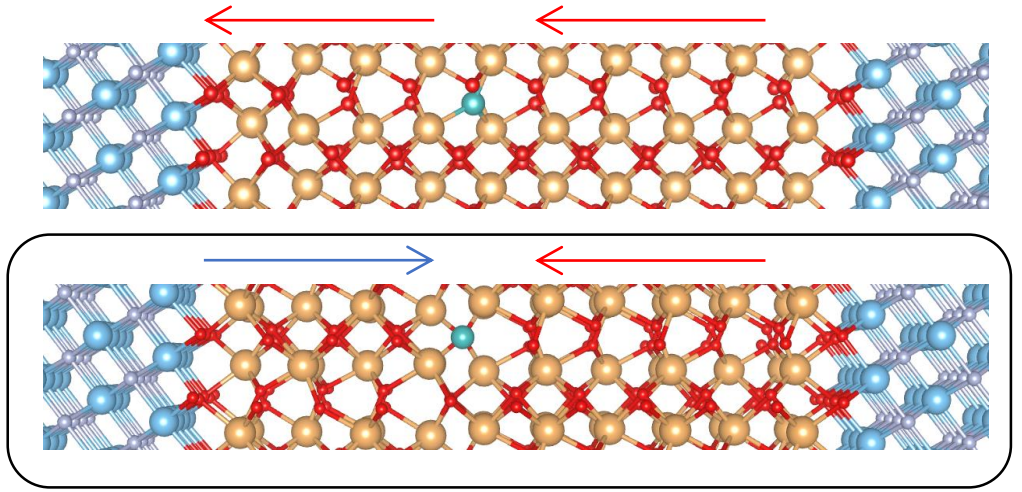

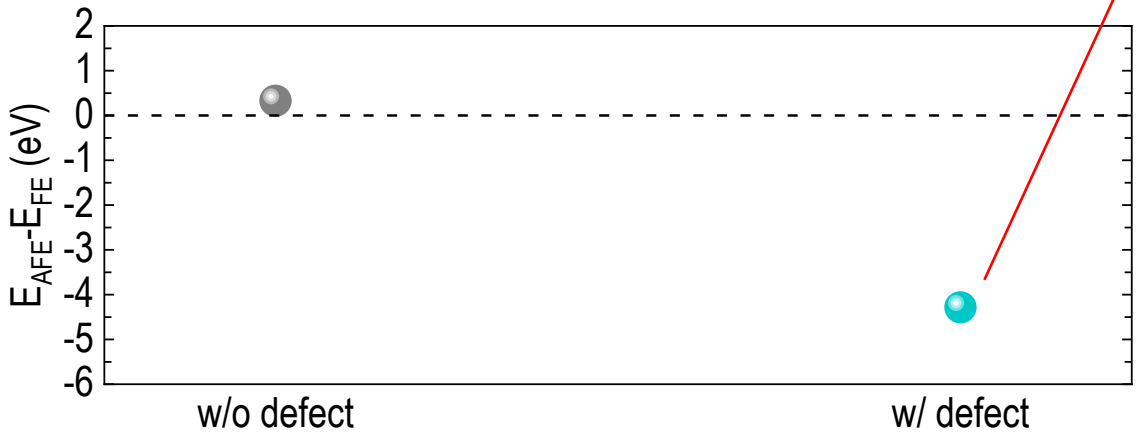

Defects prefer to be located in the middle of HfO_2

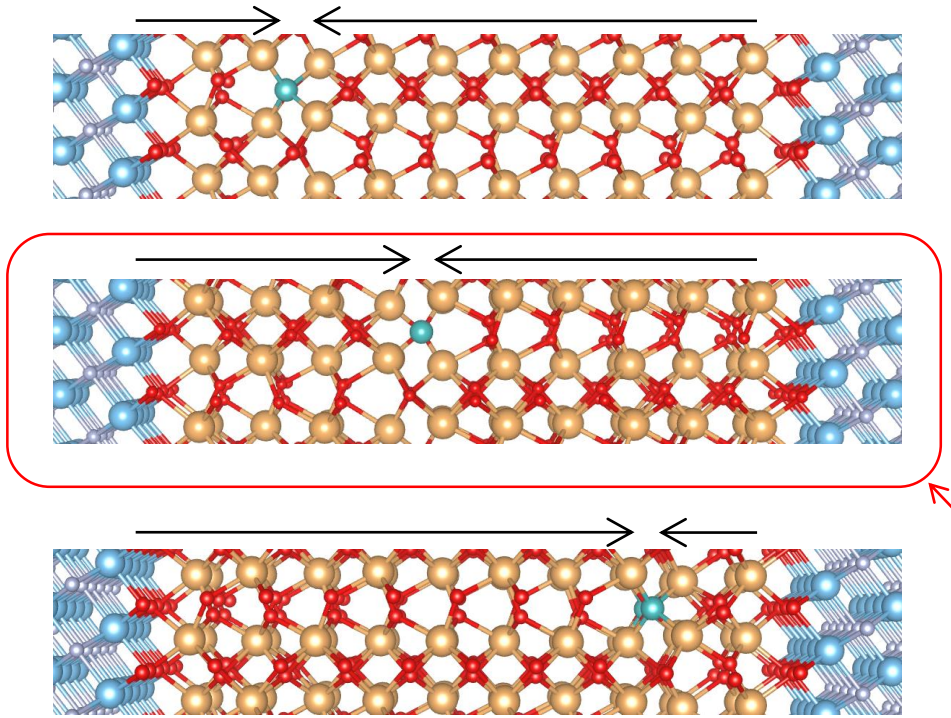

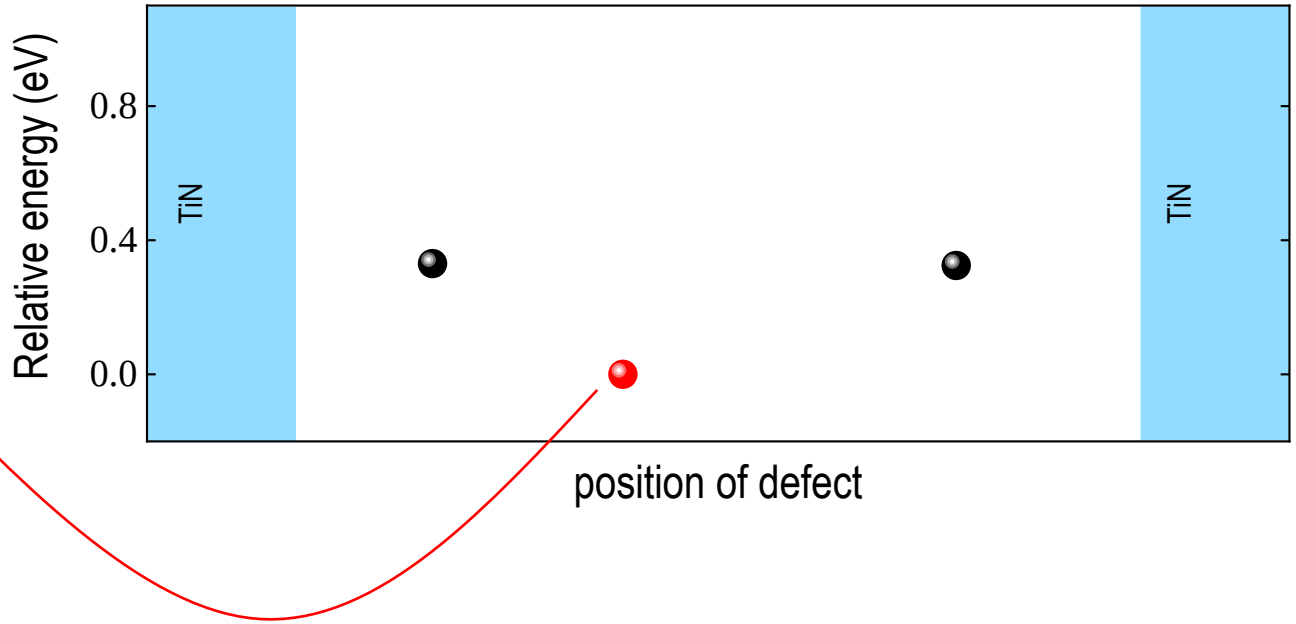

HfO_2 based Anti-ferroelectric tunnel junction(Anti-FTJ) (On state)

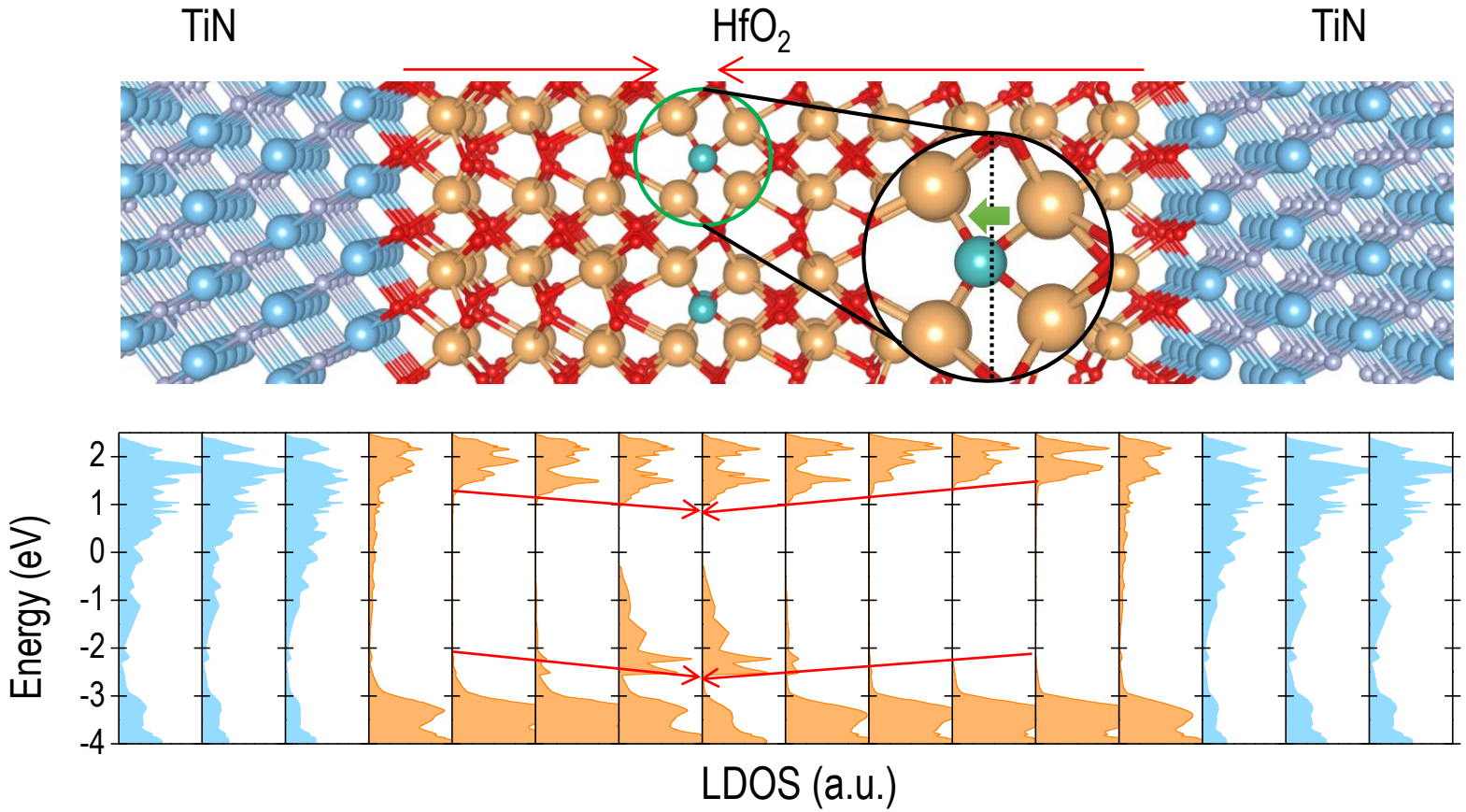

Carbon defect induce two triangular shape in the ferroelectric barrier

HfO_2 based Anti-ferroelectric tunnel junction(Anti-FTJ) (Off state)

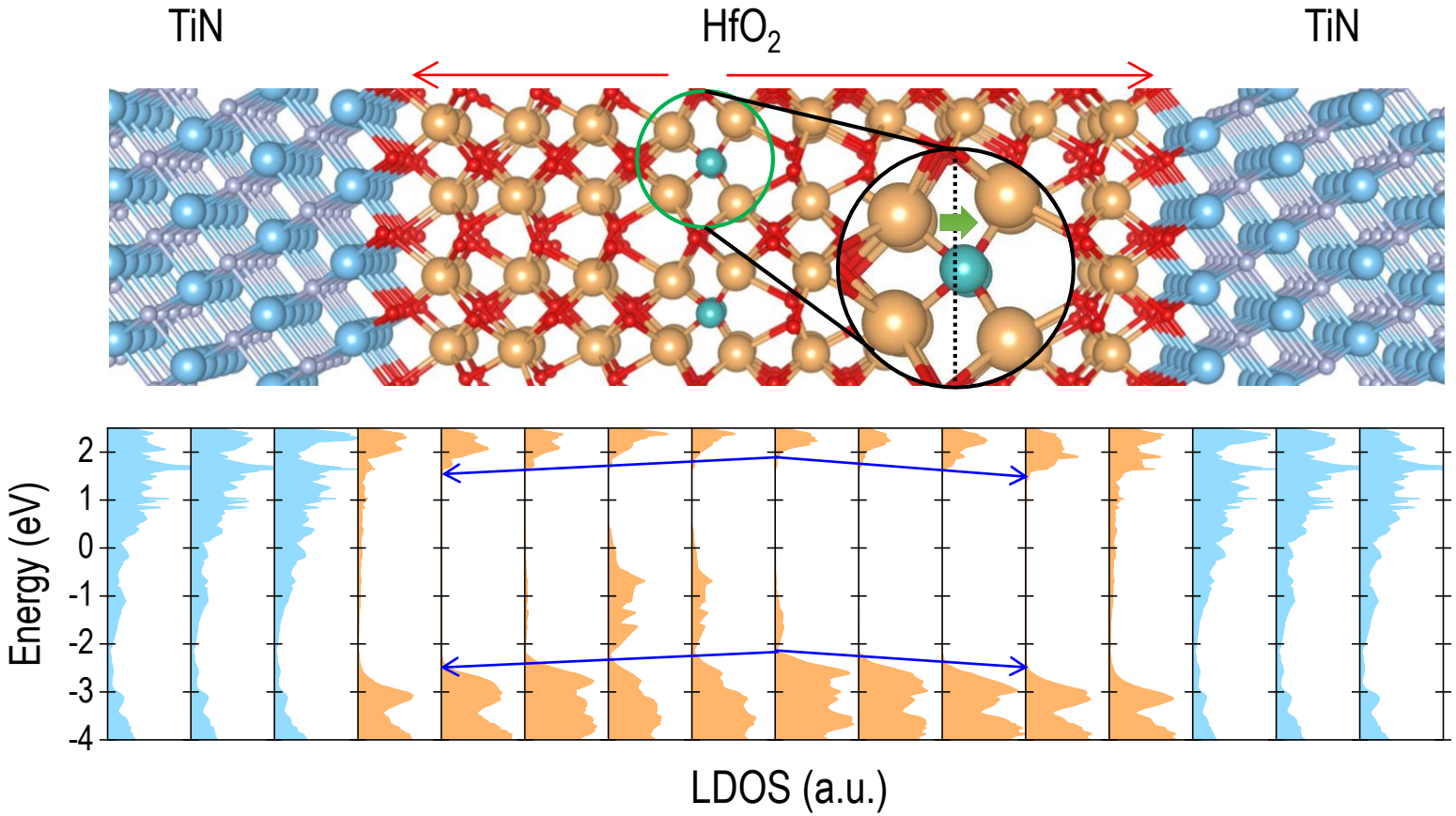

Carbon defect induce two triangular shape in the ferroelectric barrier

Summary

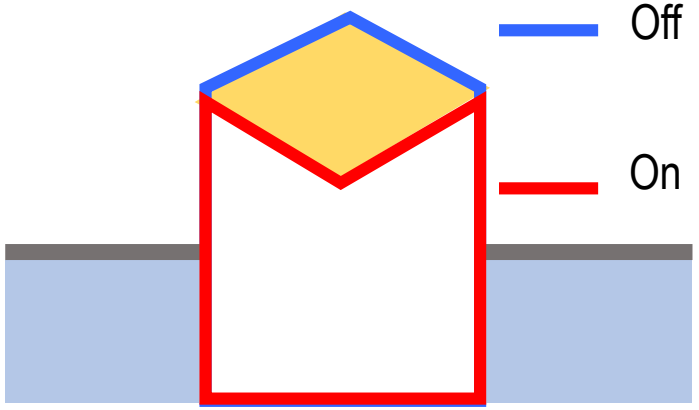

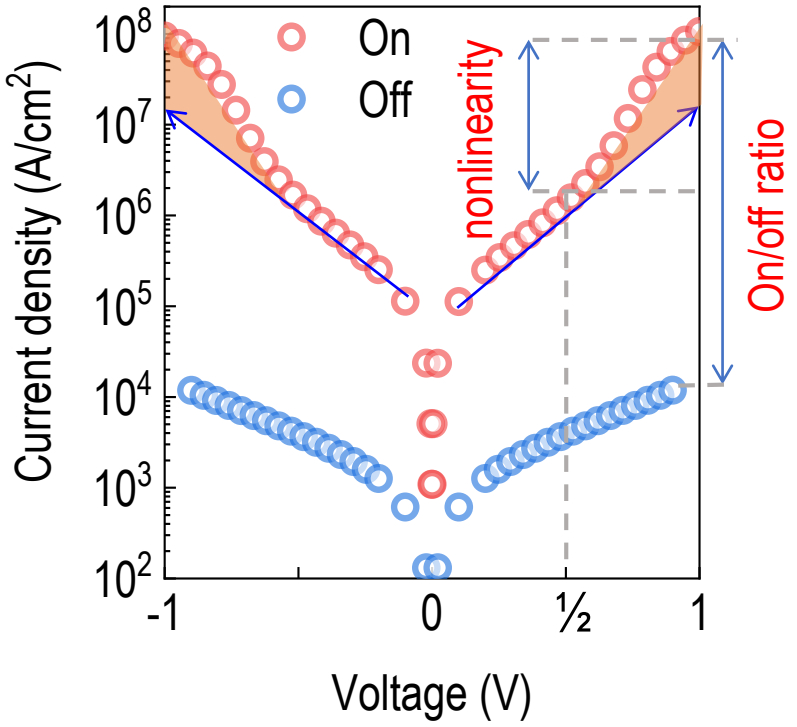

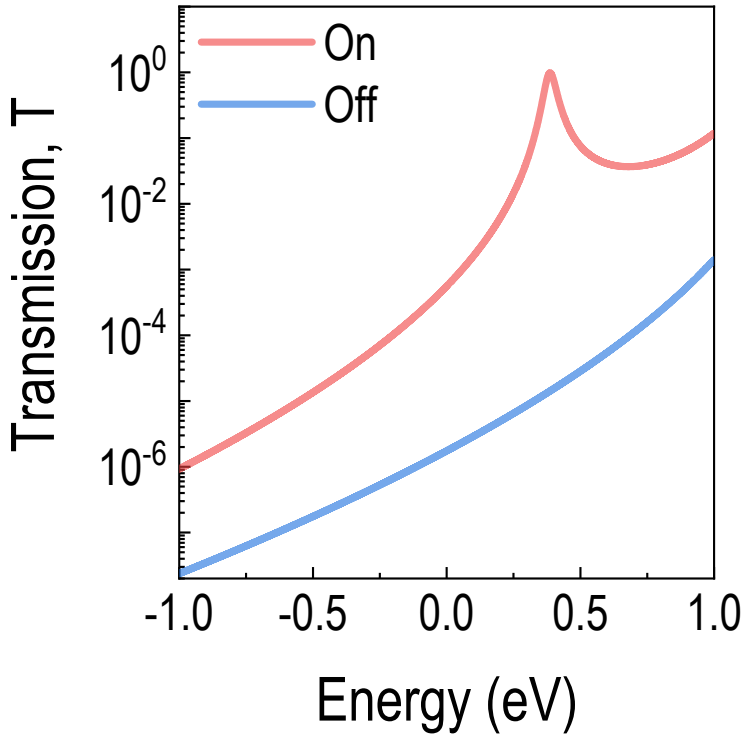

- In the on-state polarization, the resonant tunneling occurs at about 0.5eV
- 10^2 non-linearity and 10^4 on/off ratio in antiferroelectric (AFE) type HfO_2 based FTJ

Science 376, 731 (2022), Applied Materials Today (2022), Advanced Materials Interfaces 9, 2101647 (2022)

Thank you for your attention!